Faculty of Engineering and Computing
Department of Electrical and Computer Engineering

Reverse Osmosis Desalination in a Mini Renewable Energy Power Supply System

Yu Zhao

This thesis is presented for the Degree of
Master of Engineering
of
Curtin University of Technology

May 2006

ABSTRACT

The design, construction and testing of a reverse-osmosis (PV-RO) desalination system for fresh water shortage area is presented. The system operates from salt water or brackish water and can be embedded in a renewable energy power supply system, since many fresh shortage areas are remote and isolated. Special attention is given to the energy efficiency of small-scale reverse osmosis desalination systems. Limitations of conventional control strategy using toggle control are presented. Based on this, an objective of creating a small-scale reverse osmosis desalination system was set out. Initially, the background information is presented. This includes the natural resources crisis and main desalination technologies and the viability of the integration with renewable energy source.

A reverse osmosis (RO) desalination system was assembled and set up at the Curtin University of Technology, Perth, Western Australia. Supervisor Control And Data Acquisition (SCADA) system was built using a Human Machine Interface (HMI) software and a programmable logic controller (PLC). Instrumentation that included signal conditioners was made in analysis of the system characteristics. Initial testing of the system was conducted after the system design and configuration was accomplished. Testing results were used as a guideline for the development of the whole system. Modelling and simulation of the system components in MATLAB-Simulink is presented, together with a discussion of the control systems modelling and design procedure, in which the aim was to improve the efficiency of the reverse osmosis system. Simulations show the designed reverse osmosis system with Proportional Integral and Derivative (PID) controller has better performance than other controllers. This consequently leads to a lower overall cost of the water, as well as reducing full maintenance cost of the electric drives in the reverse osmosis unit. Additionally, the configuration of the remote control system through General Package Radio System (GPRS) network is depicted

After the PID control algorithm was programmed into the Programmable Logic Controller (PLC), system experiments were carried out in short durations and long durations. System performance was monitored and experimental results prove that the new control strategy applied increase the water productivity and is able to improve the system efficiency up to 35%.

Based on the data obtained from the simulations and experiments, Mundoo Island was chosen to be the location for a case study. The electric load profile of the island was derived from the Island Development Committee in Mundoo. A water demand profile was created and modelled in Matlab to be the input of the reverse osmosis system. The electric load of the reverse osmosis system was generated from Matlab simulation. This result was entered in Hybrid Optimisation Model for Electric Renewables (HOMER) simulator. Having the designed RO unit as one of the electric loads, the entire remote area power supply (RAPS) system was tested in simulations which shows the energy cost is AUS$0.174 per kWh, lower than the Island Development Committee budget estimation of AUS$0.25 per kWh. The cost of the water treatment is very promising at AUS$0.77 per m^3.

ACKNOWLEGEMENTS

I thank Professor Chem Nayar of Department of Electrical and Computer Engineering for his supervision, commitment, and support in both, the technical and personal fields throughout this work. His encouragement, constructive comments and valuable discussions are greatly appreciated.

I thank Associated Professor Bill Lawrance, who is the head of discipline of the Electrical and Computer Department. His excellent guidance and valuable comments largely helps me in many ways especially in system modelling and computer simulations.

I thank Dr Hooman Dehbonei who co-supervised this work for his light-hearted and skilled supervision and valuable advices, particularly in publishing papers and writing the thesis.

I would like to thank Rob Susanto-lee, who supported me a lot with experiments work and computer programming work. His patience and kindness inspires me along the way of the work.

I am grateful to Department of Electrical and Computer Engineering, Curtin University of Technology for providing lab facilities and equipments in which includes the crucial part of the study - revere osmosis membrane.

I wish to express my sincere gratitude to all my friends - Michael Cameron, David Schafer for their support in editing the thesis.

I am grateful to the staff at the Department of Electrical and Computer Engineering for contributions and administration, Mark Fowler, John Murry, Margaret, De-ann English. Special thanks given to Russel Wilkinson and Zibby Cielma for their expert technical assistance.

I am obliged to the Chemistry Department of Curtin University of Technology for providing the conductivity meter throughout the duration of the experiments.

I thank my family in China, for their support, concerns and encouragement from the very beginning all the way to the present day.

Finally, I thank my parents and my brother for their financial supports and prompt encouragements. Their unconditional loves spurs me on all the time. Without them, this whole experience would not have been achievable.

TABLE OF CONTENTS

LIST OF FIGURES

LIST OF TABLES

LIST OF ACRONYMS

AC	Alternating Current
CO_2	Carbon Dioxide
CITOR	Reverse Osmosis manufacturing Company, Fremantle, Western Australia
CPU	Central Processing Unit
DC	Direct Current
ED	Electrodialysis
GPRS	General Package Radio Service
HMI	Human Machine Interface
IDC	Island Development Committee
I/O	Input and output
IP	Information Package
LVD	Low Voltage Disconnect
MED	Multiple Effect Distillation
MPPT	Maximum Power Point Tracking
MSF	Multistage Flash
NASA	National Aeronautics and Space Administration
PC	Personal Computer
PV	Photovoltaic
PLC	Programmable Logic Controller
PPM	Part Per Million
PWM	Pulse Width Modulation

PVDF	PolyVinylidine DiFluoride
RAPS	Remote Area Power Supply
RMS	Root Mean Square
RO	Reverse Osmosis
SOC	State of Charge
STC	Standard Test Condition
SCADA	Supervisory Control and Data Acquisition
TCP	Transmission Control Protocol
TDS	Total Dissolve Salts
VC	Vapour Compression
VPN	Virtual Private Network
WWW	World Wide Web

LIST OF SYMBOLS

N_m	Rotational speed of the motor-pump	rpm
Q_p	Flow rate at the inlet of the membrane	l/m
K_p	Co-efficiency of the motor-pump combination	
T_m	The torque of motor	N/m
ω_m	The rotational speed of motor-pump	rad/s
Eff_{m+p}	The efficiency of the motor-pump	
p_d	The pressure differential across the pump	kPa
$p_{m,in}$	The pressure of the inlet stream of the membrane	kPa
$p_{pipe,loss}$	The pressure loss in the water pipe	kPa
m	The mass flow rate of water	l/s
g	The gravitational constant, 9.81	m^2/s
h	Total head of the water	m
V_{mot}	The voltage across the motor	V
I_{mot}	The current goes in the motor	A
π	The osmotic pressure	kPa
T	The temperature	K
R	The universal gas constant, 8.314 kPa m^3 / $kgml$ k	
$\sum X_i$	The concentration of all constituents in a solution	$kgmol / m^3$
M_f	The fee flow rate	kg / s
M_p	The permeate flow rate	kg / s

M_b	The brine flow rate	kg/s
X_f	The feed salinity	kg/m^3
X_p	The permeate salinity	kg/m^3
X_b	The brine salinity	kg/m^3
$\Delta\pi$	The osmotic pressure differential across the membrane	kPa
K_w	The water permeability coefficient	
A	The membrane area	m^2
p_p	Permeating hydraulic	kPa
π_p	Permeating osmotic pressure	kPa
$\overline{p}$	Average hydraulic on the feed side	kPa
$\overline{\pi}$	Average osmotic pressures on the feed side	kPa
M_s	The flow rate of salt through the membrane	kg/s
K_s	The membrane permeability coefficient for salt	
X_p	The permeate total dissolved solids concentration	kg/m^3
Y_p	The permeate flow rate	l/m
U	The scaled frequency that varies from 1 to 16	Hertz
F	The factual motor frequency that varies from 20 to 65	Hertz
f	The motor rated frequency	Hertz
ρ	The density of fluid	
A	A gain factor	
T_i	The integral time	s
T_d	The derivative time	s

LIST OF SUBMISSIONS

[1] Yu Zhao, Rob Susanto-Lee, Hooman Dehbonei, Chem Nayar, "Efficiency Enhancement for Reverse Osmosis Desalination in a Renewable Energy Power Supply System", *Desalination*, 2006.

[2] Yu Zhao, Rob Susanto-Lee, Chem Nayar, "PLC/SCADA Controlled Automated Reverse Osmosis Desalination", International *Conference on Intelligent Robots and Systems*, Beijing, 2006

[3] Rob Susanto-Lee, Yu Zhao, Chem Nayar, "Supervisor Reverse Osmosis Desalination Plant in an Existing Renewable Energy Power Supply Grid", *International Federation of Automatic Control*, Bansko, 2006.

[4] Ahmad Agus Setiawan, Yu Zhao, Chem Nayar, "Load Leveling by Using Reverse Osmosis Desalination in a Minigrid Hybrid Power System for Remote Island in Maldives", *Australian Universities Power Engineering Conference*, Melbourne, 2006.

ACCEPTANCE FOR PUBLICATIONS

[1] Rob Susanto-Lee, Yu Zhao, Chem Nayar, "Supervisor Reverse Osmosis Desalination Plant in an Existing Renewable Energy Power Supply Grid", *International Federation of Automatic Control*, Bansko, 2006.

[2] Ahmad Agus Setiawan, Yu Zhao, Chem Nayar, "Load Leveling by Using Reverse Osmosis Desalination in a Minigrid Hybrid Power System for Remote Island in Maldives", *Australian Universities Power Engineering Conference*, Melbourne, 2006.

CHAPTER 1 INTRODUCTION

This chapter will briefly introduce the scale of the work conducted in the research project, which includes the proposed work, objectives, main achievements and the outline of the thesis. Furthermore, it also presents the methodology of the study.

1.1 Context

The demand for fresh water is increasing in many areas around the world. This greatly influences the lives of human beings and their development. The water shortage problem has been caused by various factors such as inefficiency in water management, the deficiency of water sources, and the salinity of water, which includes underground water and stream water. Special attention is paid to the salinity of the underground water source, for the underground water provides significant amount of drinking water to human beings [2]. A salinity of 626 ppm is considered the maximum desirable salinity level. Higher concentrations are unsuitable for drinking purposes and may increase the maintenance costs for infrastructure and industrial equipment. Therefore, the salinity of underground water is a serious issue that people are confronting.

The problems of saline water also exist in Australia where its river water and underground water is salty in many areas. For example, in South Australia, the Murray River supplies drinking water to most of areas of South Australia, whereas the salinity problem of this river poses a huge threat to many users and industries despite investment in better irrigation management practices over the last decade [1].

Desalination provides a solution for resolving the problem of the water salinity. Amongst all the existing desalination technologies, Reverse Osmosis (RO) is relatively new but has already been mature in water purification industry. This

"against-the-nature" process needs considerable amount of energy which is normally drawn from the power grid. Most of the existing RO desalinations plants involve high costs in terms of initial investment, maintenance, and system inefficiencies. With the development of the membrane technology, the cost of the RO desalination unit is becoming more economical. But, their system-efficiencies are still poor.

Meanwhile, renewable energy sources are available to most of the water-shortage affected areas with capabilities that roughly match the water demands. Many designs and proposals for the RO systems were performed, where they tried to integrate the systems into renewable energy power supply systems. However, due to the high costs of the renewable energy and the low efficiencies of the desalination plants, the cost of the water produced from such systems is high. This raised an issue in which only large desalination plants are economical. However, small scale desalination systems would be ideal for the remote populations nowadays if the cost of the water treatment is low. Therefore, design of a small-scale desalination plant and enhancement of plant efficiencies has become an important issue.

This thesis summarizes the work and ideas carried out in terms of design, simulation and construction of a small-scale desalination plant that is able to be embedded in a renewable energy power supply system. The thesis states the objectives of this work followed by background information on reverse osmosis desalination and renewable energy. The work includes: system designs, system modelling, computer simulations, system construction and experiments. The significance of this research is highlighted. Further information on the RO system application is presented. The thesis finishes with conclusion and appendix.

1.2 Objectives of the Research

Apart from passively altering the production rate according to the availability of the renewable energy, most renewable energy powered RO systems only use on/off controls on the water production side (i.e. shut off unit when fresh water tank is full, turn on unit when the tank is empty). This method introduces energy inefficiencies.

This thesis includes several different control strategies that can be supplied for a renewable energy driven RO unit. Those new control strategies are to be compared

with the conventional control (on/off control). The one that produces the best performance will be adopted and programmed into a system controller to implement the strategy of energy saving.

The objective of the project is to design and construct a small-scale Reverse Osmosis (RO) desalination system with the capacity to supply quality drinking water for up to 300 inhabitants. This RO system will be competent in operating with the power drawn from the mini renewable energy power supply system previously developed at Curtin University of Technology & Regen Power Ltd [4]. The body of the prototype RO system will consist of three major parts: TECO 7200J inverter, CITOR reverse osmosis desalinator and a programmable logic controller (PLC). The feed water of the RO desalination unit is underground salty water or brackish water whose concentration of the total dissolved salt concentration (TDS) is below 10,000 ppm (parts per million). The design of the system controller focuses on exploiting new control algorithm, advancing the control strategy and improving the operation conditions for the RO system. With the new control tactics, the ultimate goal of energy saving and efficiency enhancement for the RO system can be achieved.

1.3 Research Methodology

The research methodology based on the literature review, sites investigations, system simulations, system experiments and results analysis instead of a purely theoretical study. The PLC programming language was used to implement the control strategies in the RO system. The Matlab/Simulink graphical programming tool was used in modelling for the system components. Simulations were based on the models built in Matab. Advanced control techniques (i.e. PID and feed-forward control) were used to manipulate the variable speed inverter. Short term and long term simulations were carried out during which the transient performances of the system were monitored. Simulation data were charted and analysed

The human machine interface (HMI) language was utilized to establish a user interface with the system. Empirical data were obtained from the experiments conducted in the RO desalination rig. The output of experiments was diversified by creating different system input conditions. Experimental results were collected and compared.

A case study was undertaken by selecting a location where the RO system may be suitable to be applied. Meteorological information of the area selected was gathered for the simulation in the mini renewable energy power supply system. The performance of the RO system was evaluated in a larger context.

1.4 Work Progress

After gaining the sufficient background knowledge on reverse osmosis desalination, a small-scaled RO system was designed and sized. The membrane type was decided. A reverse osmosis unit that includes a reverse osmosis membrane, high pressure pump, and AC induction motor was purchased.

Preliminary experiments were conducted. The data that were collected in the experiments provided fundamental information of the reverse osmosis membrane. The characteristics of the electric motor-pump provided the idea of saving energy and efficiency enhancement. The models of the system components were built and tested in Matlab.

Water demand profiles were created and modelled, so were the system controllers. Simulations were carried out for the purpose in evaluating the outcome of the proposed system. As the work progressed, the simulation acknowledged that the PID controller had better performance.

PLC controller was selected and configured. Sensors and transducers were purchased. Signal conditioners were built according to the conditions of the PLC input channels.

An alternative communication method (GPRS) was created using PLC Telemetry technique. This method was tested with two GPRS routers via Telstra telecommunication network at Industrial Automation Ltd.

Experiments on the RO system were conducted with different controllers. RO system parameters and results were recorded throughout the experiments in order to determine the total efficiency of the system. Establishment of the prototype RO unit had been accomplished. Data logging was taking place throughout the experiments. It

is proved that the RO system with more advanced control strategies had better efficiency. This results in reducing energy consumption in producing drinking water.

1.5 Thesis Achievements

The major achievements of this thesis are as follow:

1. Construction of a reverse osmosis desalination unit.
2. Creation of the RO system Matlab models.
3. Instrumentations in the reverse osmosis desalination unit.
4. Design and implementation of new control algorithms.
5. Design and Development of PLC program and Human Machine Interface (HMI) for the RO system.
6. Configuration of the remote control tunnel through General Package Radio System (GPRS) network.
7. Experimental data collection and analysis.
8. Case study of the application of the RO system in Mundoo Island.

1.6 Outline of Thesis Structure

In chapter1, the context of the work is set out. The objectives of the work are described. This is followed by the work progress and main achievements. The contents of the thesis are outlined.

In chapter 2, background information that includes the natural resources crisis, main desalination technologies and the viability of the integration with renewable energy source is presented. The compositions of RAPS were displayed. Special attention is given to the energy efficiency of small-scale reverse osmosis desalination system, as they are the main subjects of this research.

In chapter 3, proposed design and configuration is outlined and used as a guideline for the development of the whole system. A description of the system components and their work principles are presented. A detailed design of the RO plant is described. Finally, the configuration of the remote control system through General Package Radio System (GPRS) network is depicted.

In chapter 4, mathematical models of each component are exhibited and explained according to their specifications and data recorded in preliminary experiments. The model of each RO system component is presented in great details. The focus is on the motor-pump characteristics, the membrane features. The simulations results show characteristics of the system components.

In chapter 5, narrative of conventional control strategy- toggle control is provided. New control strategies for the RO system are explained in terms of proportion, integral and derivative (PID) control and feed-forward control.

In chapter 6, Matlab models of each control strategy mentioned in chapter 5 are created. The simulations of each control algorithms are conducted and their results are provided. Performances of the conventional and the new control strategies were assessed and compared.

In chapter 7, the construction characteristics and implementation issues regarding the prototype RO plant is presented. Experimental results are shown and analysed in light of the system performances previously derived from the simulations data. The configuration of the Programmable Logic Controller (PLC) and design of the Human Machine Interface (HMI) is displayed.

In chapter 8, a case study is carried out in Mundoo Island with the local weather data is derived from NASA meteorology institution. Having the designed RO unit as one of its electric loads, the entire RAPS system is simulated using HOMER simulation software. Simulation results are provided and analysed.

1.7 References

[1] Http://www.dwlbc.sa.gov.au/murray/salinity/index.html [accessed in 2006].

[2] Spiegler, K., Salt-Water Purification, Second edition, Plenum press, New York, 1977.

[3] Hisham T., *Fundamentals of Salt Water Desalination*, Elsevier Science B.V., New York, 2002.

[4] M-400 Series, Diesel/Battery/Inver Mini-Grid System. http://www.regenpower.com [Accessed in July 2005].

CHAPTER 2 BACKGROUND

A literature review is presented which includes water crisis of the world, renewable energy technologies, desalination technologies, renewable energy power generation systems, and development of renewable energy powered small-scale reverse osmosis desalination system whose control strategies are explained.

2.1 World Energy Crisis

The desire for fresh water in parts of the world where only seawater or brackish water is available has led to the growth, over the last 40 years or so, of a thriving desalination industry. It is dominated by large-scale municipal plants supplying large centres of population. Desalination inherently consumes a lot of energy, theoretical minimum for seawater being around $0.8 kWh/m^3$. In practice, this number is greater than $2.0 kWh/m^3$. Thus, energy cost normally dominates the total cost of desalinated water. The energy consumption of desalination also has an environmental impact, in particular the release of carbon dioxide (CO_2) into the atmosphere through the burning of fossil fuels. Prior to the industrial revolution in the 1760's, the concentration of CO_2 in the earth's atmosphere was around or below 280 parts per million (ppm), and had been for hundreds of thousands of years. Since the industrial revolution, mankind has raised this dramatically, as shown in Figure 2-1.

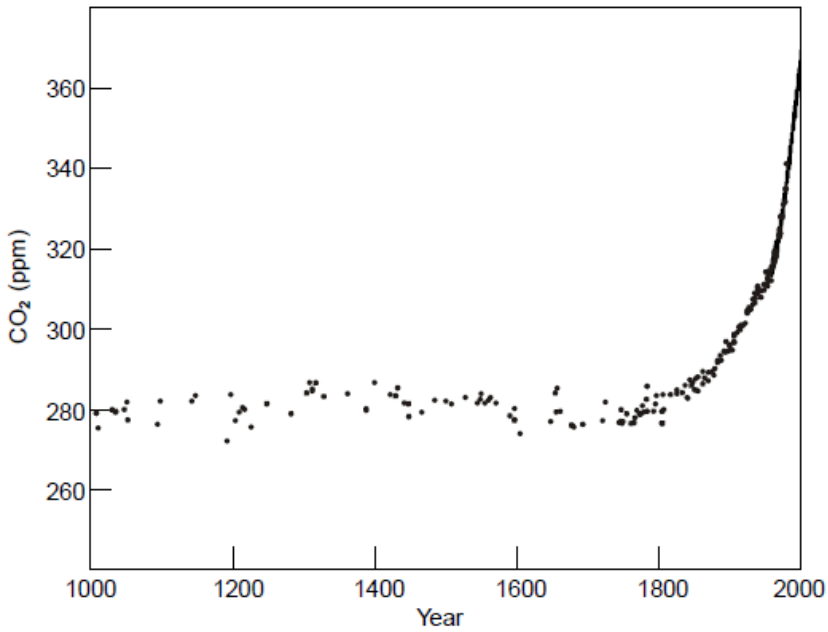

Figure 2.1 - Atmospheric carbon dioxide over the last 1000 years, illustrating the dramatic rise since the industrial revolution

(Source: Murray T, 2003)

Over the last decade one of the main reasons that the desalinations have high energy consumptions is their low efficiencies and poor reliabilities. Meanwhile renewable energy becomes an attractive and important solution for reducing the CO_2 emissions. However, the efficiencies of the renewable energy generation are not particularly high, such as average 15% for solar panels [8], 40% for wind turbines [9]. That makes the renewable energy schemes still valuable for most of the areas around the world. Even for existing renewable energy generation plants, the power they produced is more expensive than primary power generations such as thermal, nuclear, and hydroelectric. Renewable energy has natural load-matching features as a recent trend of renewable energy research is to combine renewable energy power into one generation plant together with diesel generators.

2.2 World Water Situations

2.2.1 The Portion of Fresh Water

The earth contains about $1.4\times10^{9}\,km^{3}$ of water. The hydrosphere covers approximately 70% of the planet's surface area. Nearly 97.5% of the water is salty,

which is not readily accessible for use by humans. At present, about 40% of the world's population is suffering from a serious shortage of water [10]. Throughout the world, the demand for the high quality water remains at a high level as fresh water becomes scarce.

2.2.2 Importance of Groundwater

In some events, surface water supplies may be accidentally or deliberately contaminated. For example, surface water resources may become contaminated by airborne radioactive materials and be unusable for days or years. Surface aquifers would be less vulnerable and confined sedimentary aquifers would be unaffected because of their depth, local intake areas and slow rates of groundwater movement. Consequently the confined aquifers with their level of protection and potential to provide large supplies of groundwater comprise very important, readily developable strategic resources [15]. However, Most of the underground water is salty which refers to the accumulation of salts in the soil. In general, the salinity of ground water increases with depth, although there are exceptions [1]. In drilling for petroleum people usually penetrate porous rocks containing salt water much more highly concentrated than sea water. These waters are generally too deep beneath the surface to warrant utilization. The reasons for the high salinity of the brackish ground waters in arid regions are rarely accurately known.

2.2.3 Water Situations in Australia

One of the major issues facing Australian agriculture is both dry land salinity and soil Stalinization. Especially, Western Australia is the state worst affected by dry land salinity, accounting for approximately 70 % of Australia's dry-land salinity problems. In the east, the Murray-Darling Basin is particularly affected, with an estimated 5 million hectares of land being potentially Stalinized [3].

At the same time, water use in Australia increased by some 25% between 1983-1984 and 1995-1996. This includes an increase in the use of both surface water as well as ground water. Especially, water drawn from carefully managed aquifer is no long suitable for human water consumption. In the other areas of Australia, including the southern half of the Murray-Darling Basin, saline levels are increasing by between 0.8

% and 15% annually as measured at different location[3]. Fresh water supply is largely impacted by the groundwater salinity in Western Australia, particularly in the sedimentary basins where perhaps 90% of the stored groundwater resources are brackish to saline [15].

Table 2.1

Salinity overview of each state in Australia (Source: Hayes, G, 1997)

State	Area salt affected in 1996 (ha)	Potential area affected at equilibrium* (ha)
Wester Australia	1,804,000	6,109,000
South Australia	402,000	600,000
Victoria	120,000	Unknown
New South Wales	120,000	5,000,000
Tasmania	20,000	Unknown
Queensland	10,000	74,000
Northern Territory	Minor	Unknown
Total	2,476,000	11,783,000

2.3 Saltwater

The commonly mentioned unit for addressing salt concentration is “ppm”- parts per million. 1 ppm equals 0.0001%. 1000ppm is equal to 0.1%, consequently 10,000ppm is equal to 1.0%.

The major ion in terms of positive and negative in saltwater is sodium and chlorine. Any other ions can be negligible. Meanwhile, saltwater have different varieties which can be classified as follows:

- Fresh water-less than 1,000ppm
- Slightly saline water-from 1,000ppm to 3,000ppm
- Moderately saline water-from 3,000ppm to 10,000ppm
- Highly saline water-from 10,000ppm to 35,000ppm
- Ocean water-36,000ppm of salt

Table 2.2

Typical composition of seawater with salinity of 36,000ppm (Source: Hisham T, 2002)

Compound	Composition	Mass Percent	ppm
Chloride	Cl^-	55.03	19810.8
Sodium	Na+	30.61	11019.6
Sulfate	$(SO_4)^{--}$	7.68	2764.8
Magnesium	Mg^{++}	3.69	1328.4
Calcium	Ca^{++}	1.16	417.6
Potassium	K^+	1.16	417.6
Carbonic Acid	$(CO_3)^{--}$	0.41	147.6
Bromine	Br^-	0.19	68.4
Boric Acid	$H_3BO_3^-$	0.07	25.2
Strontium	Sr^{++}	0.04	14.4
Total		100	36000

Salt water cannot be substituted for fresh water in the diet of human beings. The maximum permissible concentration of salts in drinking water depends on the type of salt, the total daily water consumption, and individual factors. The United States Public Health Service recommends that the salinity of drinking water be less than 500 parts per million (ppm) and sets 1000 ppm as the highest limit [1]. The drinking of only a few litres per day of some brackish ground waters containing high concentrations of the sulphates of sodium or magnesium often causes diarrhoea.

The amount of drinking water needed by humans is relatively small, varying between 2 and 8 litres per person daily [1] depending on the climate and occupation. Consequently, provision of small amount of high quality water by conversion of salt water presents large feasibility both technologically and economically.

2.4 Desalination Technology

At present, there are various techniques to separate fresh water from saltwater. These techniques can be classified to be two distinct groups with respect to their physical characteristics of the process. They are the thermal processes and membrane processes. The thermal process makes use of the evaporation principle of the liquids to achieve the separation of the water (solvent) from the saltwater. Whereas, membrane process makes use of filtration mechanism to extract drinking water out of saltwater.

Thermal processes include solar distillation, multistage flash distillation, multiple effect distillation, vapour compression and freeze separation methods. Membrane processes include electrodialysis and reverse osmosis principles. The following sections provide brief description and comprises of each of these techniques.

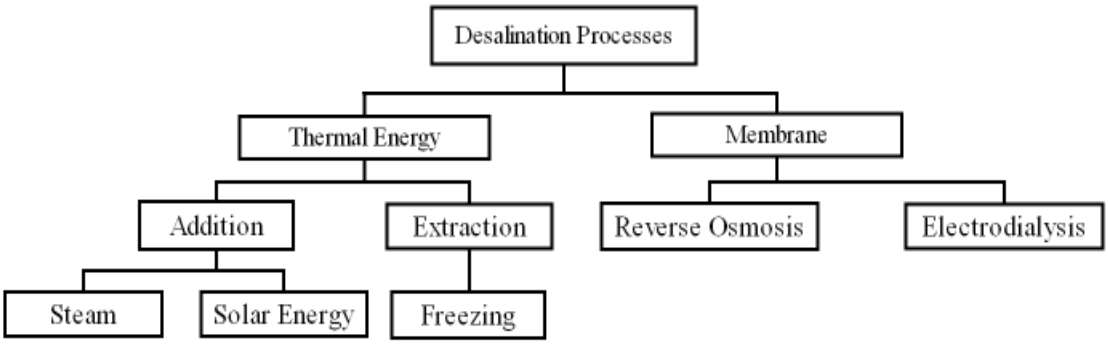

Figure 2.2 - Classification of the major desalination techniques
(Source: Hisham T, 2002)

2.4.1 Solar Distillation

Solar distillation has a greenhouse type of storage, where the desalination system borrows the energy from the sun to heat water in a container at the bottom of the storage house. This causes the water to vaporise, leaving behind any salt. The air-vapour rises up to the glass or plastic material roof and condenses. As the roof is technically built sloping, the condensed vapour drain down the roof and into side mounted troughs, from where it is pooled and transported to fresh water storages. The remaining brine concentration is removed from the aforementioned container to avoid the deposition of the salt. A still of this type is cheap to construct and easy to operate and maintain. Also, solar distillation does not require bulky electricity so it produces less pollution to the environment. However, the efficiency of this type of desalination system is modest in energy terms. The heat energy required is the latent heat of evaporation. The power requirement is about 627 kWh/m^3 [4], plus losses. At the same time, solar distillation system needs a large land area. All these limits constrain this type of technology into very small-scale applications (about 0.7m3/day). The preferable set-up locations of this system are chosen to be the places where solar radiation is high and population is low.

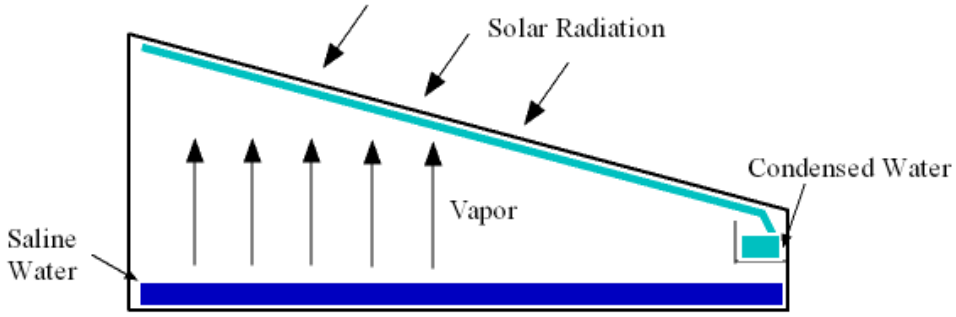

Figure 2.3 - Configuration of solar still

2.4.2 Multi-Effect Distillation (MED)

In the multi effect distillation process most of the heat energy consumed in a simple still ends up in the coolant of the condenser. Recycling this heat energy can improve efficiency several fold. Of course, the temperature of the condenser is not high enough to heat the saltwater in the original tank, but it can be used to heat a second tank held at a lower pressure. Practical distillation systems often have many tanks, known as *effects*, hence the term *Multi-Effect Distillation* (MED). MED was developed for desalination purposes during the first half of the twentieth century, but had a major practical problem with the build up of scale on the outside of the heating pipes, rather like the scaling of the heating element in an electric kettle. The efficiency of such system of various sizes is usually between 6 and 9 kWh per 1000 Litres.

2.4.3 Multi-Stage Flash (MSF)

In flash distillation, the water is heated under pressure, which prevents it from vaporising while being heated. It then passes into a separate chamber held at lower pressure, which allows it to vaporise, but well away from the heating pipes, thus preventing them from becoming scaled. Like MED, practical flash-distillation systems are divided into sections, but this time known as stages, hence the term Multi-Stage Flash (MSF). In each stage, part of the water flashes, due to a reduction of pressure and then condenses. The remaining feed water is conveyed to the next stage where its pressure will once again be reduced, causing more vapour to be produced which then condense. There can be many such stages whose number ranges from 4 to 40. Understandably, more stages will allow larger water productivities as well as having higher capital costs. With this dilemma, the stage number is one of the crucial design

aspects of a MSF unit. When first introduced in the 1960's, MSF offered slightly lower energy efficiency than MED, but this was outweighed by scaling considerations and MSF became the industry standard. Nowadays, MSF is the most widely used desalination techniques. The efficiency of such system of various sizes is usually between 10 and 14.5 kWh per 1000 Litres.

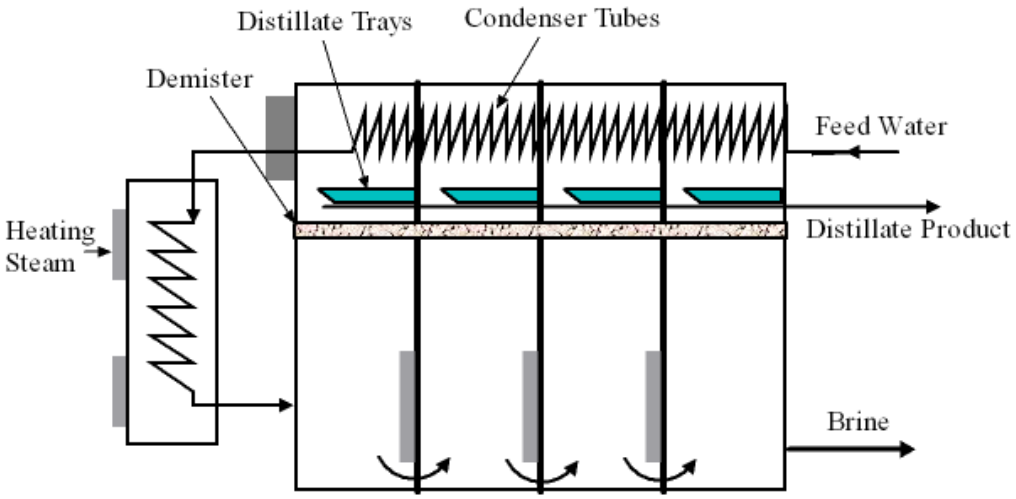

Figure 2.4 - Schematics of multi-stage flash desalination system

2.4.4 Vapour Compression

Compressing water vapour raises its temperature, which allows it to be used as a heat source. This heating steam passes through a tank of water. The vapour then can be produced and rise up to the collector at the top and move back into the compressor. This allows heat recycling in a single effect distillation process. In Thermal Vapour Compression, the compressor is driven by steam, and such systems are popular for medium-scale desalination because they are simple, in comparison to MSF. In Mechanical Vapour Compression, the compressor is driven by a diesel engine or electric motor. To increase system efficiency a heat exchanger is used to pre-heat the feed solution using the remaining heat from the product water. Furthermore, increased surface area of evaporator tubes and lower compression ratios can lead to higher productivity. The efficiency of vapour compression desalination system ranges from 7 to 15 kWh per 1000 Litres.

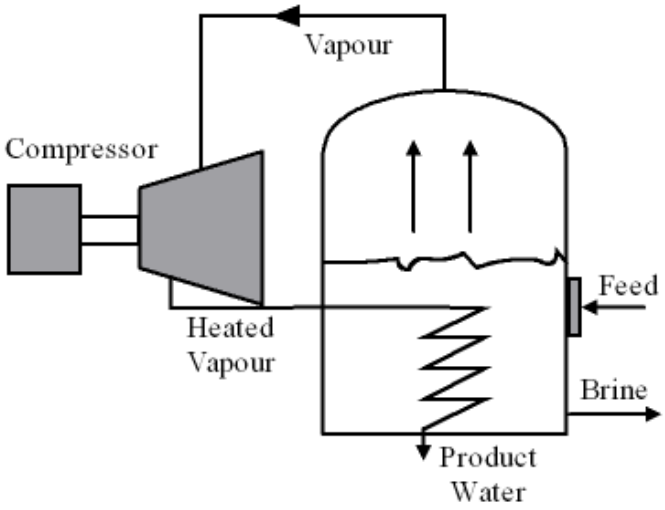

Figure 2.5 - Diagram of the Vapour compression system

2.4.5 Electrodialysis

Electrodialysis makes use of membranes. The salt ions are deliberately carried *through* the membranes, leaving behind the freshwater. Two types of membranes are required: one that lets anions through but not cations, and the other that does the opposite. These membranes are stacked alternately and held apart by spacers. The saltwater is fed into the spacer layers on one side of the stack, and a DC voltage is applied to the stack as a whole. The salt ions are attracted through one membrane or the other depending on their polarity, and by the time the water comes out of the other side of the stack, it is alternately fresh water and concentrates in the spacer layers. Reversing the polarity of the applied voltage reverses the freshwater and concentrate layers, and this can be done periodically (several times per hour) in order to reduce fouling, and is termed *Electrodialysis Reversal.* Electrodialysis was commercialised during the 1960's and is widely used today for desalinating brackish water. The energy consumption depends very much on the concentration of the feed water and so electrodialysis is rarely used for seawater desalination. Electrodialysis is considered to be the most energy efficient technology for water concentrations below 1,500 ppm [16].

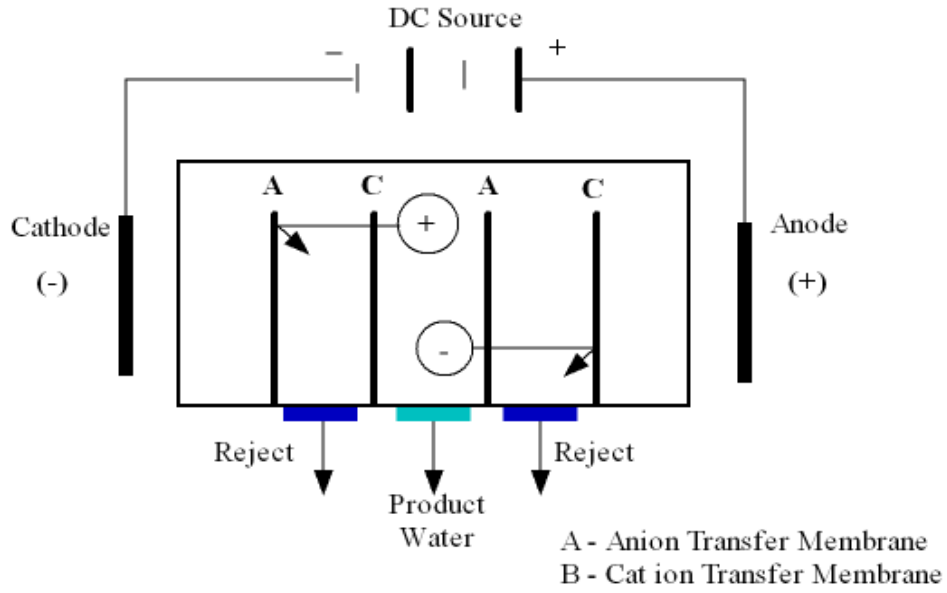

Figure 2.6 - Schematic diagram of electrodialysis system

2.4.6 Reverse Osmosis (RO)

Reverse Osmosis which was developed in 1959, is a relatively new but already mature technique for water purification. Osmosis refers to the movement of water from an area of high concentration to an area of lower concentration. Therefore, reverse osmosis is the forcible movement of water from an area of low concentration to an area of higher concentration, against the water's natural concentration gradient. In desalination, a semi-permeable membrane (a membrane which is semi-permeable allows some material to pass through, but not other materials) is used to separate water from salt and other dissolved solids.

When a semi-permeable membrane is placed between salt water and pure water which are both at the same pressure, diffusion of fresh water into salt water will occur because of nature's tendency to equalize concentrations. This process is called *osmosis*. In order for water to pass through the membrane and enable this filtration to occur, the salt-water concentrate must be pushed against the membrane with a force larger than the natural osmotic force or *osmotic pressure* [2]. The different between the exerted pressure and the osmotic pressure difference is called trans-membrane pressure. There are two types of effluent produced from the process. The first one is permeate or product water which has low salt concentration. The second one is brine which has a higher salt concentration than the feed solution. The diagram below can be seen as an illustration of this process.

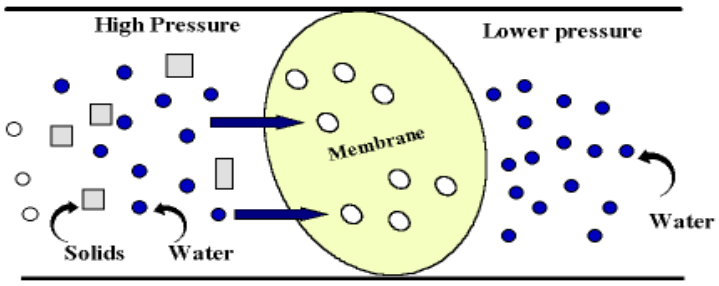

Figure 2.7 - Illustration of the reverse osmosis principle

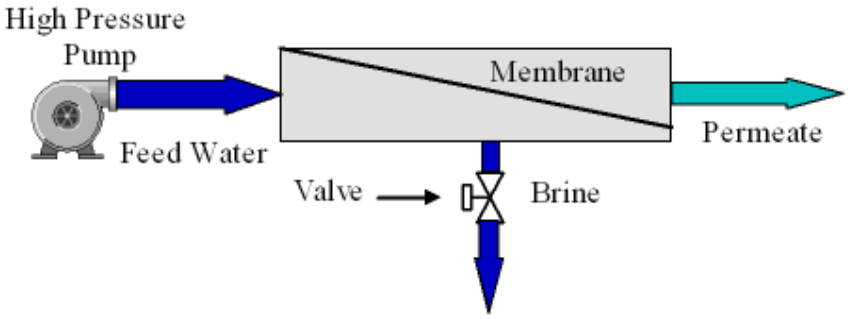

Figure 2.8 - Chart membrane compartment

2.4.7 Summary of desalination technologies

The presence of different desalination technique is summarised and can easily be seen in table 2.2 where the proportion of each desalination technology has been showed. It can be noticed that reverse osmosis has become a major technique in most large desalination production nations. The main reason for this is that, in contrast to the distillation processes just described, reverse osmosis does not involve vaporising the water. This generally leads to it being much more energy efficient. Also reverse osmosis system generally takes less energy. With all these advantages, reverse osmosis has become the major desalination technique in many developed countries (Table 2.3).

Table 2.3

Desalination production and percentages of various processes in 2000 *(Source: Hisham T, 2002)*

Country	Total Capacity M3/day	MSF (%)	MEE (%)	MVC (%)	RO (%)	ED (%)
Saudi	5253208	65.66	0.31	1.21	30.79	1.85
Arabia	5429334	64.22	0.329	1.39	32.25	1.80
USA	4327596	1.32	4.49	6.35	74.63	13.56
Kuwait	1614861	96.52	0.01	0.00	3.25	0.15
Japan	945163	3.86	2.34	0.00	84.32	7.35
Libya	701303	65.66	10.7	0.00	15.91	7.73
Qatar	572870	94.34	3.86	0.00	1.80	0.00
Spain	1233835	4.51	3.50	2.79	84.25	4.95
Italy	581478	43.76	12.4	6.53	21.67	16.24
Bahrain	473391	62.74	9.67	0.00	26.88	0.71
Oman	377879	87.31	1.111	3.70	7.63	0.24

Some parts of Australia have necessitated desalination of brackish-saline groundwater for domestic consumption and other uses due to the lack of suitable supplies of fresh water. Reverse Osmosis has been the main methods used. From 1963 to 1970, distillation of seawater and saline groundwater supplemented the Rottnest Island water supply, but ceased because of technical difficulties. In 1977, a reverse osmosis plant was constructed on the island. This plant is still operating and reduces saline groundwater of about 4000 ppm to 100 ppm, and currently produces about 0.08 GL/year [15].

Reverse osmosis has better operation efficiency than other desalination technologies. Provided renewable energy such as solar and wind energy are available, reverse osmosis is increasing in importance. Hence, reverse osmosis (RO) is the technology chosen for the designed system described in this thesis.

2.5 Small Scaled Renewable Energy Power Supply Systems

2.5.1 Renewable Energy Generation System with Grid Connection

When, connection to a centralised grid is available, often the justification for the adoption of a remote area power supply (RAPS) is based on the economic feasibility of the RAPS against drawing power from the grid. For locations where centralized grid connections are not available, RAPS is the only choice. In both of these cases, preference is given to produce energy from locally available resources, in order to supply economic and stable power for the subjected locality.

2.5.2 Standalone Renewable Energy Generation System

2.5.1.1 Diesel Generator

A diesel electric generator is an electric power source mainly comprised of a mechanical diesel engine with an output shaft connected to an electrical motor to produce electricity.

Diesel engines can burn not only diesel fuel but a range of other fuels such as natural gas heavy oil fuel. Routine inspection and maintenance of engines is required as in absence of automatic adjustments, manual adjustments need to be made periodic replacement of engine-oil, filters, belts etc are required. In addition, major overhauls are required according to manufacturers' specifications that might need replacement of major parts. 1800 rpm water cooled diesel generators can operate from 10,000 to 30,000 hours based on level of maintenance.

Sizes vary from portable stand-alone systems as small as 1 kW capacity to large fixed systems over 1000 kW supplying power into sizable grids. Figures 2.9 and 2.10 show a portable generator and a mounted generator respectively.

Various characteristics of diesel generators make them suitable for different applications. So are the common characteristics including rate of fuel consumption, engine speed, noise level and operatable time. Operation time is usually associated with engine speed. Generators with high speeds such as 3000 to 3600 rpm are

designed for shorter period operation while generators with speeds such as 1500 or 1800 rpm which are considered as low speeds can be operated for longer periods.

Diesel generators that are subjected to frequent starts and stops experience an increase in the mechanical wear on the engine. A picture of a typical diesel generator used for energy supply in remote areas is shown in figure 2.10 below.

Figure 2.9 - A portable mini diesel generator

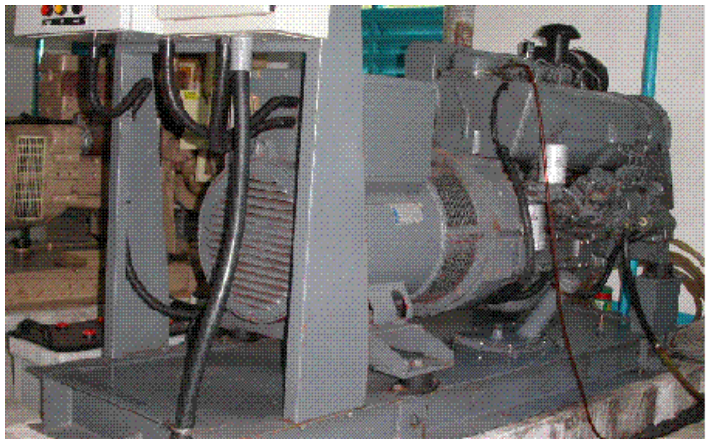

Figure 2.10 - A typical skid mounted diesel generator

2.5.1.2 Photovoltaic Generator

Photovoltaic (PV) cells, as they are more commonly referred, are produced from semiconductor wafers. PV cell operation is based on the ability of semiconductors; usually Silicon converts light directly into electricity. Photovoltaic effect occurs due to the absorption of photons into doped silicon with p-n junctions when incident light strikes its surface. The incident energy of light creates electron hole pairs. These mobile charges are then separated by the electric fields at the junction to create a voltage difference caused by the internal drift of the particles across the semiconductor. The electrical output from the cell is described by the I-V characteristic whose parameters can be linked to the material properties of the semiconductor (Figure 2.13).

There are many types of PV cells namely for instance mono-crystalline, poly-crystalline, amorphous silicon, compound thin-film, thick-film and high-efficiency cells. Figure 2.11 below shows some examples of commercially available PV cells.

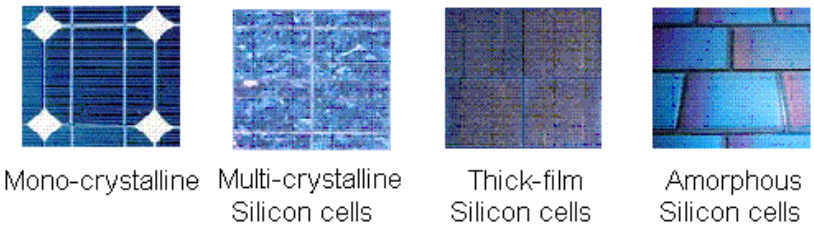

Figure 2.11 - Examples of some commercially available PV cells (Source: PV-UK, 2005)

The majority of the commercially available PV modules consist of individual PV cells connected in series in order to achieve the appropriate output voltages suitable for different applications. When the modules are arranged in series or parallel or a combination of both then they are called a PV array (Figure 2.13). Figure 2.13 shows the PV cell hierarchy in the process of PV array formation.

Figure 2.12 – Photo of a PV array (Source: PV-UK 2005)

PV panel under different temperatures are shown in figure 2.14. As can be seen, the light-generated current is proportional to the flux of photon above the band-gap energy. Increasing the temperature will increase, in the same proportion, the photon flux; this in turn generates a proportionately higher power output, shown in figure 2.15 [5].

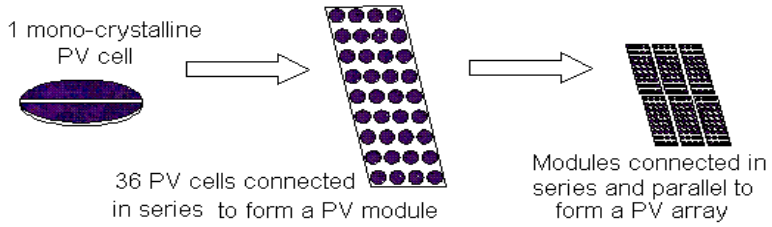

Figure 2.13 - PV cell hierarchy

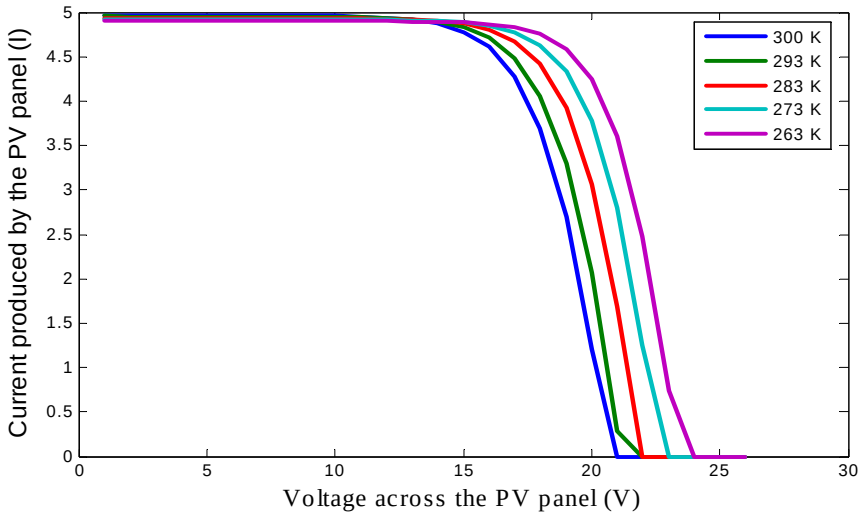

Figure 2.14- V-I characteristics of the PV panel in different temperature conditions (BP250)

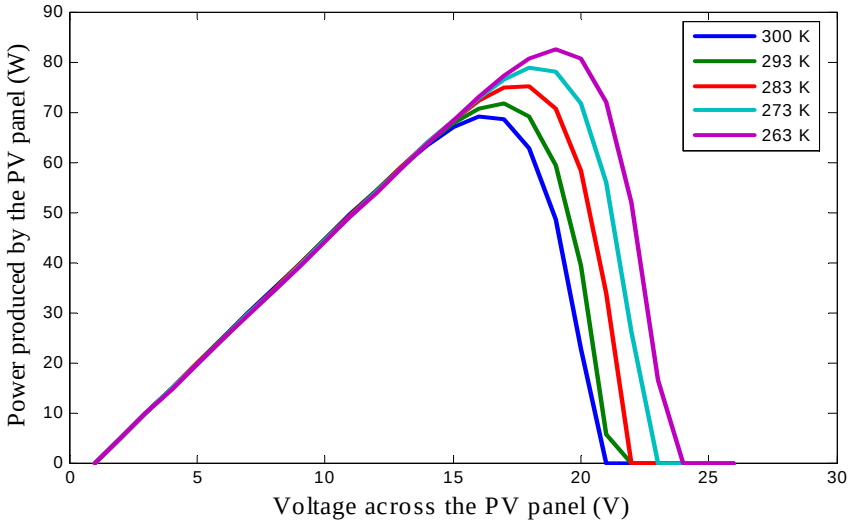

Figure 2.15 – Power output with respect to the voltage across the PV panel in different temperature conditions (BP250)

2.5.1.3 Wind Turbine

Figure 2.16 – Image of the wind turbine with two blades and three blades (Westwind)

The use of wind energy for electricity generation can be divided into two main application areas. The first and foremost of these is the commercial generation of bulk electricity through grid connected systems. The second category is the electricity generation within stand-alone systems. In contrast to grid connected systems, these are built to be used in sites where maintenance may be sporadic and technical assistance

unavailable, thus greater robustness is required in their design, incurring higher capital costs than otherwise. Grid connected turbines are used as an additional supply, complementing the conventional base load power system. In stand-alone systems, the wind can often be the sole source of energy and this should be fully taken into consideration during the design stage. Due to the inherently random characteristic of the wind, certain key aspects must be attended to in the design process of stand-alone systems. Besides the wind resource potential, the nature of the electricity load needs to be given careful consideration, in particular whether disconnection is acceptable, and if so, for how long. This consideration relates to the presence and sizing of any storage system that may be included in the system. Energy storage plays an essential role in determining system performance as the aforementioned influence on capital and maintenance costs [15]. For the design of a small stand-alone system, a key challenge is to find a good compromise between reliability and system complexity that meets the economical constraints. This is not a simple matter, and it will mostly depend on the type of load and the local resources.

2.5.1.4 Battery Bank

A battery is used to charge and store the energy from other power sources such as solar modules, wind turbines and diesel generators, and then later discharges the required amount of energy [14].

Figure 2.17 - A photo of a sealed lead-acid deep-cycle battery.
(Source: http://www.leonics.com/html/en/pd_class.php)

2.5.1.5 Rectifier

The output of diesel generators is usually alternating current (AC); therefore it needs to be rectified, regulated and controlled for battery charging. The AC power was rectified to be direct current (DC) power through a set of diode bridges that are controlled by power processing unit. The power process unit normally has digital signal generators.

2.5.1.6 Inverter

Also most electric appliances operate with 240 volt AC, 50 Hz. Therefore the DC power obtainable from the batteries needs to be conditioned. This is usually done by inverters which convert DC into AC power at the desired voltage and frequency through power switches (Figure 2.18).

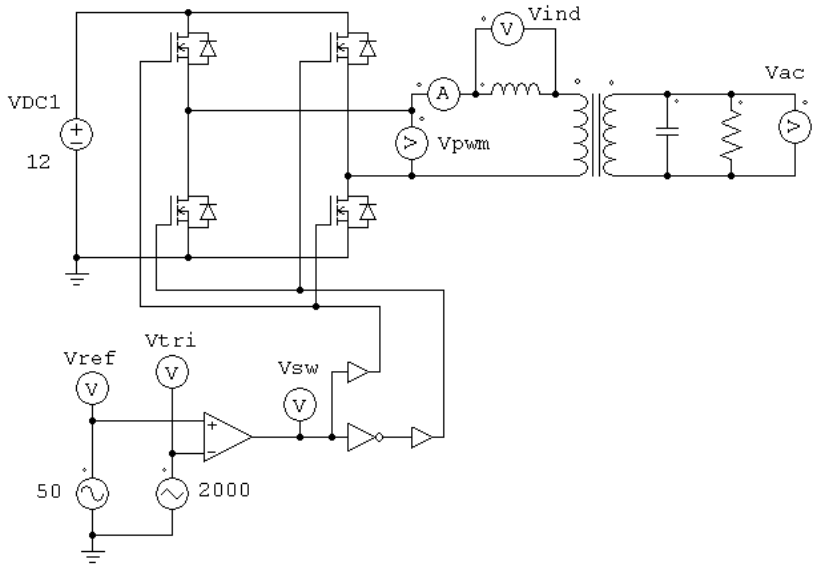

Figure 2.18 – Circuit layout of a typical inverter

Figure 2.19 – Photo of the 5 kW Apollo inverter (Source: Regen)

2.5.1.6 Charge controller

A charge controller is utilized to control the flow of electricity between the PV module, battery and the loads. Charge controller gets electricity from solar panels, charges into batteries. It also controls charge current, charge level, discharge current and discharge level. The charge controller is able to prevent battery from being damaged by ensuring that the battery is always operating within its normal charge levels. If the charge level in the battery falls below a certain level, a "low voltage disconnect" (LVD) will cut the current to the loads, to prevent further discharge. Likewise, it will also cut the current from the module in cases of overcharging. Indicator lights on the controller display the relative state of charge of the battery.

Figure 2.20 - A photo of a charge controller
Source: http://www.leonics.com/html/en/pd_class.php

2.6 Renewable Energy Powered Small Scale RO System

2.6.1 DC Motor Driven RO System without Energy Storage

2.6.1.1 System layout

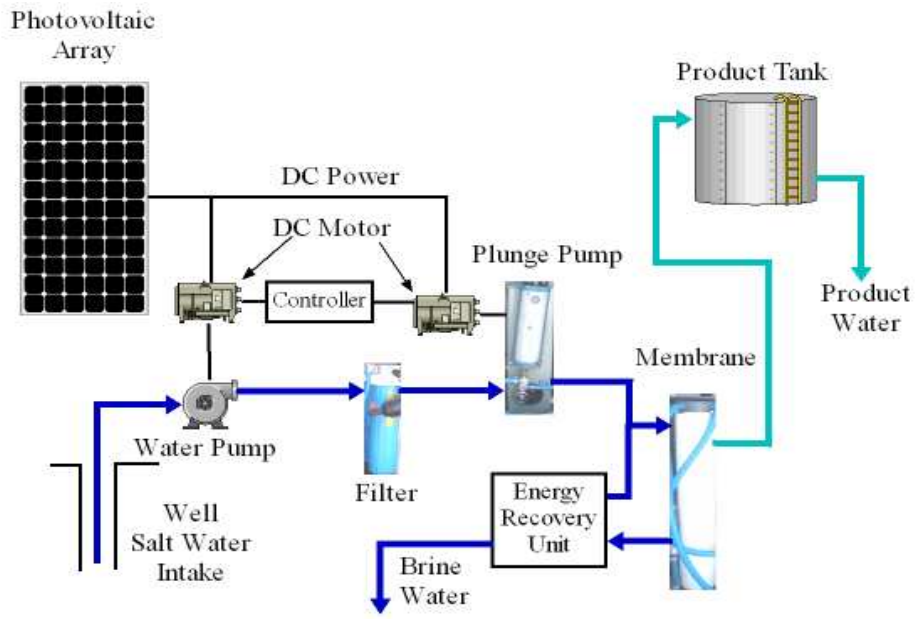

Figure 2.21 - Layout of an existing small-scale reverse osmosis desalination unit

Most small systems available today employ a high-pressure pump to produce driven-through pressure at inlet of membrane cylinders. These high-pressure pump based RO systems utilise different strategies focussed on energy saving such as energy recovery [11]. Such systems employ varieties of methods to extract as much mechanical energy as possible from the brine stream before its disposal. For example, the prototype of RO system (power rate 0.8kW) at Murdoch University (Western Australia) adopts energy that recovered from high-pressure pipe by using Clark pump [7]. The system is designed for isolated regions, autonomously operating in fluctuated weather conditions. However, its DC motor drive performs conservatively together with limited control implementation. These drawbacks highly slim the total efficiency. The water production is unpredictable as the turbulence of climates exists.

2.6.1.2 Control strategies

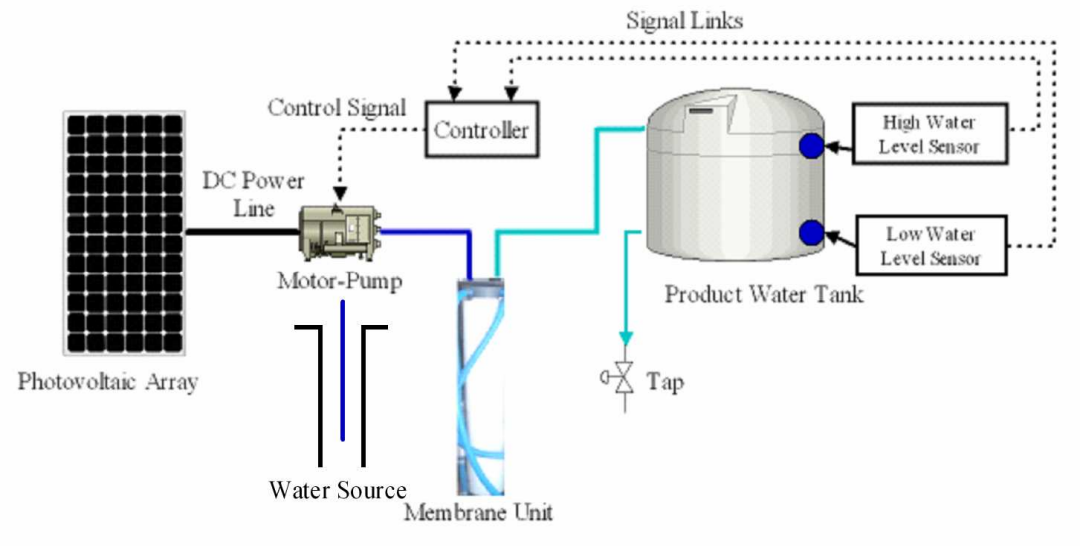

Figure 2.22 - Articulation of the control strategy in DC motor driven RO systems without energy storage

Most of the control strategies of the small scale RO systems are referred to the productivity control in term of motor control which includes the motor speed control and membrane trans-pressure controls. The latter one has been adopted to be the major control tactic and it will be discussed explicitly in chapter 4.

Apart from passively altering the production rate according to the availability of the renewable energy, most renewable energy powered RO systems only have toggle (on/off) controls on the water production side (i.e. shut off unit when fresh water tank is full, turn on unit when the tank is empty). This method introduces energy inefficiency. The RO systems introduced aforementioned mostly have controls on the motor-pump units. The trigger signal is gained from the water level sensors or float switches.

2.6.2 AC Induction Motor Driven RO Systems without Energy Storage

2.6.2.1 PV Powered RO Systems

The designs of photovoltaic-powered reverse-osmosis desalination systems were accomplished over the last decade [11]. The system operates from salt water and requires no batteries, since the rate of production of freshwater varies throughout the

day according to the available solar power. Most of these systems employ Clark pumps brine-stream energy recovery mechanisms and these, coupled with variable water recovery ratio, achieves a specific energy consumption of less than 4kWh/m^3 over a broad range of operation [11]. Standard industrial inverters, motors and pumps are employed and provide good energy and cost efficiency. Maximum power point tracking (MPPT) for the photovoltaic array is integrated and controlled by control algorithms.

A PV powered RO system was developed in UK Loughborough University in 2003. The design of the control strategy enables AC motors operating in variable speed conditions. This brings flexibilities into the RO system. It has an overall cost of water, including full maintenance, of AUS$ 4.17 per m^3 [11].

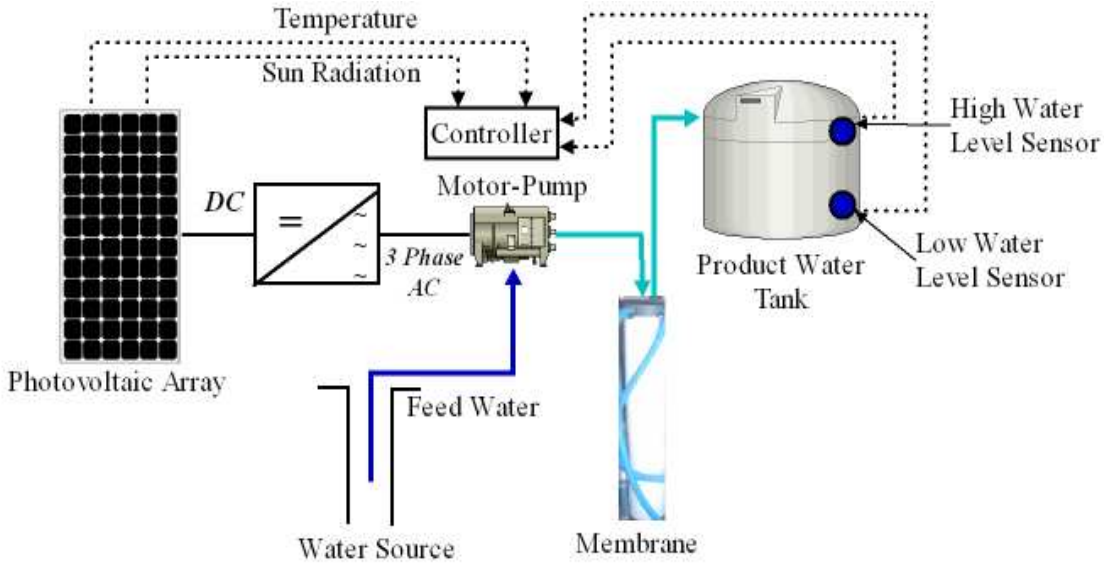

Figure 2.23 - Control strategies of PV powered RO systems without energy storage

2.6.2.2 Wind Powered RO Systems

Another idea raised in the thesis "Small-scale Wind-Powered Seawater Desalination without Batteries" by Marcos dos Santos Miranda [9] uses 2 inverters to control the plunger pump and the high-pressure pump. The pump speeds varies according to the availability of wind energy. Power is rectified to the 3-phase source directly from the wind turbine to a variable voltage DC bus to feed the inverters. It also uses a PI controller (proportional-integral) to control the motors speed. The

inverter in turn outputs three phase AC voltage to run a high pressure pump. Energy efficiency is implied in terms of control strategy and application of 3 phase electric motors. Unfortunately, the entire scheme focuses on renewable energy side of the system and has no mention of water demand side, which could result in the mismatch between supply and demand. It would also cost more pre-investment and land space to install. Meanwhile, it is exclusively designed for RO desalination, taking no interests in other electric loads. All these make the design less applicable, none the less it ideally displayed the concept of variable speed drives.

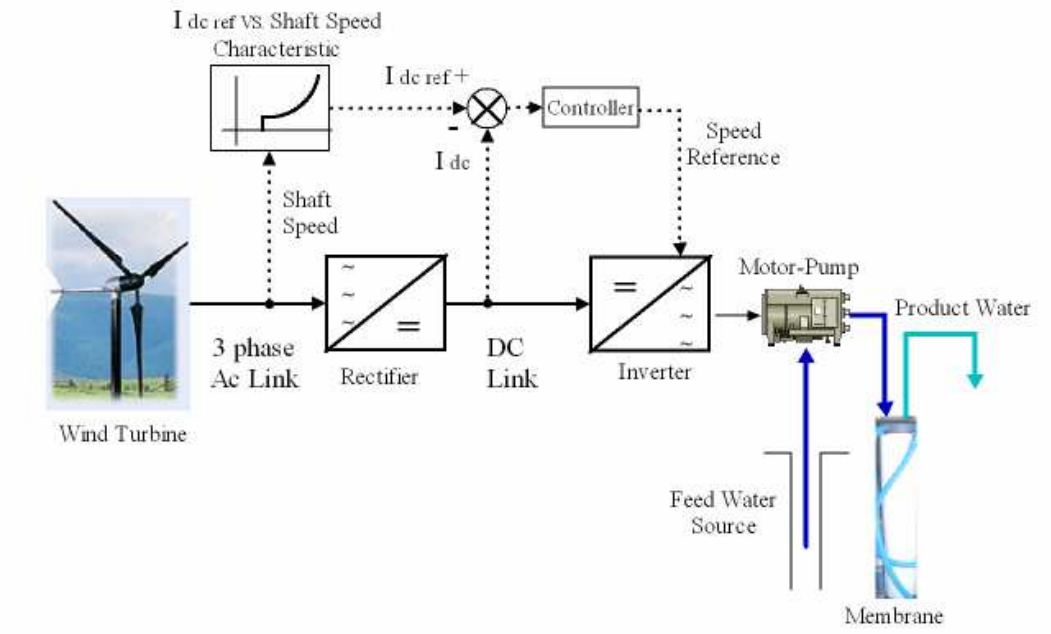

Figure 2.24 - Control strategy of wind powered RO system without energy storage

2.6.3 AC Induction Motor Driven RO Systems with Energy Storage

2.6.3.1 System Layout

With energy storages being part of the power generation system, the concept of renewable energy powered PV systems can be expanded to be broader. These RAPS systems can have more than one electric load, which introduce more conveniences to certain locations such as remote, indigenous and rural areas. Furthermore, the employment of the diesel generators enable the RAPS systems operating in fully standalone conditions with minimum impact on water supplies when renewable energy resources are temporarily not available.

A typical configuration of the RAPS system is shown in figure 2.19. RO systems act as electric loads in the system together with other loads such as lights, Televisions and Refrigerators.

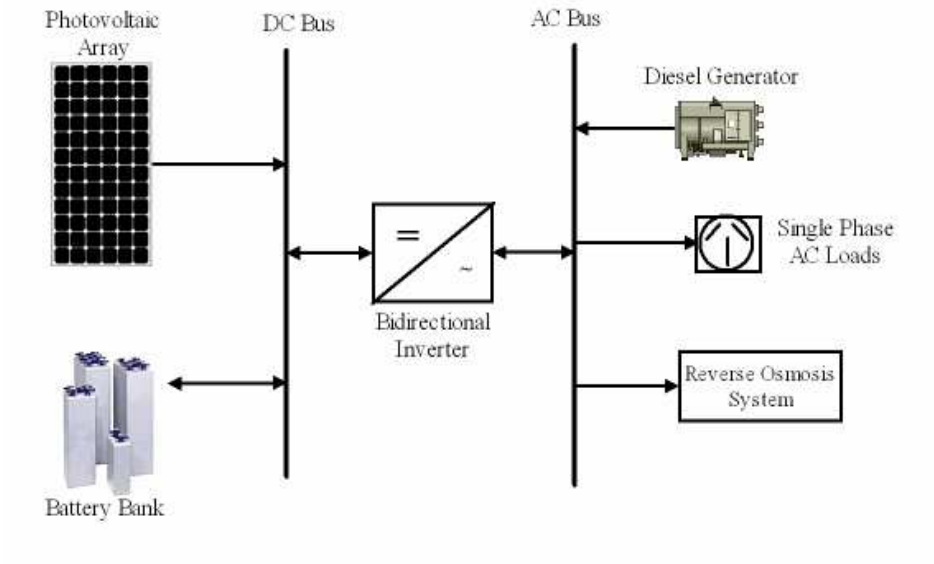

Figure 2.25 – A typical configuration of the RAPS system

2.6.3.2 Control Strategy of the RO System Embedded in a RAPS System

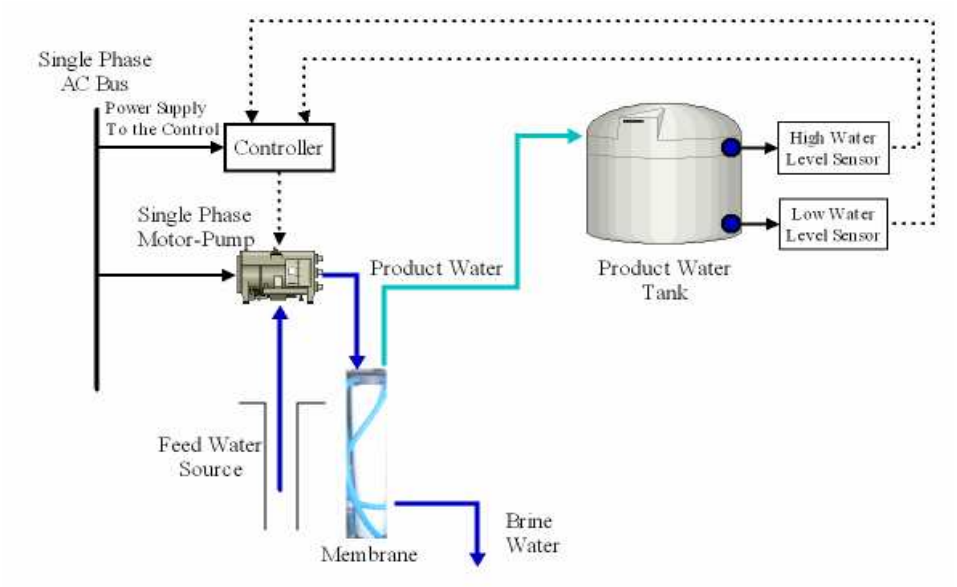

Figure 2.26 - Control strategy of the RO system embedded in a RAPS system

Most control strategies applied in the RO unit that is embedded in a RAPS system include toggle controlling tactic. That is, shut off the RO unit when the water

level in product water tank reaches high level and turn the RO unit back on when the water level in product tank hit its threshold of low value. This type of controlling is easy to implement and operate. The initial cost of the RO unit can stay low. However, it may shorten the life expectancy of motor-pumps and membranes due to the frequent start and stop time. This drawback will increase the cost of the RO system for the membrane takes up the large percentage of the total expense. Additionally, the conventional control does not take into consideration of the membrane characteristics. This may reduce the RO unit operational efficiency.

With the literature review of most RO system developed in recent 10 years, a new idea was generated in terms of electric drive speed control and load monitoring according to the characteristic of the membrane and motor-pump. The following chapters will provide the details.

2.7 References

[1] Siegler, K., *Salt-Water Purification, Second edition*, Plenum press, New York, 1997.

[2] Hisham T., *Fundamentals of Salt Water Desalination*, Elsevier Science B.V., New York, 2002.

[3] Hayes, G. 'An assessment of the National Dry-land Salinity R, D & E Program'. *LWRRDC Occasional Paper* No. 16/97, Land and water Resources Research and Development Corporation, Canberra, p.34. 1997.

[4] Marcos S., David I., *A wind-powered seawater reverse osmosis system without batteries*. Desalination (2002), 153, 9-16.

[5] Al-Alawi, A., *An integrated PV-diesel hybrid water and power supply system for remote arid regions*, Curtin University, Perth, 2004.

[6] M-400 Series, Diesel/Battery/Inver Mini-Grid System. http://www.regenpower.com [Accessed in July 2005].

[7] Jafar, M., *A model for small-scale photovoltaic solar water pumping*, Renewable Energy, 2000, 85±90.

[8] Tzen, E., Theofilloyianakos, D., Design and development of a hybrid autonomous system for seawater desalination, *Desalination* 166 (2004) 267-274.

[9] Feron, P., *Use of windpower in autonomous reverse osmosis seawater desalination*, Wind Engineering, 9(3) (1985) 180–199.

[10] Marcos, M., *Small-scale Wind Powered Seawater Desalination without Batteries*, Loughborough: PhD Thesis, Loughborough University, 2003.

[11] Murray T, *Reverse-Osmosis Desalination of Seawater Powered by Photovoltaics Without Batteries*, Loughborough: PhD Thesis, Loughborough University, 2003.

[12] Allen, A., *A geological perspective of groundwater occurrence and importance in Western Australia*, Geological survey of Western Australia, Report50, Perth, 1997.

[13] AES, *Solar Panel*, Alternative Energy Store., http://shop.altenergystore.com/XQ/ASP/ic.SUW100-SW100/QX/itemdesc.htm [Accessed in April 2005].

[14] AES, *Lead Acid Batteries*, Alternative Energy Store, http://shop.altenergystore.com/items~Cc~BATFLOOD~Bc~TROJAN~Tp~~BrandName~~CatName~Batteries%3A+Flooded+Lead+Acid.htm. [Accessed in April 2005].

[15] Kiranoudis C. T. Voros N. G., and Maroulis Z. B., " Wind energy exploitation for reverse osmosis desalination plants," *Desalination*, vol. 109, 1997.

[16] Manwell, JF, McGowan, JG. Recent Renewable energy driven desalination system research and development in North America., *Desalination*, vol 93(3), 1994.

CHAPTER 3 SYSTEM DESIGN

The RO unit is designed to be the load of an existing mini renewable energy power supply system which has renewable energy components, a bi-directional inverter, battery storage, and a single phase AC power grid. This grid provides static AC power regardless the turbulent nature of the renewable energy sources. This chapter also demonstrates the design process of system components and instrumentation.

With the renewable energy system discussed in chapter 2 (Figure 3.1), the focus of the design is on the improvement of the RO unit's efficiency. With this being the ultimate goal, the RO unit is assembled and configured as it is seen in figure 3.2.

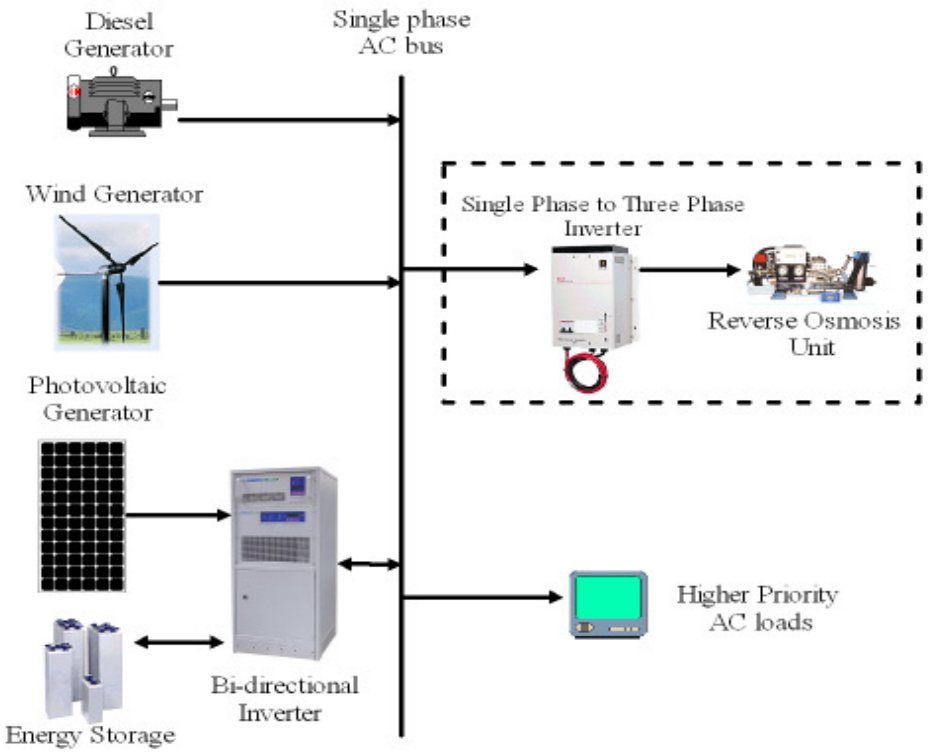

Figure 3.1 - RO system embedded in a Renewable Energy Power Supply

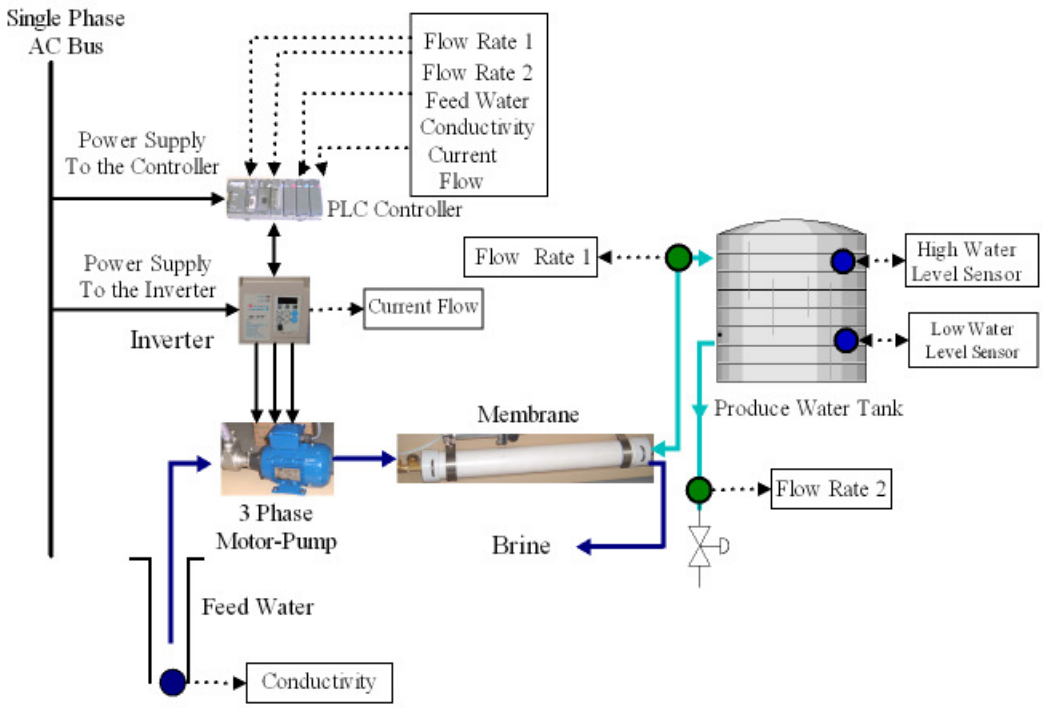

Figure 3.2 - Layout of the proposed RO system

3.1 Reverse Osmosis Membrane

Since the first membrane was produced in late 1950's, the membrane technology has been greatly developed and had a broad classification which consisted of polymer, thin film composites, etc. Generally, the cost of the membrane can take up to 15- 40% of the total investment of the reverse osmosis desalination plant and must be replaced periodically [18].

Commercially, there are three types of RO membrane available: plate-and-frame, hollow fibre, and spiral wound. Spiral wound units are popular because of their widespread utilisations, low cost and easy availability from manufactures. The spiral wound membrane was chosen from the main type of RO module design available in the market when the initial research for this thesis was carried out.

3.1.1 Membrane Structure

A spiral wound module has three layers: one spacer layer, and two membrane layers. Those two sheets of the membrane are sandwiched together with one another with a sheet of the polyester tricot in between. All layers are wrapped around a

product water collection tube (Figure 3.3). The edges of all layers are sealed except the end of the product water collection tube. As the feed water is pumped through the unit with high pressure, the solvent permeates through the membrane from the higher salt concentration to the lower salt concentration side. Driven by the high water pressure, these solvents then flow towards to the centre of the unit and end up being pooled into the product water tube, which has an opened end, where the product water flows out.

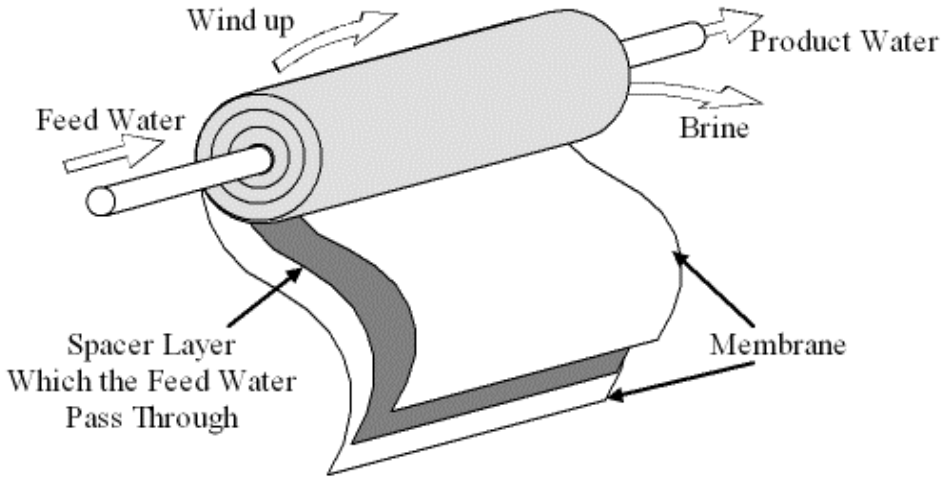

Figure 3.3 - Spiral wound membrane schematics

3.1.2 Membrane Specification

A Filmtec, spiral wound membrane was selected due to its low energy requirement [2] is shown in figure 3.4. It is a type of polyamide thin-film membrane which needs only 6.9 bars to let the water through. Its operation limit is listed in table 3.1.

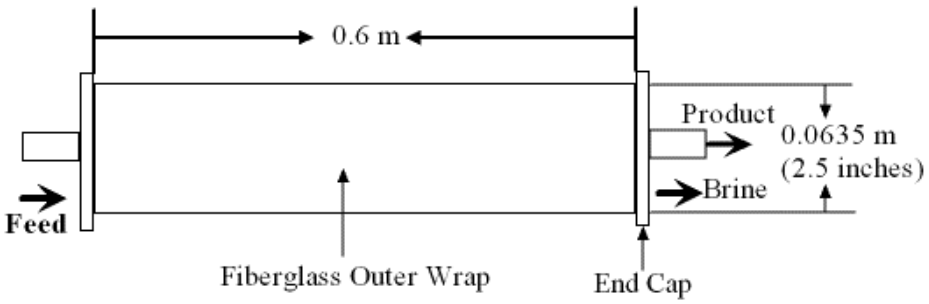

Figure 3.4 - Dimensions of the selected membrane compartment

Table 3.1
Specification of the RO membrane

Items of the membrane specification	Constraints
Max Permeate	1400 litres/day
Maximum Operating Temperature	$113^0 F$ ($45^0 C$)
Normal Operation recovery ratio	15%
Maximum Operating Pressure	600 psi (41bar)
Operation pressure	0-25 bar
PH Range continuous Operation	2-11
Free Chlorine Tolerance	<0.1ppm
Salt rejection	99%

The membrane cylinder contains one membrane with a diameter of 2.5 inches, which is used to desalinate salt water that up to 10,000 ppm [1].

Universally, a person needs about 3 litres of drinking water per day. This membrane has capacity to cater for small communities (300 inhabitants). An energy recovery system is enclosed in many small size reverse osmosis units. In the proposed RO system, the average pressure in the concentrate pipe is not significantly high (around 10 bars). Meanwhile, the selection of the high pressure pump (rotary vane pump) restrains the performance of the energy recovery unit. Therefore, after careful consideration, the energy recovery unit was not chosen to be part of the design. However, as the energy consumption always plays an imperative role, the adoption of an energy recovery unit will be listed as a future research item.

3.1.3 Membrane Maintenance

3.1.3.1 Filter Cartridge

The filter of the membrane unit will become fouled or clogged up over time. When it is not allowing sufficient feed water through – the pump will take in air through the joints and threads. This will cause the pump to run roughly. As the time for this to occur depends on the quality of the feed water and operational

times, it will vary the times for replacement of the filter cartridges greatly from system to system.

3.1.3.2 Membrane Cleaning and Sterilizing

The membrane will be contaminated by the growth of bacteria on its surface, and also the product water. Monthly cleaning and sterilizing is required to keep the quality of the water at an acceptable standard.

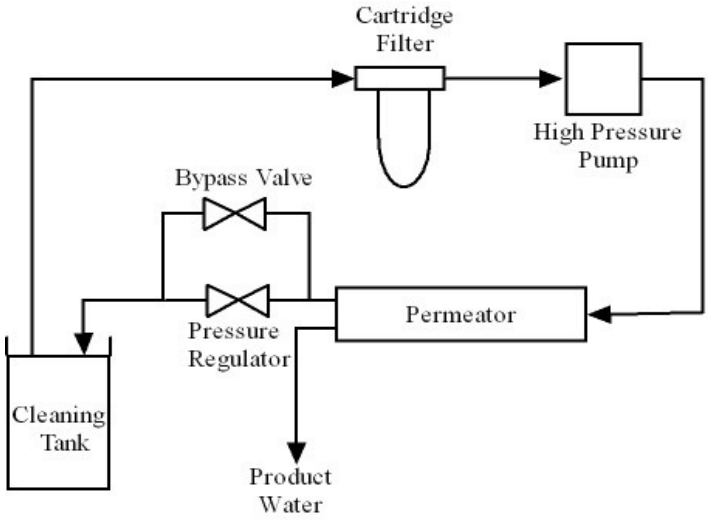

Figure 3.5 – Reverse osmosis system set-up for cleaning and sterilising purpose

A) Cleaning

Refer to the schematic diagram figure 3.5 and set up the closed circuit for cleaning using a bucket (20 litres capacity) to draw the cleaning chemical. The solution is to go through the filter; then the pump; membrane; then back to the bucket.

1. Making the cleaning solution – dissolve 200 grams citric acid (2 %) in 10 litres of fresh water in a bucket with 20 litres capacity. Draw the solution through the filter, then the pump; the membrane; then return solution to bucket.

2. Put bypass valve to start position. Immerse the inlet of the pump into the aforementioned solution and switch on the desalination pump which sucks the

cleaning solution up through the filter, pass it over the membrane and return it to the bucket. Do not pressurise the system. Allow to run approximately twenty minutes. Stop the pump and allow it to stand for three or more hours. If convenient, allow to soak overnight.

3. Temporarily connect the return line to the bucket (to discharge to waste). Start pump and let the flow almost empty the bucket.

B) Sterilizing

Membrane sterilizing should be carried out immediately after cleaning. Form the same closed circuit as for cleaning procedure. This time, the solution to be used is sodium metabisulphite 1% (preservative). Make solution by dissolving 100 grams of this chemical in ten litres fresh water. Then allow solution to circulate for 10 minutes. Leave the solution to stand until desalination system is to be used again. It is quite normal for the solution to remain inside the system when not in use as it prevents the growth of algae.

When the desalination system is to be operated, establish the feed water to the waste system as normal. The first litre of fresh water produced will have minimal traces of the preservative. This chemical is harmless. It will quickly disappear.

3.2 Activated Carbon filter

Carbon Filters contain a deep bed of activated carbon as the filter media. Carbon is a highly adsorbent material with a very high capacity for the removal of tastes/odours, chlorine and Trichlormethane.

The filter media is held within a cylinder (Figure 3.6). The filter media sits on top of a gravel bed and a centre tube passes through the media. Normal service flow is down through the filter bed and back up the centre tube. During backwashing, the flow is reversed flushing sediment out of the filter bed.

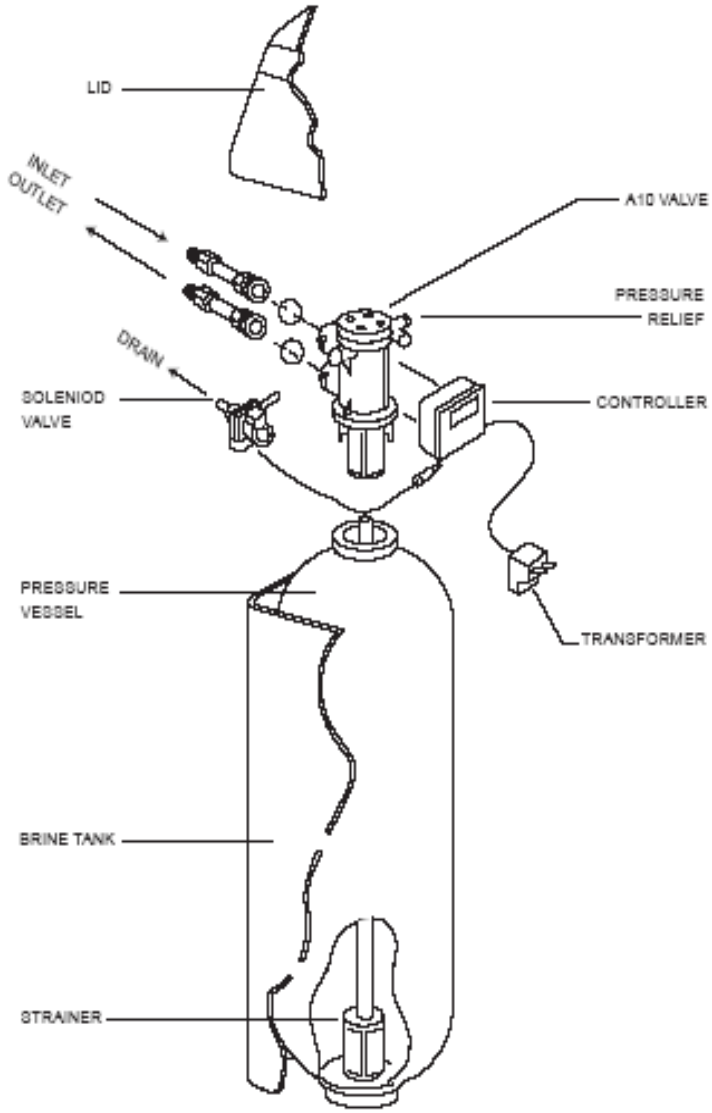

Figure 3.6 - The assembling of carbon filter (Source: CITOR)

3.3 High Pressure Pump

A high pressure pump drives salty water through membrane cylinder. A Fluid-o-Tech high volume rotary vane pump (Figure 3.7) was chosen as it has superior performance and stability at low pressures. Its flow rate ranges from 500 to 1000 litres/h at 1450 rpm. The maximum pressure that can be delivered is 16 bars.

Figure 3.7 - Image of the rotary vain pump (Source: http://www.fluidotech.it)

A contact is mounted at the pump outlet to detect the no flow fault. If the contact is active, the system will produce an alarm and notify operators/users.

3.4 Three-phase Motor

The three-phase electric drive performs better than the DC and the single-phase AC drive. It is also easier to control in variable speed conditions. Hence, a three-phase 4 Pole induction motor (CMG SLA) was selected. Its normal work-voltage is 220-240 V (delta connected), as its frequency is 50 Hz. When it works with 240 V, 50 Hertz power supply, it delivers 0.37 kW power. And it has water proof insulation. It has been used as a variable speed drive to vary the pressure of inlet water of the membrane unit. By changing the line frequency through a single phase to three phase inverter, the speeds are varied which also varies the water pressure.

Figure 3.8 - Image of the AC induction motor
(Source: http://www.aer.co.uk/acatalog/CMG_Electric_Motors_SLA.html)

3.5 Single-Phase to Three-Phase Inverter

The inverter chosen for the RO system is a commercially available one: 1kW single phase to three phase inverter. It is an all-digital, mini size inverter (TECO Speecon 7200J) It converts power from single phase AC to three-phase AC and feed this power to the motor-pump unit whose rated power is 0.37kW. This inverter has small delays in response to input power.

The inverter is mainly used as a device for varying the speed of the motor drive with the inductor motor's characteristic with a constant value of V/f. By changing line frequency (f), the speed of the motor drive is altered in the inverter's power range [8]. Also, the inverter has relay inputs and an analogue input. The relay inputs are used for switching on and off the motor. The analogue input accepts 4-20mA signals and is used for setting the frequency reference.

3.6 Sensors and Transducers

Sensors and transducers are selected for extracting the data out of the system. These data feed into the controller (described in section 3.7). So, the sensors and transducers selected preferably have digital or analogue signal output which can be stored and read by the controller. Most of chosen meters and transducers have a 4-20mA analogue signal output channel because 4-20mA analogue signal output has become commonest industrial standard due to its robust feature as compared to the 0-10V analogue signal output. Some of the meters need an output signal conditioner because they do not provide the 4-20mA output directly as it is discussed in the following section (3.6.1). Bearing this in mind, the process of the instrumentation was carried out with the equipment as specified.

3.6.1 Flow Sensor

The most significant measurement in a water supply system is the flow of water. Knowledge of flow is needed to bill customers, check the efficiency of pumps, monitor for leaks, and help control or limit the delivery of water. There are several types of flow meters commercially available such as the differential pressure flow

meter, turbine flow meter, and the vortex shedding flow meter. At this point, two turbine flow sensors were chosen due to their lower error rate compare to the other types of flow meter [10]. The sensor is constructed with PolyVinylidine DiFluoride (PVDF), which is a highly non-reactive and pure thermoplastic fluoropolymer. It is also known as KYNAR and utilises sapphire for the turbine spindle and bearing assembly which enhances the accuracy and improves long term reliability [23]. It also has connections for both 8 mm and 12 mm diameter hoses which are common fitting size for the water hose in the designed RO system (1.5cm diameter). The range of the flow this type of sensor can measure is 0.05 -9 Litre/minute which can cover the operational flow rates range in the system.

The flow passing through meters can be reflected by different frequency pulses. A frequency to current converter is connected to the signal link of the flow meter used in order to get 4-20mA current output. This selection process involved in using two signal conditioner (Frequency to voltage converter and voltage to current converter) because of the availability of the frequency to voltage converter and the high expense of a frequency to current converter (costs around US$400). Hence, one of the flow sensors has a direct connection to a frequency current converter. The output current signal (4-20mA) is fed into one of the channels on the PLC analogue input module (Discussed in section 3.7), whereas, another flow sensor is linked to a frequency voltage converter which hooks up with a voltage current converter where another PLC analogue input channel is obtained its input current signal. Because the frequency current converter and the frequency voltage were already available in the laboratory, with aforementioned scheme, a voltage (0-10V) to current (4-20mA) needs to be built by purchasing and configuring a voltage to current conversion chip. The flow rates are to be totalised in PLC register.

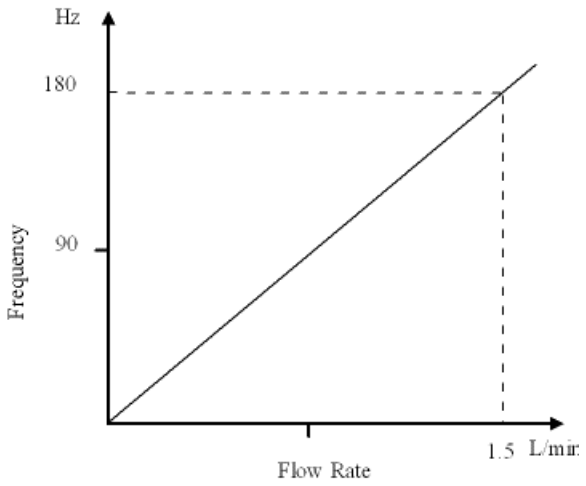

Figure 3.9 - Characteristic of the selected flow meter

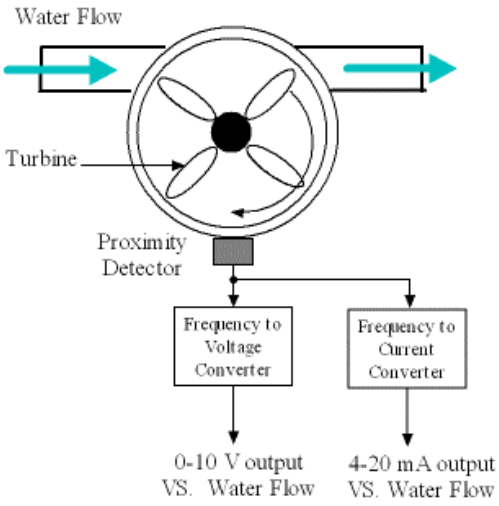

Figure 3.10 - Structure of the flow meter

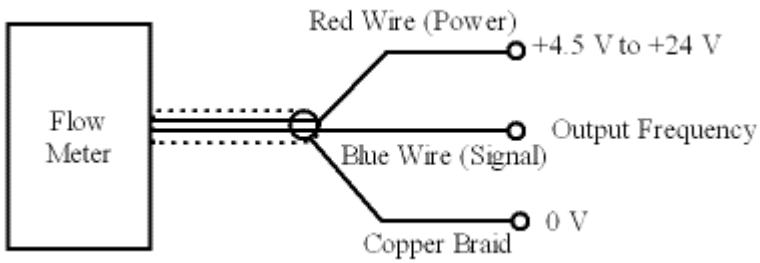

Figure 3.11 – Wiring in structure of the selected flow meter

3.6.1.1 Frequency to Current Converter

The frequency current converter is a device for indication and monitoring of periodical signals which occur in almost all areas of process automation, i.e. from frequencies in general and speeds in specific.

The input signal sequence is evaluated and converted into a frequency by a µ-controller in accordance with the cycle method. The µ-controller calculates a current proportional to the input frequency and produces it with a digital analogue converter in respect to the selected measurement range's limit value.

The analogue signals which can be selected are: 0-20mA and 4-20mA. For matching with the chosen PLC signal type, the analogue signal type of converter was selected to be 4-20mA. The pulse output produces the input frequency which is subdivided by the adjustable factor of (1-9999). The calibration was carried out by setting the minimal and maximum frequency, the flow sensors can produce into the converter.

3.6.1.2 Voltage to Current Converter

A voltage to current converter was chosen because there was only one frequency to current converter available in the laboratory, as commercial product frequency to current converter was prohibitively expensive. Therefore, a voltage to current conversion chip was purchased and configured.

Figure 3.12 shows the configuration layout of the voltage to current inverter. A n-channel MOSFET transistor was purchased to be one of the major components in this configuration. All of the components of the circuit were tested and soldered in a PCB board using drawing tool (Protel2000). This circuit board was then fixed into metal boxes with EMC (electromagnetic) shielding protection.

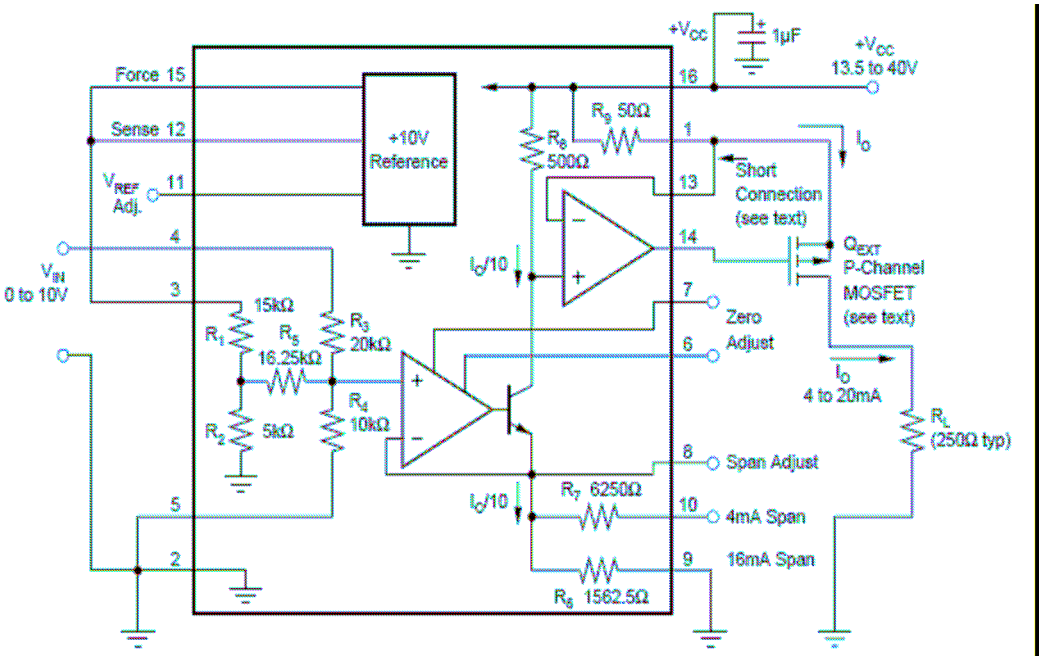

Figure 3.12 - Configuration circuit of the voltage to current signal conditioner (Source: http://focus.ti.com/lit/ds/sbos141a/sbos141a.pdf)

3.6.2 Water Level Float Switch

Water level float switches are used to alarm the system when the water level is high or low in the product tank. Using the principle of water buoyancy, float switches act as normal switches triggered by the water level and provide on and off signals to the controller to indicate the system states. When the water hits high level, the high water level will be triggered. The output signal of the switch will jump from 0 to 1. Figure 3.13 presents an image of the float switch used in this project.

Figure 3.13 – Image of a float switch (Source: http://www.smarthome.com/7197.html)

3.6.3 Conductivity meter

A conductivity meter is used to determine the salinity level in the raw water tank. This meter needs to be calibrated every time when it takes measurement. The correct reading of the conductivity will help to determine the performance of the RO system in different water conditions. In the early stage of the experiment (described in chapter 6), a conductivity meter with 4-20mA signal output was borrowed from Endress the Hauser Pty, Ltd. The reading of the feed stream conductivity was fed into PLC in analogue format, which was then stored into one of the registers. The data in this register was taken by designed HMI and put up on the computer screen.

3.6.4 Power meter

The Fluke energy meter (Figure 3.14) was selected to show the instantaneous power flow driven by the motor-pump, totalise power with respect to time and determine energy consumption over the testing period. This meter has an optical RS 232 port for data communication with computers. A software package was provided by the manufacture with this meter. This software will allow the user of the meter to monitor and record the data from meter via RS 232 port.

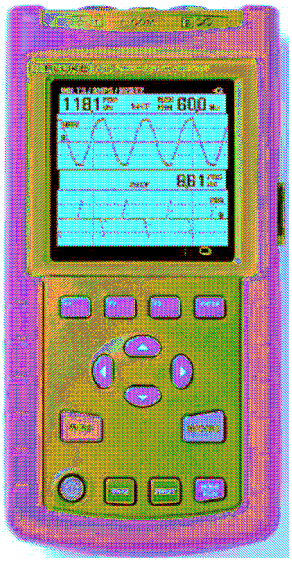

Figure 3.14 - Image of the fluke energy meter
(Source: http://au.fluke.com/auen/home/default.htm)

3.6.5 Temperature Meter

A temperature indicator helps to determine if the system is working in suitable conditions, and also assists in estimating the water productivity. In a faulty condition, it will trip the whole system. For the designed RO system, temperature was only taken into consideration but was not one of the variables of the system due to limitation of the lab instruments and the variable nature of the temperature.

3.6.5 Battery Bank State Sensor

A battery bank state sensor is used to indicate the state of charge of the batteries. This state of charge is monitored, and when the SOC (state of charge) is too low it will alarm and trip the system. In the experiment conducted in the later stage of the project, a batter bank state sensor was not part of the system because the renewable energy power supply system was purposely sized and the SOC never went lower than 60%. However, due to the important role of the battery state of the charge, a battery bank state sensor was included in the original design to show the delicate nature of the RO system.

3.7 PLC and HMI

A Koyo DL205 PLC (Programmable logic controller) is used for process control and data acquisition (Figure 3.15). Because the control logics can be programmed into this device, it makes for a flexible and powerful tool. The PLC has fixed I/O (inputs and outputs) or configurable (virtual) I/O, which is more commonly referred to as the modular PLC. The selected modular PLC consists of a back-plane with a built-in power supply, a Central Processing Unit (CPU) and the I/O modules. The back-plane facilitates the base onto which the other modules are connected to. The CPU is where the program logic is stored and executed, and is the module that a programming device connects to for downloading the program logic. The I/O modules are used to facilitate the monitoring and control of the process plant, which is configured to suit the application. The CPU gathers the required information from the I/O cards via a bus on the back-plane.

Figure 3.15 - Image of the selected Koyo PLC
(Source: http://web2.automationdirect.com/static/manuals/d2user/d2uservol1.pdf)

For the RO system, different modules were chosen to fit the signal conditions. Analogue input and output, digital input and output modules were selected. Their configurations are shown in table 3.2.

Table 3.2
Selected Modules of PLC

Module Name	Module Function
D2-06B-1	DL205 6 slot back-plane and 110/220VAC power supply
D2-260	DL260 CPU (with built-in PID loop capability)
H2-ECOM	Ethernet module for communications to the HMI and programmer
D2-16ND3-2	16 channel 24VDC digital input module
F2-08AD-1	8 channel 4-20mA analogue input module
D2-08TR	8 channel 5-30VDC or 5-240VAC relay output module
F2-02DA-1L	2 channel 4-20mA analogue output module

A Human Machine Interface (HMI) is typically a personal computer (PC) connected via a communications link to the PLC to aid in process visualisation allows the monitoring and control of the process [10]. This process control via an operator interface is also known as Supervisory, Control and Data Acquisition, or SCADA. Control functions such as starting pumps and controlling inverter speed can be done via onscreen pushbuttons or direct set-point entry respectively. Process alarms such as pump faults and low flows can be logged and alarmed for later analysis of faults or events. Analogue values such as tank levels and flows can be monitored over a period

of time by using trend charts. Citect SCADA HMI is used for this project. Below is the screen shot of the graphic builder of Citect SCADA.

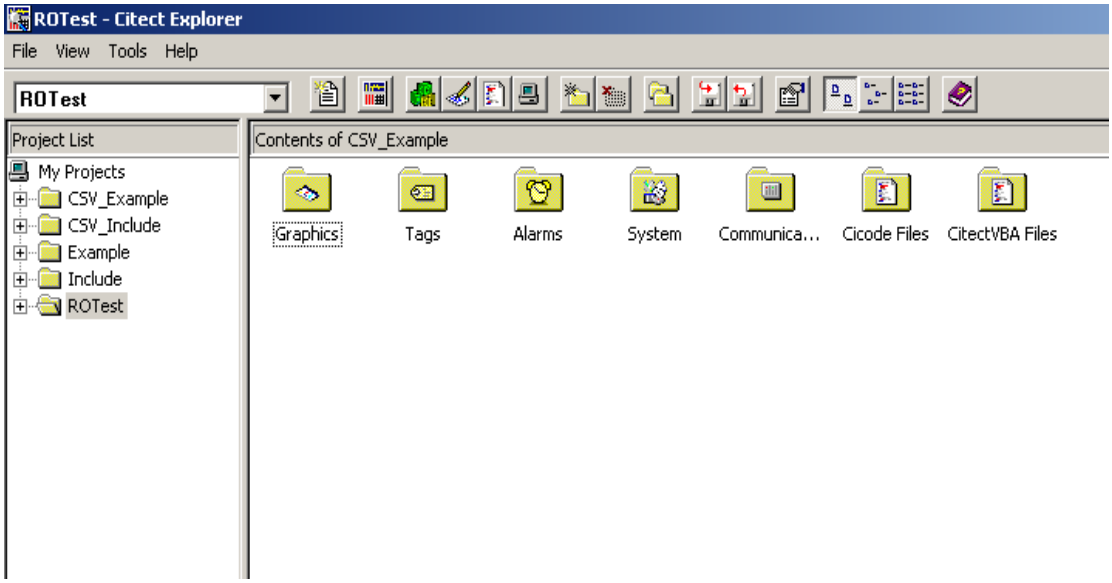

Figure 3.16 Screen shot of the Citect graphic builder

3.6.1 Ethernet Communication

The PLC can communicate with the HMI application on the PC via RS232C port by means of the host link protocol [2]. However, Ethernet is used as the main communication method because of its greater connection speed and its ability to communicate over longer distance. Whereas RS232C is a point to point connection, where there is only one master and one slave unit. Ethernet enables multi-drop network, where there can be one master and multiple slave units.

3.6.2 Telemetry

A remote monitoring system can also be implemented using GPRS (General Packet Radio Service communication) which is a new area being exploited in PLC remote control field. A VPN (Virtual Private Network) was established between the remote PLC Controller and the PC through the public mobile internet service (Figure 3.17, 3.18, and 3.19). A Local IP address was assigned to the PLC control, and also to the GPRS router. A public IP address was allocated to the GPRS router once after it was logged on the internet through the mobile network. Private keys were used for both ends of the transmission link in order to secure the system information from

being stolen. The Information Packet (data) is transported via the Ethernet port in TCP/IP protocol. This enables transfer rates of up to 100K/s.

Therefore, with the greater flexibility, system operators will be able to change PLC codes, check errors, and log data in real time wherever the GPRS service is accessible. GPRS remote control reduces the noise effect and hazard to the locals, for the RO system can generate extensive amounts of noise. It also gives the operators extra rooms for monitoring the system by remote data logging. With outstanding convenience of the communication method, remote data logging can be done any place where internet services are available. The explicit configuration of the Sarian MR2110 GPRS router can be found in appendix.

Figure 3.17 Photo of the selected GPRS router

Figure 3.18 Photo of the selected GPRS mobile phone (blackberry)

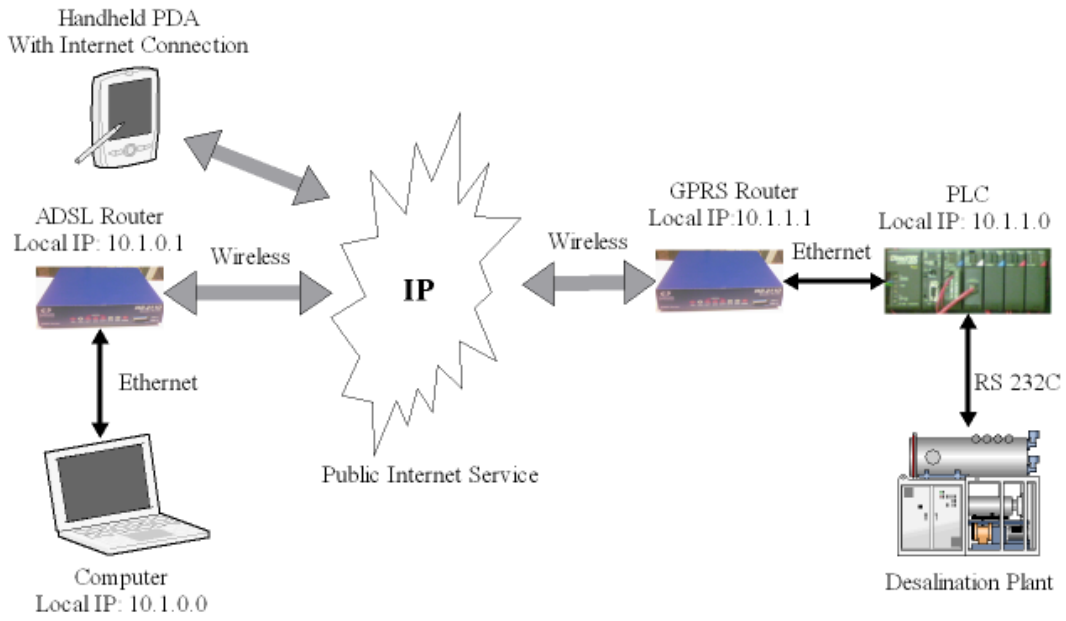

Figure 3.19 - Configuration of the telemetry via GPRS network

3.7 References

[1] Nayar C. V., Phillips S. J., James W. L., Pryor T. L., and Remmer D., "Novel wind/diesel/batter hybrid energy system." *Solar energy*, vol. 51 pp. 65-78, 1993.

[2] Tzen, E., Theofilloyianakos, D., *Design and development of a hybrid autonomous system for seawater desalination*, Desalination 166 (2004) 267-274.

[3] Ahmed N., *Application of a PAPS for the Maldives*. Perth: Masters Thesis, Curtin University of Technology, 2005.

[4] CITOR, Instruction Manual-Designator, Perth, 2005.

[5] Ashari M. and Nayar C. V., "An optimum dispatch strategy using set points for a photovoltaic (PV)-diesel-battery hybrid power system," *Solar Energy*, vol.66, 1999.

[6] DL205 User ManualVolume 2, Automationdirect.com Incorporated, http:// www.Automationdirect.com [accessed 2005].

[7] Citect HMI, Manual of the SCADA, http://www.citect.com/products-and-services/citect-hmi.html [accessed 2005].

[8] Hisham T., *Fundamentals of Salt Water Desalination*, Elsevier Science B.V., New York, 2002.

[9] Data sheet, XTR110 Voltage to current converter, http://focus.ti.com/lit/ds/sbos141a/sbos141a.pdf, [accessed 2005].

[10] Specification sheet, liquid flow sensor duel range, RS Components Pty Ltd, 2005.

[11] Specification sheet, Sarian MW3520, West Yorkshire, 2006.

[12] Application note 21, Configure a Sarian to be an L2TP over IPSEC VPN server, West Yorkshire, 2006

CHAPTER 4 SYSTEM COMPONENTS MODELING

In this chapter, procedure of RO system modeling is presented in forms of various mathematic models as well as the Matlab models built according to the data acquired from the preliminary tests. System components characteristics were depicted and plotted. Model of the RO membrane and power consumption of the system were created in Simulink (A binding product of Matlab).These Simulink Models were tested in the operation range of the system components. The simulation results were charted and analyzed.

4.1 Component Modelling and Data Fitting

The initial strategy for processing the experimental data from a number of the components, as part of the determination of the sub-models, was to use the polyfit function in Matlab [7]. This routine is useful for discovering complex polynomial relationships between two variables, but that is also its main limitation. Since many of the components in the system have variables that depend on more than one input variable, an alternative procedure was sought.

4.1.1 Modelling Procedure

It was noticed that even for the single input-output system, the adoption of a more flexible modelling procedure that is the one that was not based merely on polynomial relationships could be helpful for reducing the curve fitting errors.

A more refined modelling procedure was applied instead, which considered the influence of more than one variable on any other variable. This procedure, referred to as “Linear-in-the parameters Multiple Regression”, is described [1]. It was also implemented in Matlab and consists of a data regression routine, which fitted the data

points to a predefined non-linear relationship, through least-squares error minimization. To calculate the coefficients of a predefined non-linear model, the further deduction is needed, as explained below.

For instance, to calculate the relationship between an output variable, Y_1, and two input variables, X_1 and X_2, the following non-linear model (linear-in-the-parameters) can be defined:

$$Y = f(X_1, X_2) = k_1 + k_2 X_1^n X_2^n + k_3 X_1^{n-1} X_2^{n-1} + \cdots\cdots + k_{n-1} X_1 X_2 \qquad (4.1)$$

Where

Y_1 is the variable wanted as the model input;

X_1 and X_2 are the variables used as the model inputs.

For example, in the RO unit specified in chapter 3, the flow rate of permeate is Y_1; the frequency of supply power is X_2, and the conductivity of the feed water is X_1. Y_1 varies in accordance with the variations of X_1 and X_2. Usually, this relationship can be revealed by a three dimensional chart. This means the output water flow rate can be plotted with respect to the power supply frequency X_2 by using the polyfit function. A string of equations can be produced because of different conductivity levels.

Of all the equations generated from the original experimental data set, relationships amongst their coefficients in can be discovered by comparing their correspondent curves. The final non-linear equation of polynomial can be inferred if there is any relations can be found amongst those coefficients.

The RMS error between the original data and the model fit would be calculated, and if needed, the target non-linear relationship adjusted, giving a different target equation. An RMS error of less than 5% was used as a guideline for the suitability of the data fitting. This tolerance was obtained for most of the derived models [7].

Another guideline used was the overestimated system warning that Matlab would produce if the data matrix were rank deficient, i.e. if it did not have linearly

independent columns. This indicated that the established non-linear model was not suitable and a different target matrix X would be chosen.

4.1.2 Components Models

The purpose of modelling the components individually was to gain their characteristics within the expected range of operation of each component during the operation of the system. All the components were tested and the models established for operation within the testing range. The models are not guaranteed to work outside the test range and although this approach may limit the applicability of the models in other applications, it was found to be satisfactory in the scope of this work.

The inverter used in the system is a standard commercialised inverter for its convenience of manipulation and low price. Its work principle is V/f adjustment which were tested and plotted, and the efficiency curve of the inverter was discovered by comparing the input power and output power. This curve was fitted in Matlab in order to find its mathematical equation which was used in modelling the system efficiency subsystem.

The pump used in the system is a high pressure rotary vain pump, it was expected that the flow rate and developed pressure would be directly related to the rotational speed and applied shaft torque. The water was considered as incompressible, hence, the pump modelling was of a direct input and output relationship. As it is connected to a three phase induction motor, the output water flow rate of the pump follows the dynamics of the motor's speeds.

The RO membrane model and parameters were obtained from the manufacturer's specification sheets. From previous investigations (discussed in chapter 2) regarding the RO membrane characteristics, it is predicted that the permeate flow rate will increase as the applied pressure across the membrane ramps up. The change of the permeate flow rate will be nearly linear to the variations of the feed water conductivity [2]. At the later stage, preliminary experiments were conducted and the characteristic of the membrane was plotted and formulated. Reverse osmosis membrane model was built in Matlab using the data collected during the experiments. This will be discussed in the following sections.

The RO system power consumption was trended with respect to the motor frequency during the preliminary experiments. Matlab model of the total energy consumption was established and simulated in Matlab.

4.1.3 Simulation Method

The MathWork' software package Matlab contains a simulation tool-Simulink. It is a type of graphical programming language that is capable of providing a programming environment in which mixed continuous and discrete systems can be simulated [7]. This makes it suitable to implement, test and evaluate the proposed RO system. Simulink includes a comprehensive library that provides many function blocks. These functions block can be imported into the project window and programmed to be able to interact with other function blocks. Particularly, one of the function blocks is called *user defined function*; it allows system transfer functions to be stored in the format of mathematic equations. This feature largely eases the procedure of the modelling for the RO system.

Simulink also allows for the division of a simulated system into a number of subsystems [8]. These subsystems can be modelled and tested individually and then interconnected later. This makes great convenience to build the subsystems such as reverse osmosis membrane, power consumption, product water tank and control systems.

After the components are assembled, the whole system can be simulated over an unlimited time. The simulated results can be exported to Matlab's database by defining a workspace (i.e. a function block allows to store the data into Matlab database) and connecting it to the output of the system. These data are saved in array format and can be plotted out by using *plot* command in Matlab console window. Meanwhile, an oscilloscope function block and discrete display function block can be attached to any interconnecting line to monitor the corresponding signal's behaviour. This gives a quick overview and examination over the constructed systems [1].

Another useful feature of Simulink is *Mask* that enables the user to reduce the number of input dialogue boxes of the model. This is achieved by wrapping the boxes into a subsystem. Hence, users will not have to open each block in the subsystem and

enter the parameters every time, instead, key in the values on the mask dialog block. These values will be automated passed on to the function blocks in the subsystem. This advances the modelling for the RO system and simplifies the simulation procedures.

4.2 Variable Speed Inverter

4.2.1 Working Principle

Because, an off the shelf inverter is chosen for the system, the internal control strategy of this inverter is unknown. For this reason, the thesis does not include great details of the inverter itself but and test results in terms of the V/f chart as well as a brief introduction about the theory of single phase to three phase conversion.

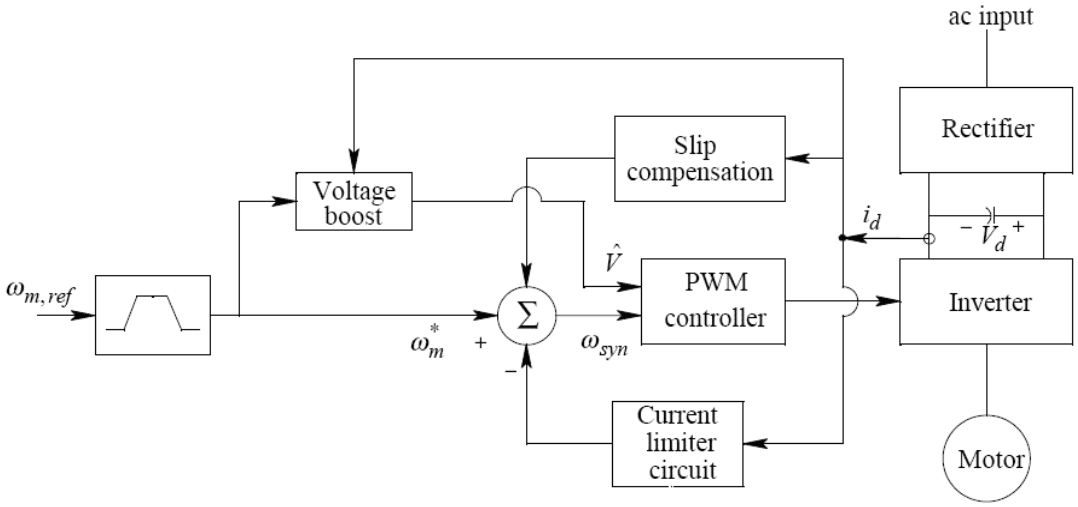

Figure 4.1- Overview of inverter speed control (Source: Mohan, N., 2003)

The inverter is used for controlling the speed and torque of the electric drive. It regulates its output voltage and frequency by using PWM (pulse width modulation). Shown in figure 4.1, PWM is generated by an internal controller that usually contains a sine wave generator or square ware generators depending on its features for functionality. Applying the relation of V/f, the flux density inside of the motor is maintained regardless the variations of motor speed. With this fundamental variable speed principle, inverters can change the operation power intake and speed of the motor drive.

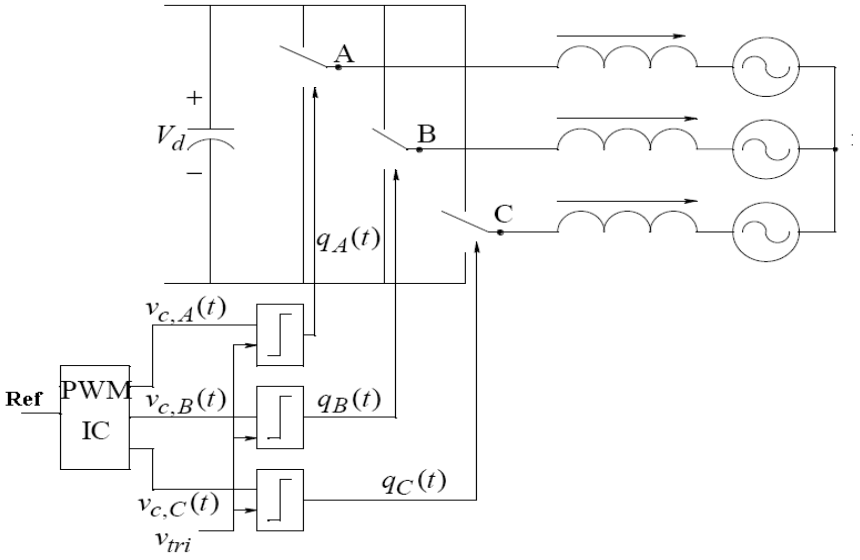

Figure 4.2 - PWM regulations for speed control (Source: Mohan, N., 2003)

From the data obtained in RO motor tests, the V-f characteristics was discovered and can be seen in figure 4.3, the relationship between motor frequency and line to line voltage of this inverter was plotted, which keeps linear from 20 to 50 hertz with each load conditions (different feed water conductivities). The curve starts becoming levelled around 50 Hertz. This phenomenon reveals the voltage constraint (270V) for this type of inverter [3].

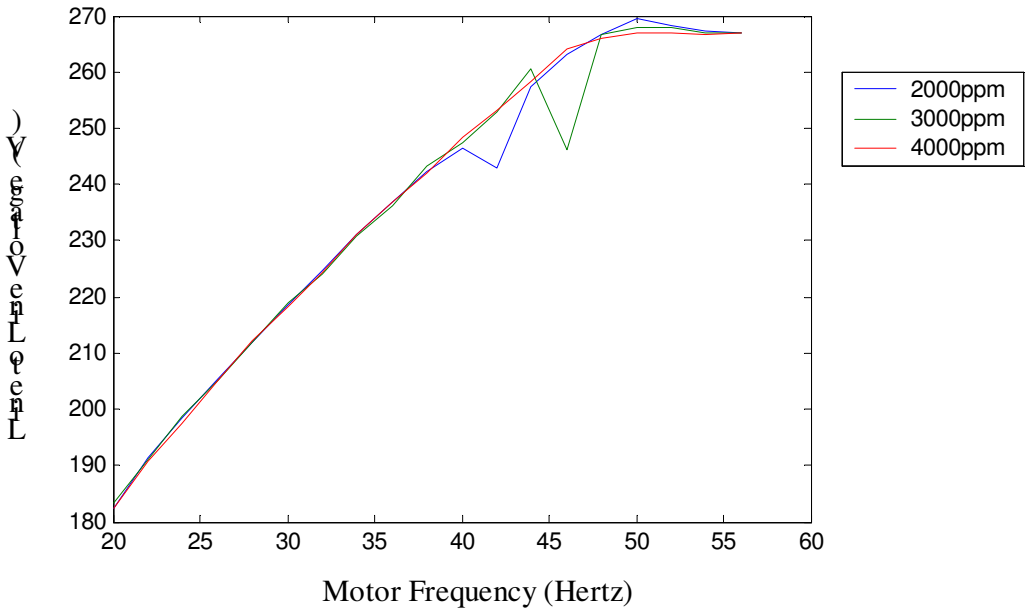

Figure 4.3 - The curve of the V/f

4.2.2 Matlab Model for the Inverter

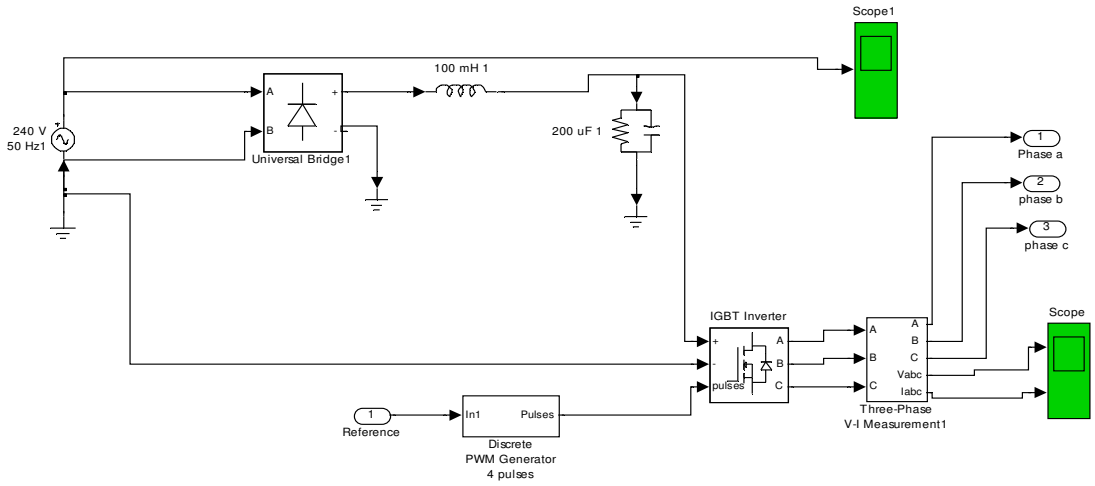

Figure 4.4 - Simulink Model of the inverter

Several function blocks (such as IGBT inverter, universal bridge, and low-pass filter) were used in the model of the inverter. The basic route for power flow is illustrated as meanwhile can be seen in figure 4.4. Single phase AC current is rectified to be DC current, which then is converted to be three phase AC current through high speed switches (transistors) controlled by the PWM signal generator. A reference signal is required for the signal generator to set up the certain values for the line to line voltages and frequencies which lead to motor speed variations.

4.3 Motor-pump

The combination of the motor-pump is the driven force in the RO system. It is found more straightforward to characterising them altogether than individually. Hence, the aim of the motor pump modelling is to establish a mathematic model according to the empirical data and find the relation between the electrical and fluid energy as well as the correlation between the motor frequency and the RO system power consumption.

4.3.1 Mathematical Model of the Motor-Pump

For the rotary vain high pressure, the flow rate at the inlet of the membrane is proportional to the rotational speed of the motor [4], which can be given by:

$$K_p \times N_m = Q_p \tag{4.2}$$

Where

N_m is rotational speed of the motor-pump, rpm (revolution per minute);

Q_p is the flow rate at the inlet of the membrane, litres/minute;

K_p is the co-efficiency of the motor-pump combination.

The power that is delivered by the motor-pump is given by [5]:

$$P_{m+p} = T_m \times \omega_m \times Eff_{m+p} \tag{4.3}$$

Where

T_m is the torque of the motor, N/m;

ω_m is the rotational speed of the motor-pump, rad/s;

Eff_{m+p} is the efficiency of the motor-pump.

The power that is imparted to the liquid by the motor-pump is [4]:

$$P_{liquid} = \frac{Q_p \times p_d}{36} \times 1000 \tag{4.4}$$

Where

Q_p is the flow rate at the outlet of the pump, litres/h;

p_d is the pressure differential across the pump, kPa;

As $P_{m+p} = P_{liquid}$, which gives the equation:

$$T_m \times \omega_m \times Eff_{m+p} = \frac{Q_p \times p_d}{36} \times \frac{1000}{3600} \tag{4.5}$$

Substitute equation [1] into [4]

$$T_m = \frac{K_p}{129.6 \times Eff_{m+p}} \times p_d \tag{4.6}$$

Since,

$$p_d = p_{p,out} - p_{p,in}, p_{p,out} - p_{pipe,loss} = p_{m,in} \tag{4.7}$$

Where

$p_{p,in}$ and $p_{p,out}$ are the water pump inlet and outlet pressure, respectively;

$p_{m,in}$ is the pressure of the inlet stream of the membrane, kPa;

$p_{pipe,loss}$ is the pressure loss in the water pipe, kPa.

Meanwhile, the length of the water pipe in the actual RO unit is small, so the pressure loss $p_{pipe,loss}$ is negligible.

Hence the relationship between the motor torque and inlet water pressure of the membrane is:

$$T_m = \frac{K_p}{129.6 \times Eff_{m+p}} \times (p_{m,in} - p_{p,in}) \tag{4.8}$$

4.3.2 Matlab Modelling for the Motor-Pump

4.3.2.1 Characterization of the water flow rate

From the motor-pump test, data relates to characteristic of motor speed and flow rate of the pumped water were retrieved and plotted. By using data fitting function, an equation was generated within minimal error range.

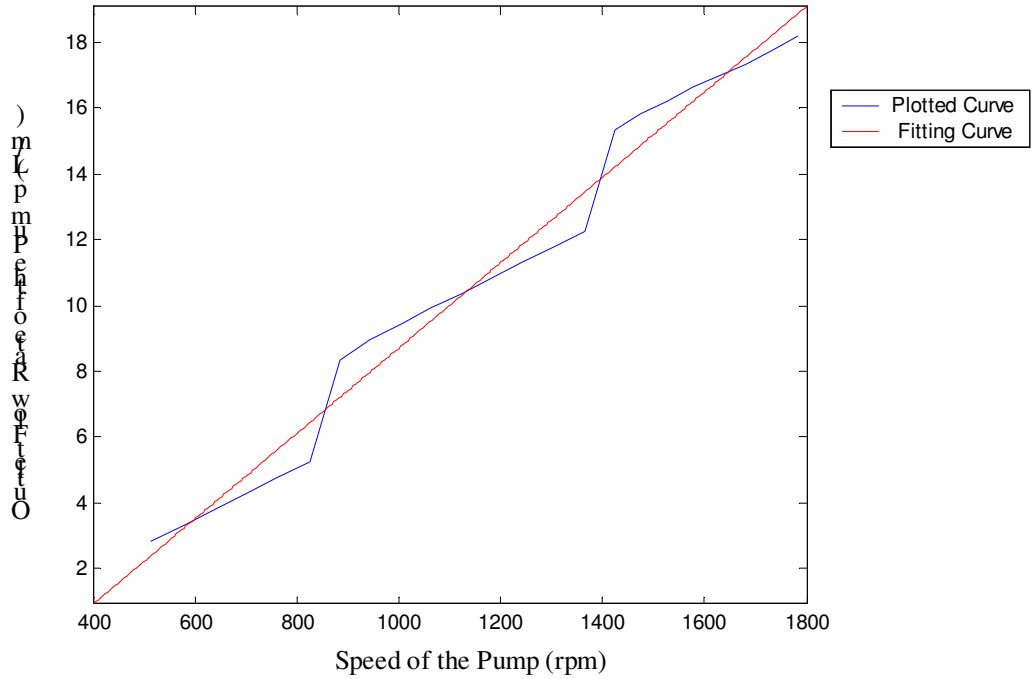

Figure 4.5 Data plotting and fitting of the outlet flow rate of the pump with respect to the pump speed

As can be observed in figure 4.5, fitting curse thread through the sample points, consequently, an equation was derived and given by:

$$Q_p = 0.012 \times N_m - 4.3 \tag{4.9}$$

Where

N_m is rotational speed of the motor-pump;

Q_p is the flow rate at the inlet of the membrane.

4.3.2.2 Efficiency of the Motor-pump

The efficiency of the motor-pump is another factor would influence the performance of the RO system. The higher efficiency can offer greater water delivery ability to the motor-pump. Another test was carried out in the aim of obtaining the efficiency curve of the motor-pump combination.

Table 4.1

Essential parameters for the motor-pump efficiency test

$100kPA \approx 10m$ static head
Gravitational constant $9.8m/s^2$

The hydraulic power required to pump water to the certain head is determined by the following equation [6]:

$$P_{HYD} = m \times g \times h \tag{4.10}$$

Where,

m is the mass flow rate of water, litres/second;

g is the gravitational constant, 9.81;

h is total head of the water, meter.

The motor power derived from the renewable energy power supply system through the variable speed inverter can be calculated by the following equation:

$$P_{MOT} = V_{MOT} \times I_{MOT} \tag{4.11}$$

Where,

V_{mot} is the voltage across the motor, V;

I_{mot} is the current goes in the motor, A.

Then, the efficiency of motor-pump combination unit can be characterised by the following efficiency expression:

$$Eff_{m+p} = Eff_m \times Eff_p = \frac{P_{HYD}}{P_m} = \frac{m \times g \times h}{V_m \times I_m} \tag{4.12}$$

From the test data, the efficiency curves are plotted with feed water conductivity 2000 and 3000 respectively. It can be noticed that there is not significant discrepancy between those two curves, indicating that the feed water conductivity is not the parameter having influence on the motor-pump efficiency.

Although curves show that the efficiency of motor-pump change in an unexpected way, i.e. step up at certain motor frequencies, it helps to know the characteristics of the motor-pump. Meanwhile, Observed in figure 4.6, the possibility of maintaining the water flow rate by providing less motor frequency can be anticipated. Less power will be consumed by the motor when the supply frequency is reduced (seen in figure 4.7)

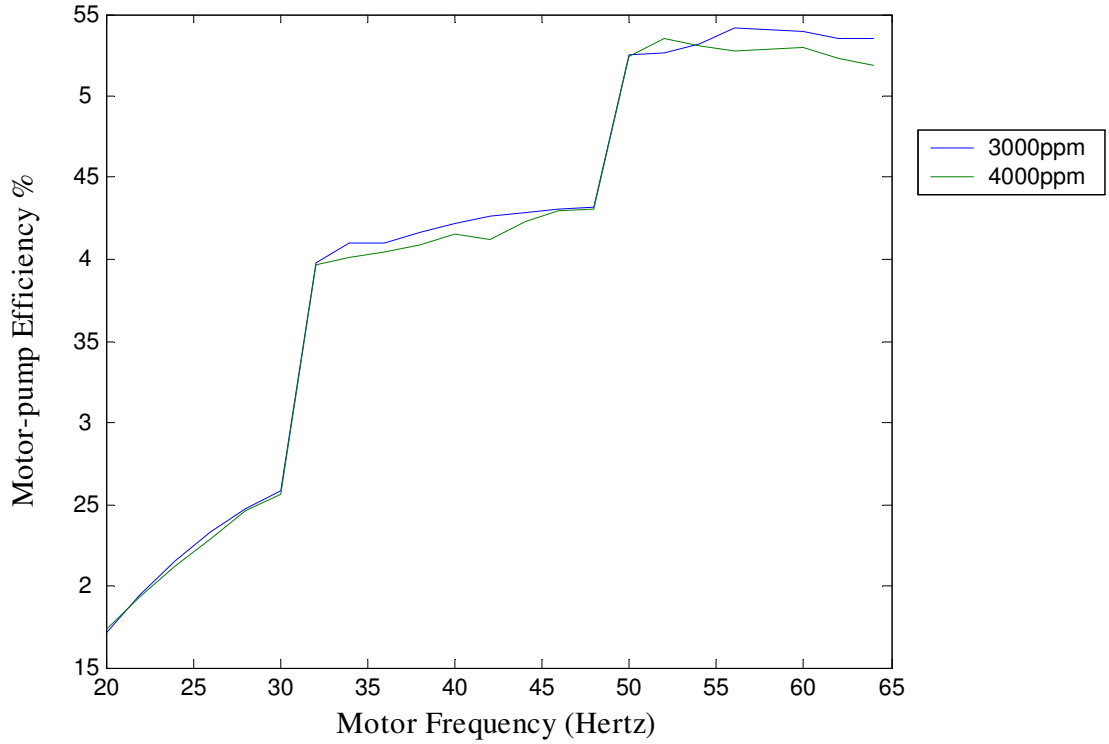

Figure 4.6 - Motor-pump Efficiency vs. the Motor Frequency

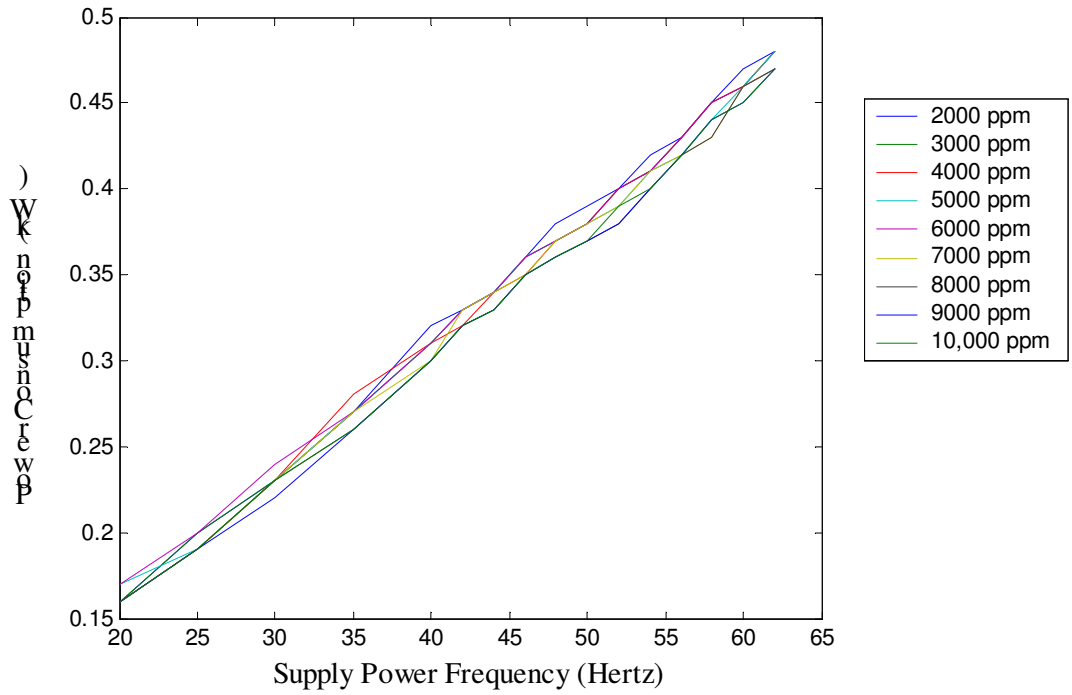

Figure 4.7 - Power Consumption vs. Supply Power Frequency

4.3.2.3 Matlab Model of the Motor-Pump

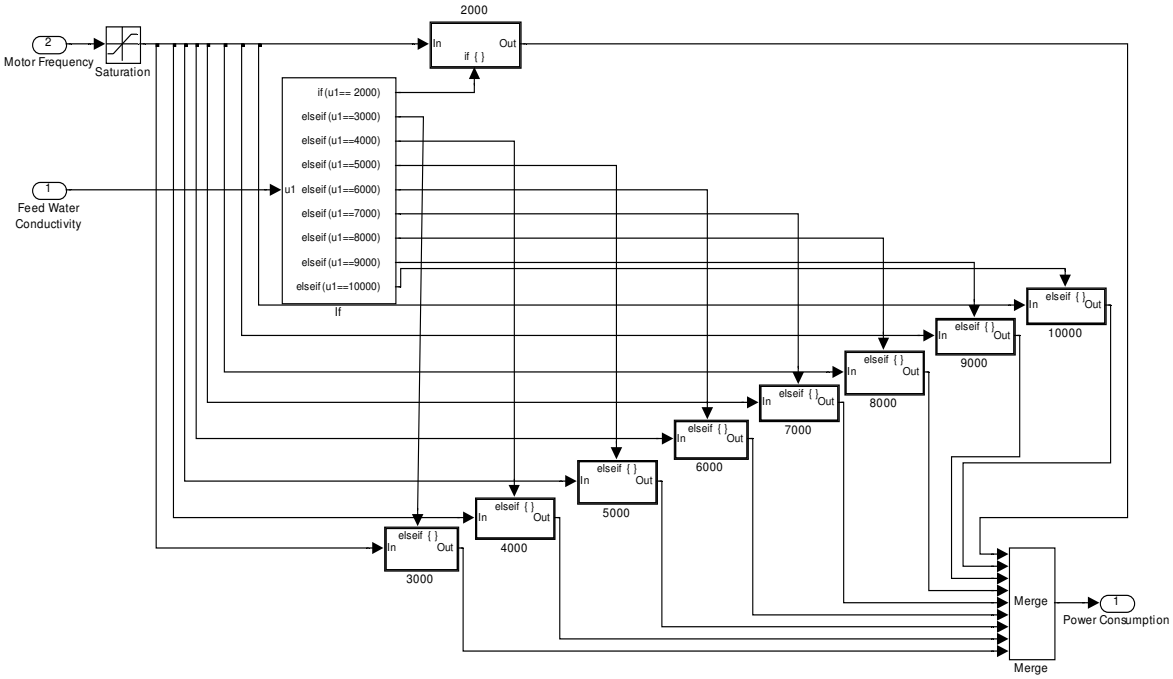

Figure 4.8 - Simulink Model of the Total Power Consumption of the System

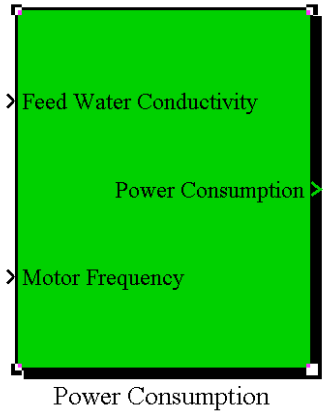

Figure 4.9 - Mask of the Simulink Model of the Total Power Consumption

A subsystem about the power consumption of the RO system was built in Simulink. A *if* function block was used to create an auto-selector for different condition where the feed water conductivity varies from 2000 to 10000ppm. Each condition leads to a scenario in which an action was taken according to the input of its function block. This subsystem was masked and placed together with other subsystems (will be described in the following sections). Every time before the simulation, the feed water conductivity shall be entered by clicking on its subsystem dialogue block.

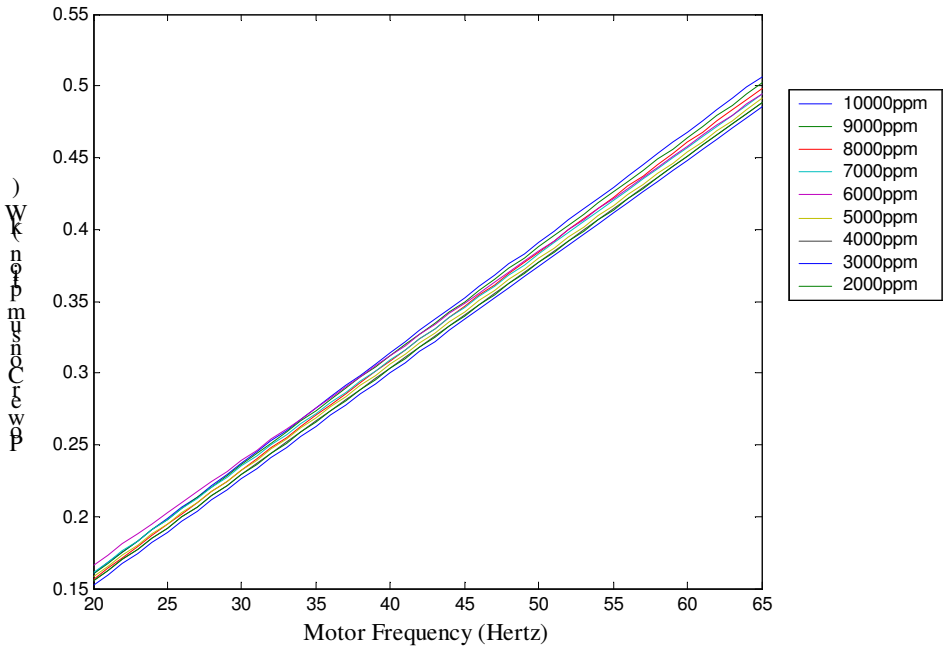

Figure 4.10 - Simulation Results from the Simulink Modelling

4.4 Reverse Osmosis Membrane Modelling

The modelling of the reverse osmosis membrane was carried out from depicting the mathematical model for the membrane. Then, a series of experiments were conducted. After that, with the experimental data, the characteristics of the membrane was visualised in Matlab. Its transfer function was discovered with two input variables, using data fitting function in Matlab.

4.4.1 Mathematical Model of the Membrane

4.4.1.1 Osmotic and Operating Pressure

The osmotic pressure, π, of a solution can be determined experimentally by measuring the concentration of dissolved salts in the solution. The osmotic pressure is represented by the following equation [9].

$$\pi = RT \sum X_i \tag{4.10}$$

Where

π is the osmotic pressure , kPa;

T is the temperature, K;

R is the university gas constant, 8.314 kPa $m^3 / kgml$ k;

$\sum X_i$ is the concentration of all constituents in a solution , $kgmol / m^3$.

An approximation for π may be made by assuming that 1000ppm of Total Dissolved Solids (TDS) equals to 75.84 kPa of osmotic pressure [9].

When the operation pressure is set equal to the sum of the above resistances the net permeate flow rate across the membrane would be minimal or equal to zero. Therefore, the operation pressure is set at higher value in order to maintain economical permeate flow rate.

4.4.1.2 Permeate Mass and Salt Balance

$$M_f = M_p + M_b \tag{4.11}$$

$$X_f M_f = X_p M_p + X_b M_b \tag{4.12}$$

Where

M_f is the feed stream flow rate, kg/s;

M_p is the permeate flow rate, kg/s;

M_b is the brine flow rate, kg/s;

X_f is the feed salinity, kg/m^3;

X_p is the permeate salinity, kg/m^3;

X_b is the brine salinity, kg/m^3.

4.4.1.3 Water transport

Rate of water passage through a semi-permeable membrane

$$M_p = (\Delta p - \Delta \pi) \times K_w \times A \tag{4.13}$$

Where

M_p is the rate of the water flow through the membrane, Kg/s;

$\Delta \pi$ is the osmotic pressure differential across the membrane, kPa;

K_w is the water permeability coefficient;

A is the membrane area, m^2;

Δp and $\Delta \pi$ represent the net hydraulic and osmotic pressure differential across the membrane, respectively.

$$\Delta p = \overline{p} - p_p$$

$$\Delta \pi = \overline{\pi} - \pi_p \tag{4.14}$$

Where

p_p and π_p are the permeating hydraulic and osmotic pressure, respectively, kPa;

$\overline{p}$ and $\overline{\pi}$ are the average hydraulic and osmotic pressures on the feed side, respectively, kPa.

And they are given by:

$$\overline{p} = 0.5(p_f + p_b)$$

$$\overline{\pi} = 0.5(\pi_f + \pi_b) \tag{4.15}$$

Where

p_f and π_f are the hydraulic and osmotic pressure of the feed stream, respectively, kPa;

p_b and π_b are the hydraulic and osmotic pressure of the reject stream, respectively, kPa.

4.4.1.4 Salt Transport

The rate of salt flow through the membrane is defined by

$$M_s = (\overline{X} - X_p) \times K_s \times A \tag{4.16}$$

Where

M_s is the flow rate of salt through the membrane, kg/s;

K_s is the membrane permeability coefficient for salt;

$M^3/m^2 s$. X_p is the permeate total dissolved solids concentration , kg/m^3;

A is the membrane area, m^2.

$$\overline{X} = \frac{M_f X_f + M_b X_b}{M_f + M_b} \tag{4.17}$$

Where

X_f and X_b are the feed and reject salt concentrations, ppm.

Equation (13) and (16) show that:

- Water flow rate through membrane is proportional to net driving pressure differential $(\Delta p - \Delta \pi)$ across the membrane [9].
- Rate of salt-water flow is proportional to concentration differential across the membrane $(\overline{X} - X_p)$ and is independent of applied pressure [9].

The fact the water and salt have different mass transfer rates through a given membrane creates the phenomena of salt rejection, no membrane is ideal in the sense that it absolutely rejects salts; rather the different transport rates create on apparent rejection. Equation 4.13 and 4.16 displays that increasing the operating pressure will increase water flow without changing salt flow, thus resulting in lower permeate salinity.

4.4.2 Characteristic of the Reverse Osmosis Membrane

In previous section, the mathematical equations are used for reverse osmosis membrane to give fundamental ideas. However, more illustrations are needed to characterise the RO membrane. Similarly to the testing that carried out on the motor-pump, the membrane testing consisted of assessing the performance of the motor-

pump and gathering the information while the electric drive is in steady-state operating conditions.

The feed stream characteristics changed in the tests. They were: pressure, flow, and conductivity. Worth to mention that the feed water temperature was not taken into consideration during the tests due to the steady feature of the temperature (i.e. always around 25^0C while the testings were carried out) over long period (8 hours). But, more information about this interesting point will be briefly presented in chapter 7 and reserved for future exploration in this field where the variations of the feed water temperature will effect on the output water of the RO membrane.

The RO membrane characteristics were shown in figure 4.11 and 4.12. It is found that the permeate flow rates is proportional to the motor frequency. Especially when the motor frequency is above certain values, e.g. beyond 30 Hertz, the inlet flow rate of the membrane starts curving when the feed water conductivity is 1000ppm. However, the relation between feed stream conductivity and permeate flow is almost linear when the motor frequency is set as fixed value. And all those linear curves are in parallel (refer to figure 4.12).

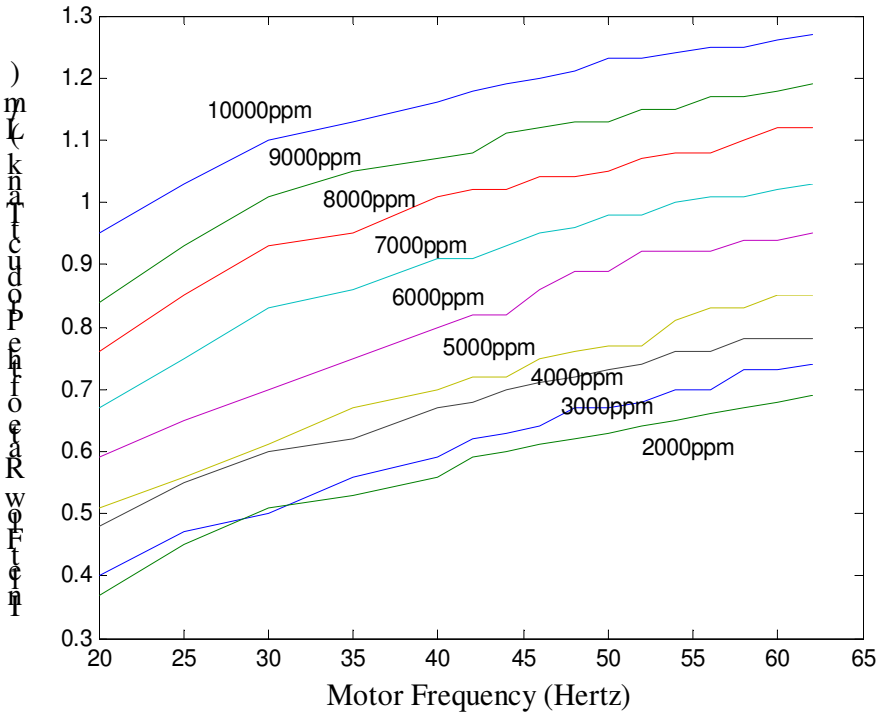

Figure 4.11 - Inlet flow rate of the product tank vs. motor frequency

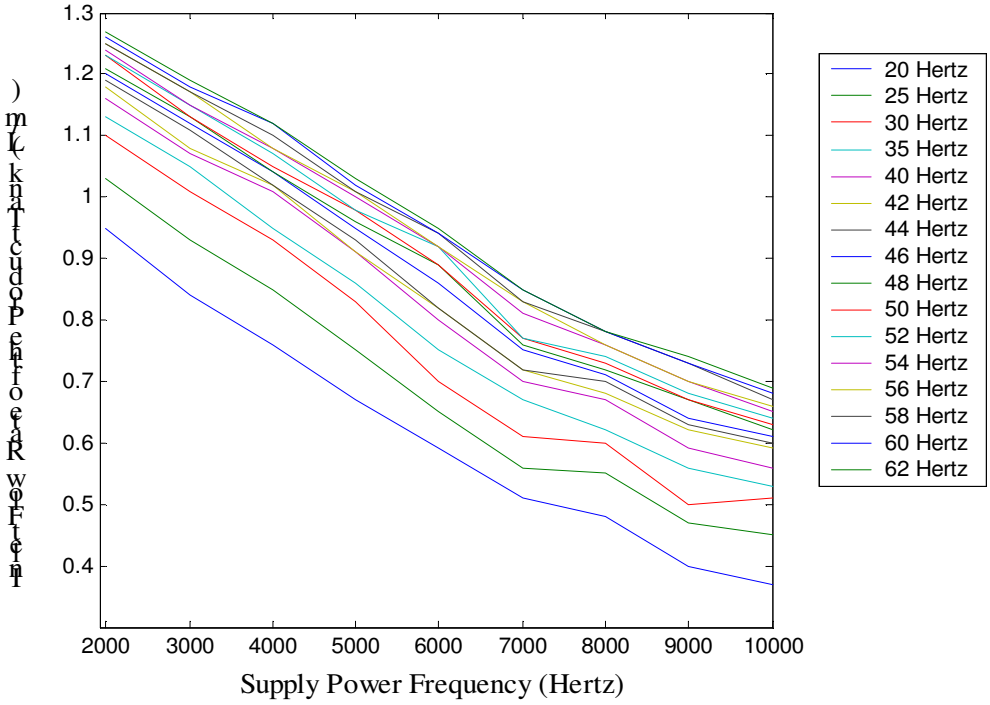

Figure 4.12 - Inlet flow rate of the product tank vs. supply power frequency

4.4.3 Matlab Model of the Membrane

4.4.3.1 Data Fitting and Equation Generation

Using 3-D plot function in Matlab, the relation amongst permeate flow rate and motor frequency was visualised in the larger extent, characterization of the membrane was further articulated (figure 4.13). The work of finding an appropriate equation for interpreting the membrane performance is largely benefited by those graphical data aforementioned.

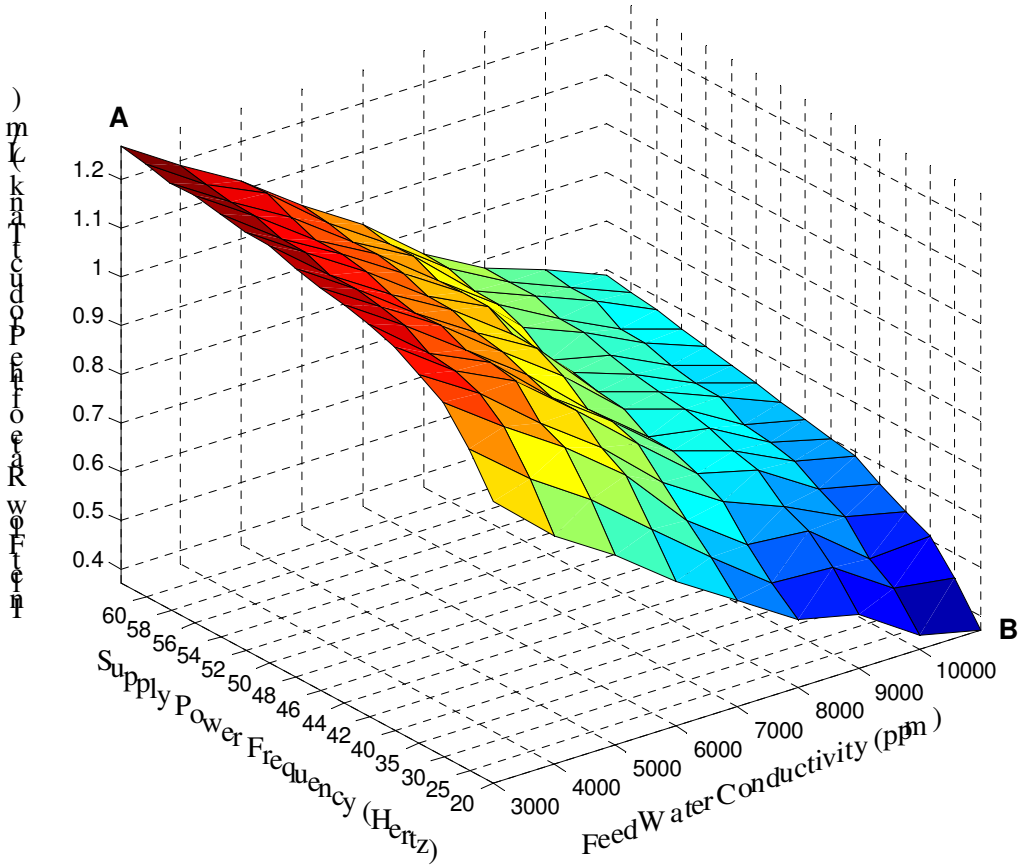

Figure4.13 - Inlet Flow Rate of the Product Tank corresponding to Motor Supply Power Frequency and Feed Water Conductivity

Modelling the water permeation process through a semi-permeable membrane is not a simple task and relationships between variables are far from obvious. Surely, the equation produce in the format of polynomial will not be the only one that can represent semi-permeable membranes, but amongst the one tested; it was the one which provided the best matching between the measured data and model outputs. And this relation can be represented in form of the mathematical equation shown as below.

$$Y_p = k_1 X_1^3 + k_2 X_1^2 + k_3 X_1 + k_4 X_f + k_5 \tag{4.18}$$

Where

Y_p is the permeate flow rate, litres/minute;

X_1 is the motor frequency, Hertz;

X_f is the feed water conductivity, ppm;

k_1, k_2, k_3, k_4 are the coefficients of the variables.

From the characteristics of the membrane revealed in figure 4.11, by using the polyfit function in Matlab, the relations amongst the motor frequencies and permeate flow rates are discovered within different feed water conductivities. The values of coefficients k_1, k_2, k_3, k_4, k_5 and a constant were recorded from each generated equation. For the error's rate the fitting shall be kept minimal, the mean values of k_1, k_2, k_3, k_4 were selected and listed as below.

Table 4.2
Mean value of the coefficients

Name of the coefficients	Mean value of the coefficients
K_1	0.0002
K_2	-0.0067
K_3	0.0824
K_4	-0.000071
K_5	0.98

Figure 4.12 shows that the product flow was in a linear relation with the feed water conductivity. This means there was a possibility of inferring an equation for each individual coefficient. To apply this idea, data fitting function was used; the equations were produced and substituted into the equation 4.18. And the final equation for the membrane productivity with respect to the motor frequency and feed water conductivity is presented that consists of two input variables in form of 3rd order polynomial and is given as:

$$Y_p = 0.0002X_1^3 - 0.0037X_1^2 + 0.0824X_1 - 0.000071X_2 + 0.98 \quad (4.19)$$

Where

X_1 is the motor frequency, Hertz;

X_2 is the feed water conductivity, ppm.

4.4.3.2 Simulation of the Membrane Performance

As shown in figure 4.14, using the generated equation 4.19, the functions blocks were created to represent the equation. Those blocks are available in *math operation* category. A *clock* function in *source* category was chosen to give a constant rising input values from 0-16. These values, then, were used to be as motor frequency that is input into the RO system. In reality, the variation of motor frequency spans from 20 to 65 Hertz. Thus, the inverter output frequency needs scaling utilising the equation given by:

$$U=0.36\times F - 6.11 \tag{4.20}$$

Where

U is the scaled frequency that varies from 1 to 16 Hertz;

F is the actual motor frequency that varies from 20 to 65 Hertz.

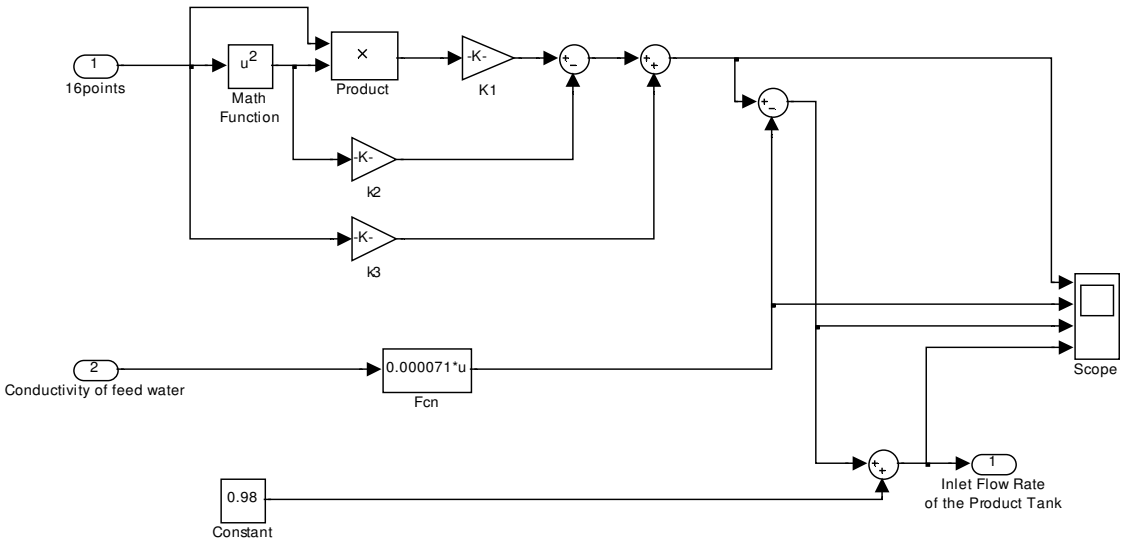

Figure 4.14 – Simulink representation of the product flow dynamic model

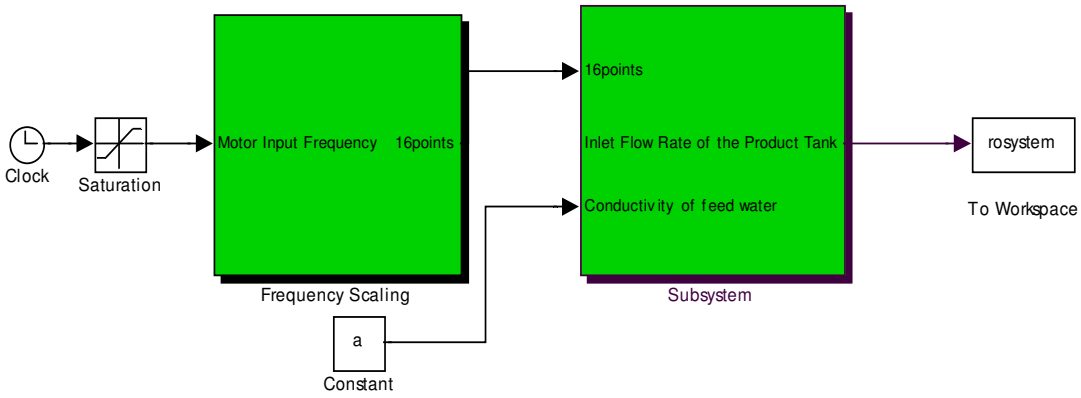

Figure 4.15 - Simulink Models of the RO membrane

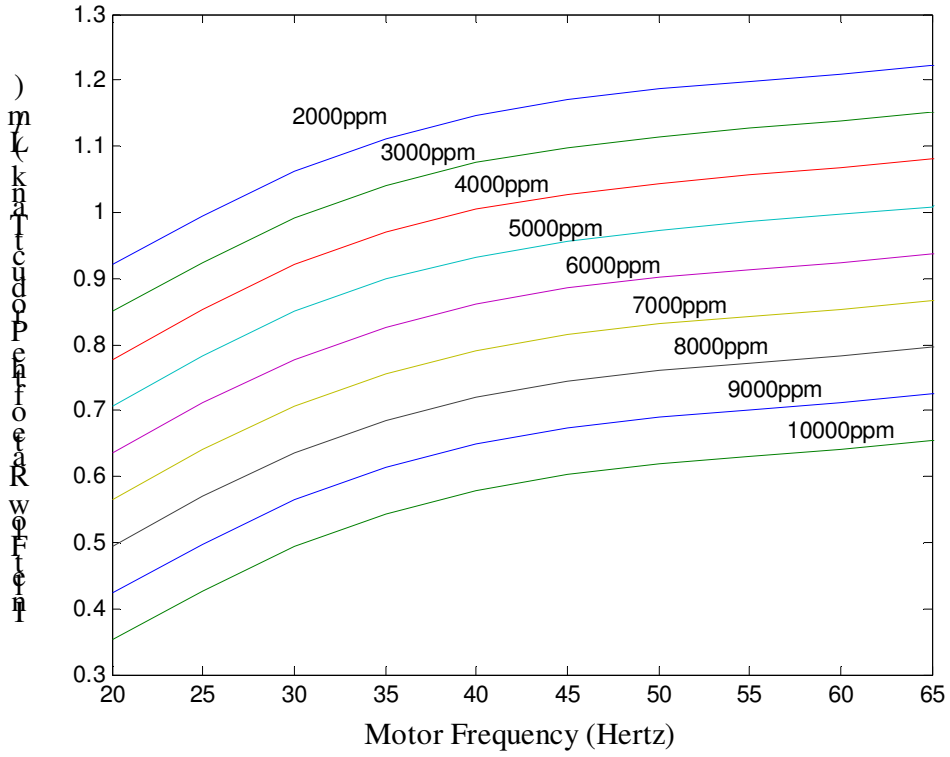

Figure 4.16 - Simulation Result of the RO Membrane Model

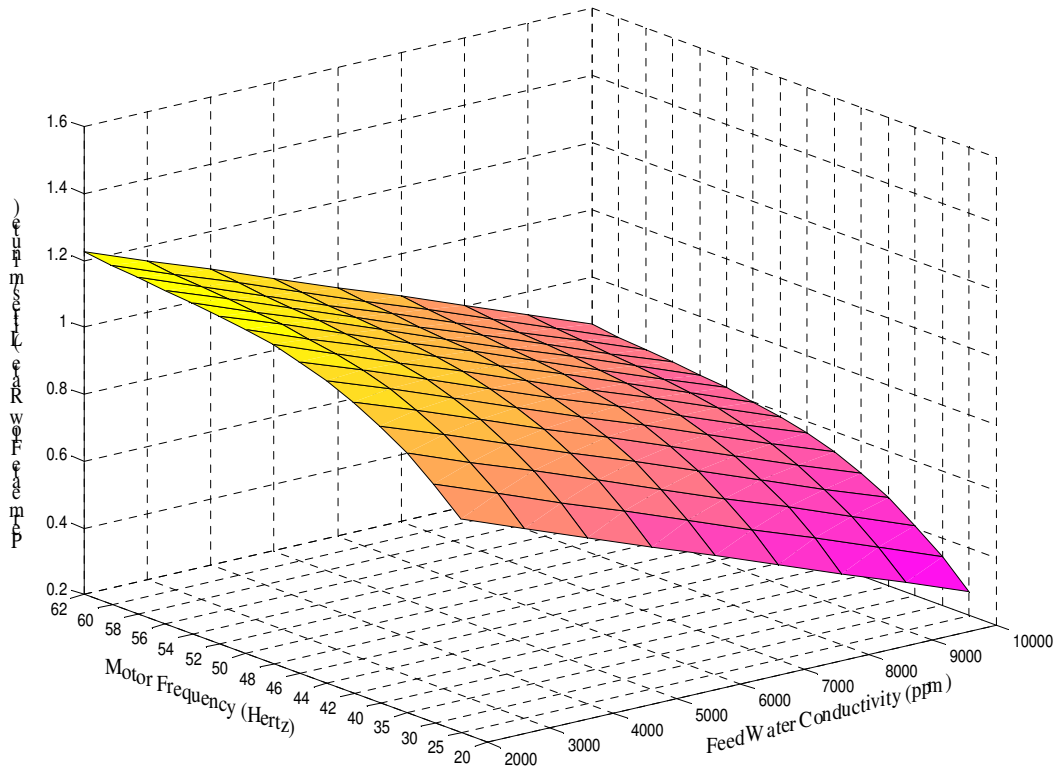

Figure 4.17 – Simulation result for the water productivity surface in series of the motor frequencies and feed water conductivities

Simulation of the membrane yielded the news graphs (figure 4.16, 4.17) that are literally the clones of the original ones (figure 4.11, 4.13) but in the better "appearances".

4.5 Correlation between the Torque and the Permeate Flow

In accordance to the previous discussion, it is believed that the relation between inlet salt-water pressures and permeates flow of the membrane can be represented by:

$$M_p = K_m \times p_{m,in} \tag{4.21}$$

Where

M_p is the flow rate of product water, Kg/s;

K_m is the coefficient of the membrane;

$p_{m,in}$ is the feed stream pressure, kPa.

Substitute 4.9 into 4.8, and the torque can be represented by:

$$T_m = \frac{K_p}{129.6 \times Eff_{m+p}} \times (\frac{M_p}{K_m} - p_{p,in}) \tag{4.22}$$

This can be simplified to be as following formula:

$$T_m = K_1 M_p - K_2 \tag{4.23}$$

Where,

$$K_1 = \frac{K_p}{129.6 \times Eff_{m+p} \times K_m} \tag{4.24}$$

$$K_2 = \frac{K_p \times p_{p,m}}{129.6 \times Eff_{m+p}} \tag{4.25}$$

Throughout the deduction above, the values of K_m, $p_{p,in}$, K_p, Eff_{m+p} need to be determined by using the laboratory methods. Worth mention is that, K_m, K_p, Eff_{m+p}, $p_{p,in}$ are the parameters that researchers assumed out of the normal behaving of each components. In fact, all of them might keep changing as $p_{m,in}$ (inlet pressure of the membrane) varies. Therefore, the real parameters of each equation can be revealed as:

$$K_p = X_1 (p_{m,in}) \tag{4.26}$$

$$Eff_{m+p} = X_2 (p_{m,in}) \tag{4.27}$$

$$p_{p,in} = X_3 (p_{m,in}) \tag{4.28}$$

$$K_m = X_4 (p_{m,in}) \tag{4.29}$$

Thus, substitute equation 4.26, 4.27, 4.28, 4.29 into 4.25, the final expression for motor toque is:

$$T_m = \frac{X_1(p_{n,in})}{129.6 \times X_2(p_{n,in})} \times [\frac{M_p}{X_4(p_{m,in})} - X_3(p_{m,in})] \quad (4.30)$$

4.6 Start-up of the Motor:

For the three-phase electric drive, starting current can be 6 to 8 times the rated current of the motor [5]. If large currents are drawn even for a short time, the current rating required of the inverter will become unacceptable large.

At starting, the rotor speed N_m is zero, and hence the slip speed N_{siip} equals the synchronous speed N_{syn}. Therefore, at start-up, a low line frequency must be applied in order to keep N_{slip} low, and hence avoid large starting currents.

For the motor in the RO system, as it is a 4 pole electric drive, assumption is built that the motor needs to develop a starting torque of 150 percent of the rated in order to overcome the starting friction.

Since,

$$N_{syn} = \frac{2\pi \times f_{rated}}{p/2} \quad (4.31)$$

Where

P/2 is pole in pairs;

f is the motor rated frequency, Hertz.

Therefore,

$$N_{syn} = \frac{\omega}{2\pi} \times 60 = f \times 60 = 1500 \text{ rpm}$$

Meanwhile, it is known that:

$$N_{rate} = 1345 \text{ rpm}$$

So,

$$N_{rate,slip} = N_{syn} - N_{rate} = 1500\text{-}1345 = 155 \text{ rpm}$$

At start-up, the rate slip speed of the motor is:

$$1.5 \times N_{rate,slip} = 155 \times 1.5 = 232.5 \text{ rpm}$$

Hence, for 4-pole machine, the start-up Frequency is

$$f_{start} = (\frac{N_{syn,start}}{60}) \times \frac{p}{2} = \frac{232.5}{60} \times 2 = 7.75 \text{ Hz}$$

However, 20 Hertz was chosen to be the starting frequency for the motor for the safety purpose. Because the lower start speed will generate much more heat in the motor than in high speed, which could damage the motor. Also, the lower start frequency will risk the motor from stalling if any unpredictable high level load occurred at that time.

4.7 Product Water Tank Modelling

The product tank is modelled in Matlab and shown below. It automatically calculates the water level in the storage tank and reports this value to the system controller (whose information will be displayed in chapter 6). The water tank capacity is a changeable parameter that is required to confirm before the simulation for RO system happens.

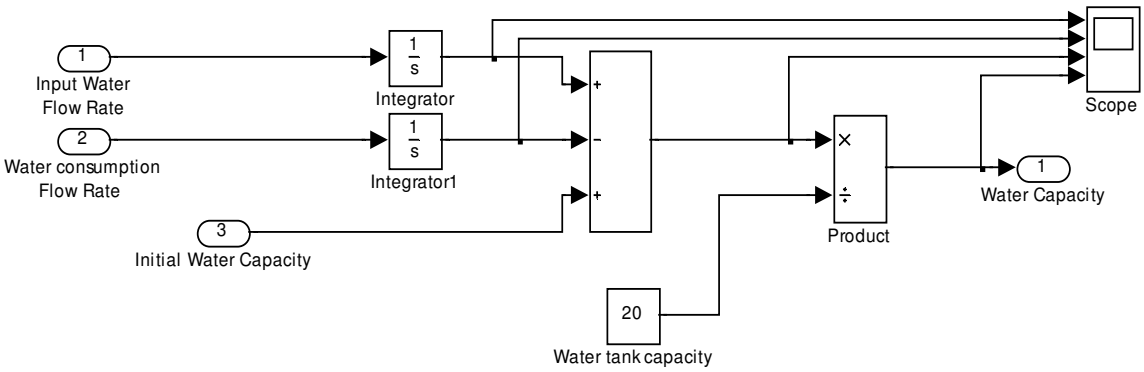

Figure 4.18 - Simulink model of the product tank

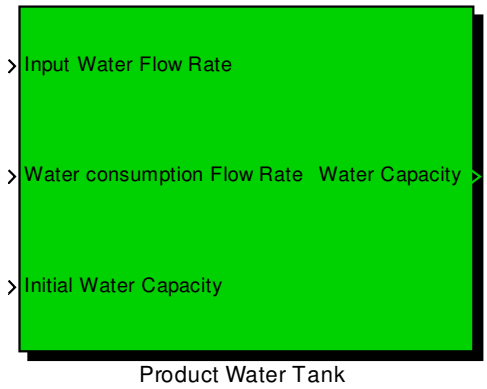

Figure 4.19 – Masked model of the product tank

4.8 Saltwater Modelling

The proposed system is designed for desalinating brackish/saline water whose salt concentration range from 2,000 to 10,000ppm. For experimental purpose, brackish water or natural saltwater is not available, the use of the NaCl solution is a common workaround used in laboratory tests, allowing standardization and repeatability in test conditions and results. This alternative was adopted in this work.

During the test (discussed in chapter 7), saltwater was simulated by dissolving pool salt in tap water that was contained in the water tank. The amount of salt dissolved in water can be measured either as a per cent, in parts-per-thousand (ppt), or in part-per-million (ppm), (where 10ppt=1%=10000ppm). The common parts-per-thousand measurement is the weight of the salt in pounds per thousand pounds of water (about 125 gallons). Pond-keepers often talk about the pounds of salt per hundreds gallons of water. Since 100 gallons of pure water weights about 800 pounds, one pound of salt per hundred gallons equates to a salinity of 1.25 ppt (0.125% or 1250ppm), (1 ppt=0.8 pounds per hundred gallons).

The definition of the compounds per cents are given as [10]:

1 pound/100 gallons=1250ppm

If assume that salt concentration is 2,000ppm

Hence

$$\frac{1250}{2000}=\frac{1/100}{x/100}$$, x=1.6 pound salt/100 gallons water

Convert it to unit of ppm according to the relation:

1 gallon water= 4.546 litres water

1 pound salt=0.454 kg

Therefore, for the saltwater of 2000ppm, the weight of salt per litre water is:

$$\frac{1.6\times 0.454}{100\times 4.546}=0.001596\,\text{Kg/litre}$$

Table 4.3
Weight of the salt in one litre water for different conductivities

PPM	Weight of the salt per litre
2000	0.001596
3000	0.002394
4000	0.003192
5000	0.00399
6000	0.004788
7000	0.005586
8000	0.006384
9000	0.007182
10,000	0.00798

4.9 Inlet pressure of the pump

Since, physically the pressure of the fluid is

$$p_{p,i}=\rho g h \tag{4.32}$$

Where

ρ is the density of fluid;

g is $9.81 m/s^2$;

h is height from motor-pump to water level in the tank.

Particularly,

$$\rho = \frac{m}{V} \tag{4.33}$$

Where, m is the water mass, V is the total volume of the fluid.

Using the equation 4.13, the liquid density with different conductivities were calculated and tabulated as shown below.

Table 4.4
Liquid Density in different conductivities

Conductivity (ppm)	Liquid Density (kg/m^3)
2000	2.596
3000	3.394
4000	4.192
5000	4.99
6000	5.788
7000	6.586
8000	7.384
9000	8.182
10,000	8.98

So, the inlet pressure of the high pressure pump can be calculated by using equation 4.32 when the water vertical distance between the water level in the feed water tank and the inlet of the high pressure pump. For example, when feed water conductivity is 3000ppm, the vertical distance is 0.43 meters; the inlet pressure of the pump is 21.64184 kPa.

4.10 References

[1] The Mathworks. *Matlab Documentation (Using MATLAB Version 6.5)*, 2001.

[2] Slater, CS, Brook, CA, III. *Development of a simulation model predicting performance of reverse osmosis batch system*, Separation Science and Technology, 1992, 27(11), 1361-1388.

[3] TECO Speedon, *Inverter Instruction Manual*, TECO Electric & Machinery Co., Ltd, Taipei, 1997.

[4] Igor J., Joseph P., Pump Handbook, McGraw-Hill Companies, New York, 2001.

[5] Mohan, N., Electric Drives-an integrative approach, MNPERE Minneapolis, Minnesota, 2003.

[6] Bill. L., *Photo-votaic System for Vineyard Irrigation at Yandanooka*, Curtin University, Perth, 2004.

[7] The MathWorks Inc., Natick, and MA 01760-1500. *SIMULINK (R), Dynamics System Simulation for MATLAB (R) Version 2.2 edition*, 1998.

[8] Al-Alawi, A., *An integrated PV-diesel hybrid water and power supply system for remote arid regions*, Curtin University, Perth, 2004.

[9] Hisham T., Fundamentals of Salt Water Desalination, Elsevier Science B.V., New York, 2002.

[10] Spiegler, K., Salt-Water Purification, Second edition, Plenum press, New York, 1977.

[11] William B.L. and Wichert, B., " A versatile PV module simulation model based on PSI/e," *Solar Energy*, vol.52, 1994

CHAPTER 5 CONTROL STRATEGIES

The objectives of efficiency improvement for the RO system are depicted in this chapter. The conventional control (toggle control) is explained. The major control strategy (PID control, feed-forward control) applied in the RO system is displayed from the basic principle to its functionality in practice. Followed by The application of the PID control in PLC, the control algorithms are further explained in the form of the flow chart. This lays a ground for the arguments in the following chapters.

5.1 Objectives of the Control

Conventional control strategies for RO systems embedded in RAPS system described in chapter 2 are based on the toggle control principle which assesses the water level in the product tank. When the water level goes below the threshold, the desalination unit starts and continues to run until the product water tank is full [2]. This control has the advantage of easy operation and maintenance. But, it introduces extra energy consumption caused by unpredictable start/stop times and turbulence of the water demands. Thus, to improve this simple performance, new control strategies are needed.

The main purpose of designing new control strategies for the RO system is to enhance the system's efficiency and save energy, explicitly by reducing the on-off cycle of the motor-pump unit, while at the same time attempting to adjust the system to operate around the maximum efficiency points and preventing the membrane from being over-used and damaged. These objectives will consequently minimise the total cost of the RO system maintenance, reduce the electric burden of renewable energy power supply system, lower the price of the power provided by RAPS grid and benefit customers.

With the flexibility of the variable speed drive and PLC controller, the RO system now is competent to fulfil the aforementioned control objectives, particularly in perspectives of saving energy and increasing the life expectancies of the RO motor-pump.

The renewable energy power supply system in which the RO system can be embedded has been its own control system that was previously developed at Curtin University of Technology [1]. It produces power in single phase AC format for maximally 26 kW electric loads. The performance of that system has been tested and the test results were promising and optimistic. All these were taken as the supporting materials for designing the control logics in the RO system as one of the electric loads of the renewable energy power supply grid. Having this background, the process of designing the control strategies is discussed as below.

5.2 Control Techniques

There are two major control techniques for the RO system that can integrate into a RAPS system: toggle control and load following control; the latter one has not yet been largely implemented. Therefore, it is the one which will receive the greatest focus.

5.2.1 Toggle Control

Toggle control also known as on/off control is the most commonly used techniques in control systems because it is easy to implement and cheap to run. This control strategy is largely used in the systems that include storages tanks, i.e. water tanks. For example, as seen in figure 5.1, a water pumping system has a water tank for storing the water pumped out of a well. The systems will shut down when the water level reaches its highest point that is usually set at 80 percent of the total tank capacity. The system will start again when the water level hits the low level set-point. This cycle will continue while the water consumption goes on. This control technique is considerably simple but less efficient. However, this type of control is being used by most of the existing RO systems.

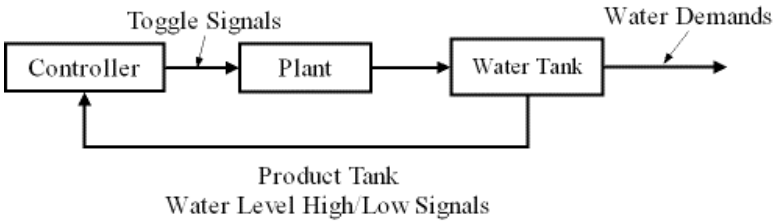

Figure 5.1 Toggle control in water supply system

5.2.2 Load Following Control

The load-following control monitors the systems' output to determine its input values. This type of control enables systems to adjust inputs to match system's output conditions. Because the Load-following control regulates the output of the systems, it consumes less energy compared to the aforementioned toggle control. There is a large category regarding load-following control, however, selected control ideas are depicted in the following sections in connection to the best suitability for the RO system.

5.2.2.1 Feedback PID Control

Notice that most of the processes of RO systems have system output variables, such as flow rates and conductivities. The values of these variables are very useful in determining the outputs of the RO systems if they can be fed back to the system and compared with the desired ones [5]. This process, based on the block diagram in Figure 5.2, can be called closed loop control.

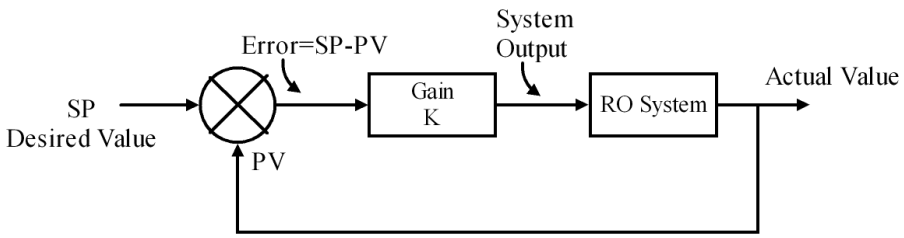

Figure 5.2 - Proportional closed loop control

The required values, denoted by set-points, is compared with the actual value PV (Process Variable), for process variable, to give an error E, which is simply given as:

$$E = SP - PV \tag{5.1}$$

This is multiplied by a gain, K, to give an OP (Output) from the control mechanism where

$$OP = KE = K(SP - PV) \tag{5.2}$$

This output causes a change in the plant, giving the output PV. Generally, PV will be directly related to OP, given by the below equation:

$$PV = A \times OP \tag{5.3}$$

Where

A is a gain factor.

Combing the equations (5.1) to (5.3), another relationship between PV and SP is given by:

$$PV = \frac{AK}{(1+AK)} \times SP \tag{5.4}$$

That is the system signal PV will follow the SP multiplied by a scaling factor AK/ (1+AK). The term AK is know as the open loop gain, and is often denoted by G, which can be written as:

$$PV = \frac{G}{1+G} \times SP \tag{5.5}$$

It can be seen that for large values of G, the error between PV and SP will be small. For example, when G=10, PV=0.91SP

A large value of G can be obtained by using a large value of gain, K. However, unfortunately, in practical systems this often leads to instability.

A modified type of control strategy is shown in figure 5.3 where the output signal is the sum of the error plus the time integral of the error, i.e.

$$OP = K(E + M\int Edt) \tag{5.6}$$

This is known as PI control, which stands for proportional plus integral control.

The integral term will cause OP to change as long as there is an error and OP will only be constant when the error is zero and SP=PV. A PI controller thus provides zero error in the steady state without the need for a high gain.

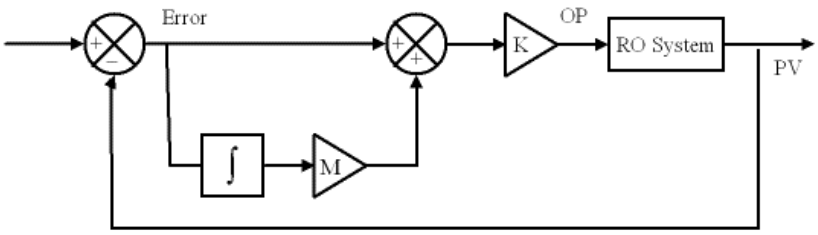

Figure 5.3 PI control block chart

In practical controllers, the term M in equation (5.6) is replaced by $1/T_i$ giving

$$OP = K(E + \frac{1}{T_i}\int Edt) \tag{5.7}$$

Where

T_i is known as the integral time.

The reason for this change arises out of the underlying mathematics.

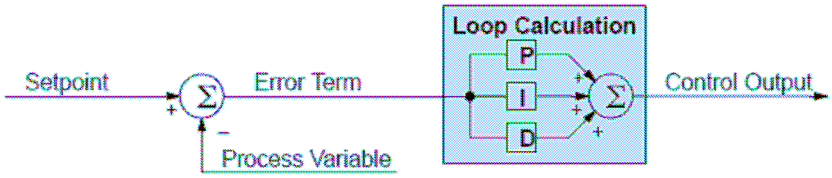

Figure 5.4 - PID control

A Further modification is shown in figure 5.2. Here a time derivative (rate of change) term has been added, giving

$$OP = K(E + \frac{1}{T_i}\int Edt + T_d \frac{dE}{dt}) \quad (5.8)$$

This is known as a three terms or PID (proportional, integral and derivative) controller. The multiplier T_d is known as the derivative time.

The derivative term brings two benefits. Because it responds to the rate of change of error it will alter the output, when the set-point changes rapidly. The derivative term can also make the system more stable and reduce overshoot.

PID control is useful for controlling and regulating the flow rate of the RO system that is subject to the turbulences from the environment such as the temperature, conductivity of the feed water and users' ambient demands. All of these will produce a change in PV, the controller will detect them and modify OP to make PV=SP again, and remove the effect of the disturbance.

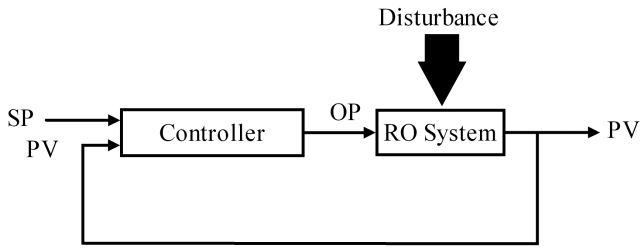

Figure 5.5 - The effect of a disturbance

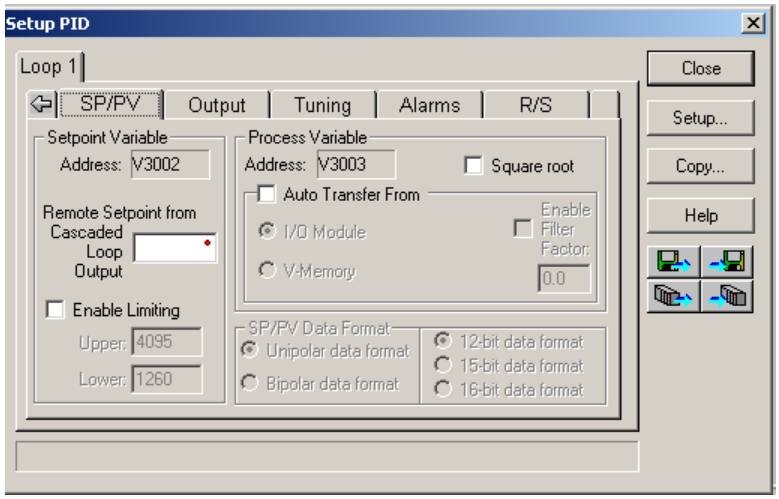

Figure 5.6 - Screen Image of the Configuration Window

PID loop can be set up in the PLC control by using PID set-up tool included in the controller itself. In addition, auto-tuning was used to tune the PID loop to achieve the best performance.

5.2.2.2 Feed-forward Control

Feed-forward control is an enhancement to standard closed-loop control. It is most useful for diminishing the effects of a quantifiable and predictable loop disturbance or sudden change in set-point [4]. Use of this feature is an option available on DL260. However, it's best to implement and tune a loop without feed-forward, and adding it only if better loop performance is still needed. The term "feed-forward" refers to the control technique involved, shown in the diagram below. The incoming set-point value is fed forward around the PID equation, and summed with the output.

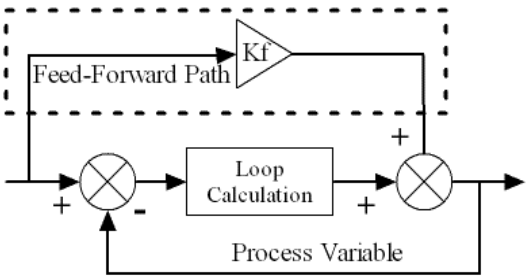

Figure 5.7 - Feed-forward Control

In the previous section on the bias term, we said that "the bias term value establishes a "working region" or operating point for the control output. When the error fluctuates around its zero point, the output fluctuates around the bias value." When there is a change in set-point, an error is generated and the output must change to a new operating point. This also happens if a disturbance introduces a new offset in the loop. The loop does not really "know its way" to the new operating point... the integrator (bias) must increment/decrement until the error disappears, and then the bias has found the new operating point. Suppose that we are able to know a sudden set-point change is about to occur (common in some applications). We can avoid much of the resulting error in the first place, if we can quickly change the output to the new operating point. If we know (from previous testing) what the operating point (bias value) will be after the set-point change, we can artificially change the output directly

(which is feed-forward). The benefits from using feed-forward are: The SP–PV error is reduced during predictable set-point changes or loop offset disturbances. Proper use of feed-forward will allow us to reduce the integrator gain. Reducing integrator gain gives us an even more stable control system. Feed-forward is very easy to use DL260 loop controller, as shown below. The bias term has been made available to the user in a special read/write location at PID Parameter Table location V+04 [3].

5.3 Control Strategies for the RO Unit

From the system efficiency characteristics plotted in figure 5.8, it is found the total efficiency of the system reaches its climax when the motor frequency is around 25 Hertz and decreases as the motor frequency continues. Whereases, the power consumption keeps going up while the motor frequency increases. Furthermore, in figure 4.11, the flow rates of the product water do not increase dramatically in the high motor frequency range. In another word, the differences of the flow rates between high motor frequency and low frequency are not that significant. This means that the energy saving can be achieved by keeping the motor frequency low when the water demands are not large. And the controller will bring the motor frequency up only when the water demand reaches a very high level.

In regards to the aforementioned ideas, new control algorithms were created. It automatically monitors and controls the system to improve the performance of the RO unit as well the mini renewable energy power supply grid. It mainly has three parts explained in the following sections.

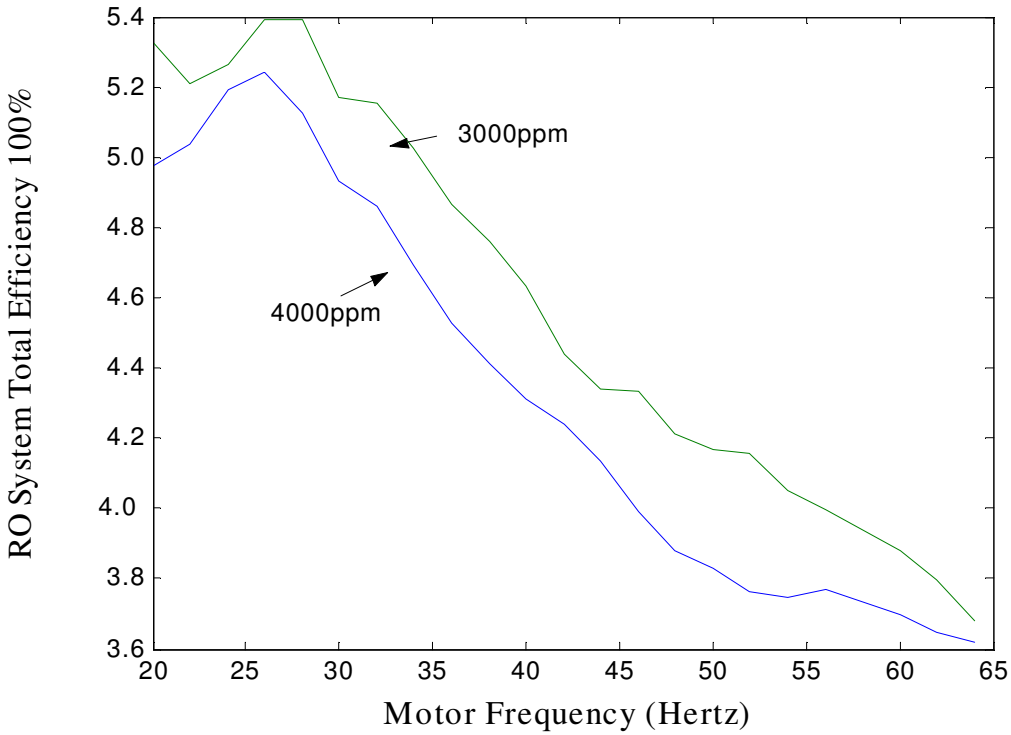

Figure 5.8 - RO system total efficiency vs. motor frequency

5.3.1 Design of the Control Strategy in PID Loop

Proportional-Integral-Derivative control is used to change the motor's speed when sensors show a variation from preset intended values. 20 Hertz is assigned as start-up frequency, which prevents the motor from stalling.

Alternatively, a feed-forward control closed loop can be used to adjust the speed of the motor drive by monitoring the difference between the water input and output rates of the product tank. It is useful for diminishing the effects of a quantifiable and predictable loop disturbance or sudden change in set-point. The feed-forward control technique will be implemented and tested at the next stage of the research.

The PID set-point is assigned as the difference between the product tank inlet and outlet flow rates [5]:

$$SP = \text{Inlet flow rate} - \text{Outlet flow rate} \tag{5.9}$$

This set-point is set to zero, meaning that the PID shall maintain its output when the inlet flow is equal to the outlet flow. Hence when the PID process variable is

greater than zero, the PID output will reduce until the minimum speed of 20 Hertz is reached. When the PV is less than zero, the PID output will increase to its maximum output value. This maximum output value i.e. efficiency thresholds, is gained from the preliminary pump tests, which proved that the increase in productivity is negligible after a certain motor speed.

Preliminary tests are conducted on the RO unit. In the first test, with different salinities or conductivities, the flow rates of product water were recorded as the frequency of the motor driver was varied from 20 to 62 Hertz. The transient power of each stage is trended as it is shown in figure 4.7. It is found that the power consumptions at each saline level follow similar trends. This can be concluded that the powers drawn by motor-pump are very similar, regardless the saline level of the raw water. Meanwhile, in all those conditions, the power consumptions change linearly.

Notice that, from water production Diagram (Figure 4.11), the product water flow rates do not change insignificantly after the power output into the RO pump reaches certain points. Hence, the thresholds in different conductivities are determined and set-up in a PID tuning parameters. For example, from 20 Hertz up to a maximum of 62 Hertz, the flow rate of output water does not vary greatly when the conductivity is 2000 PPM, etc.

This algorithm promotes energy efficiency when there is little demand for water, such as at night time; the tank is filled slowly, requiring less energy. Depending on the size of the product tank, it may also avoid frequent motor starts and stops, decreasing start up energy requirements and extending motor life. When there is a higher demand for water, the system will increase to its speed points where delivers it maximal productivity using minimal energy required.

5.3.2 Flow Chart of Control Process

A control process was created in consideration of the PID control, system alarms and maintenance. For example, as can observed in figure 5.11, the controller will check and verify any alarm before virtually switching on the RO motor-pump. This is crucial for process control in industry [4]. And, during the operation cycle of the PID

loop, system raised alarms can trip the entire RO system. In the end, the membrane will be flushed automatically by a flushing pump.

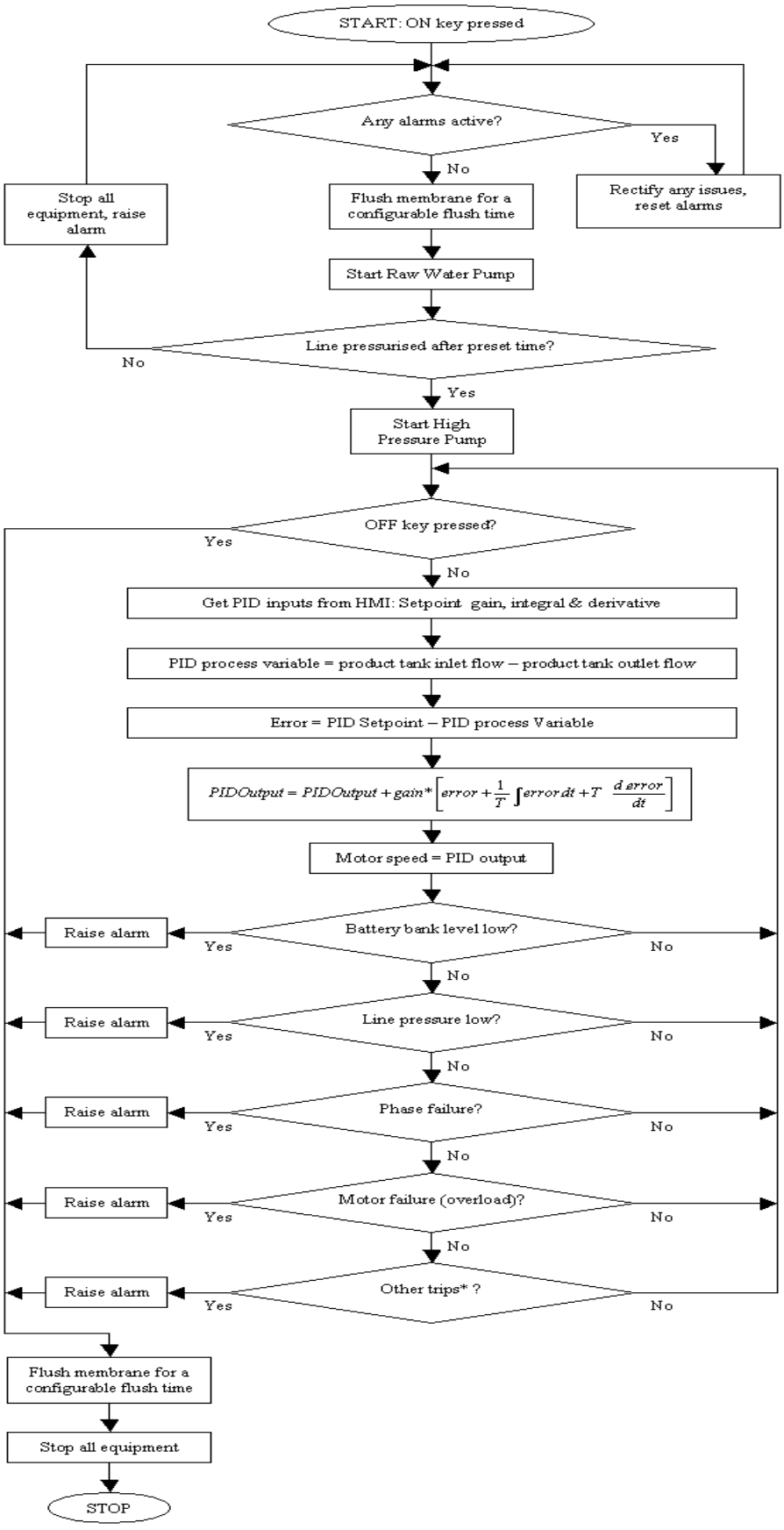

Figure 5.11 Flow chart of the load following control

5.4 Reference

[1] Http://www.regenpower.com [accessed July 2005].

[2] Al-Alawi, A., *An integrated PV-diesel hybrid water and power supply system for remote arid regions*, Curtin University, Perth, 2004.

[3] DL205 User ManualVolume 2, Automationdirect.com Incorporated,2002

Http:// www.Automationdirect.com [accessed 2005]

[4] Rohner, P., *PLC*: automation with programmable logic controllers, UNSW Press, Kensington, 1996.

[5] Norman A. *Instrument for Process Measurement and Control*, CRC Press, New York, 1997.

[6] Norman S. Control Systems Engineering, third edition, Hon Wiley & Sons, INC, Brisbane, 2000.

[7] Richard C., Robert H., *Modern Control Systems, tenth edition*, Pearson Education Australia Pty. Ltd., Sydney, 2005.

CHAPTER 6 RO SYSTEM SIMULATION WITH CONTROL SYSTEM AND WATER DEMAND MODELLING

The control system was modeled with a PID controller and a toggle controller in simulink. Details of each model were displayed. The system was simulated within operation constraints and component specifications. The simulations time was set for short terms as well as long terms. The simulations results from PID control and toggle control were compared.

6.1 Water Demands Modelling

6.1.1 Water Demand Profile

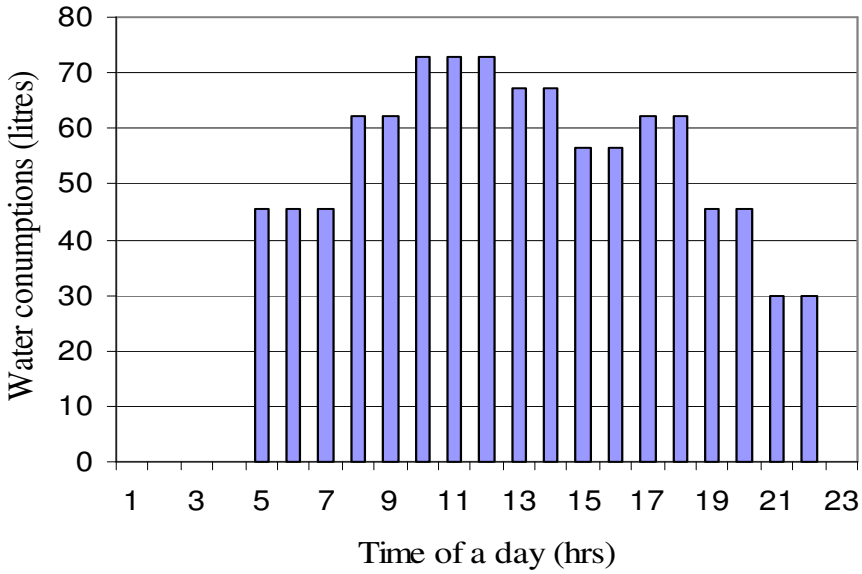

Figure 6.1 – A daily water demand chart

The designed RO system is capable of providing drinking water for a community or area whose total population is within 300 inhabitants (mentioned in chapter 2). A daily average water demand profile of 300 inhabitants was created based on the work done by E.T. Kaikhurst [1]. Generally, the average drinking water demand is around 3 litres per day. From the system design specification, the water demand for an area of 300 residents is 900 litres. Considering the waste factor of 1.2, the total water demand is 1080 litres per day. Meanwhile, taking into account the general human water intake habits and temperature variation during a day, the drinking water demand should reach the highest at around noon and hit the lowest level at around midnight. A generic drinking water profile for 300 inhabitants is shown in figure 6.2. It shows the highest drinking water demand is 72 litres per hour and lowest figure is 30 litres per hour. The total drinking water demand is 1003 litres per day.

6.1.2 Matlab Model of 24 Hours Water Demand

Pulse generators were used in simulink to simulate the water demand scenarios under various situations. The parameters of the pulse generators were set according to the specifications of the DC product water pump described in chapter 3. Over the period of a day, different water demands can be revealed by setting different signal turn-on periods in the pulse generators (Figure 6.3). For example, high water demands were reflected by high turn-on frequency. The amplitude of the pulses stands for the output flow rate and do not need changing because the DC product water pump does not have variable speed features. An auto-selector is used in modelling the 24 hour water demands. It switches amongst the input channels sequentially according to the input signal of the control port. For example, when the input signal for the control port equals to 1, the auto-selector connects the port 1. A digital clock is chosen to supply the input signal for the auto-selector. The sample time of this clock is 3600 seconds means that it extracts the readings of time once every 3600 seconds as simulations go on. The value of time is divided by a constant value-3600. This provides the linear stepping signal start from 1 to 24 which can be used to control the switch. The Matlab model of 24 hour water demands is shown in figure 6.4.

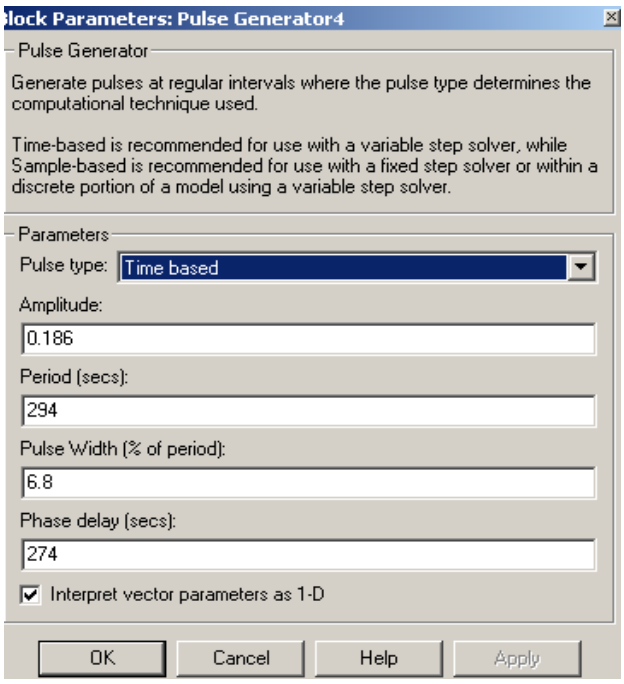

Figure 6.2 – Parameter set-up window for pulse generator

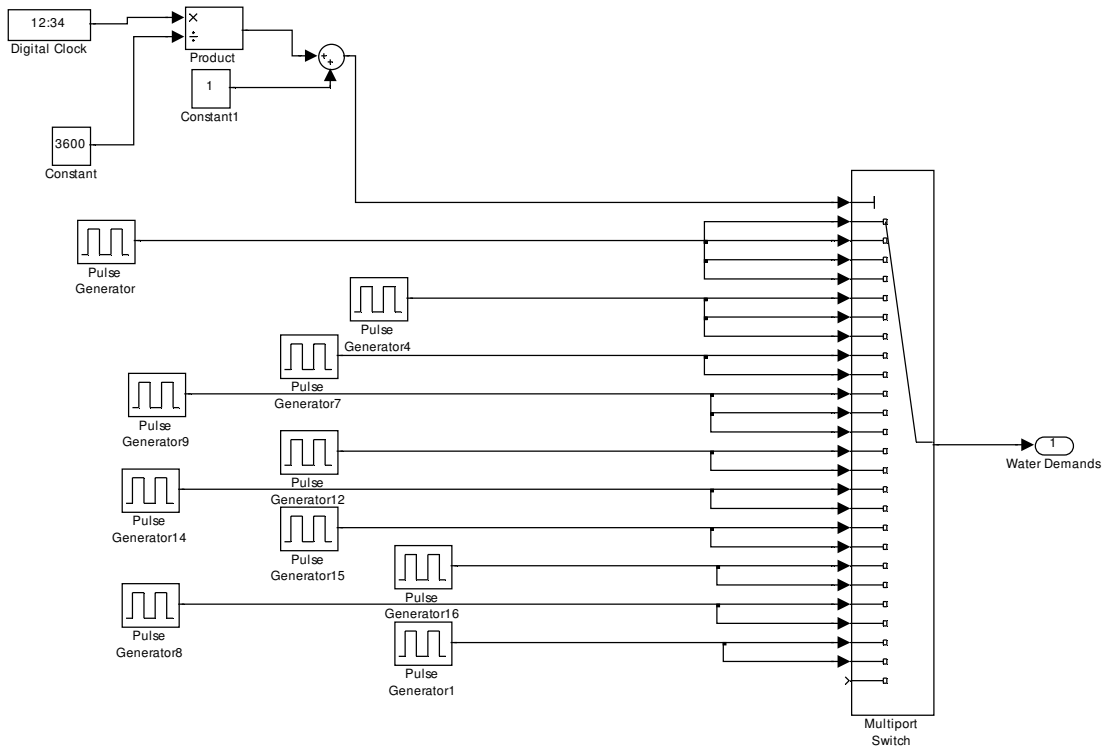

Figure 6.3 – 24 hours Water Demands Model

Over the 24 hours in which water demands were modelled, the total water consumption is 1003 litres. This model was tested and masked. Figure 6.5 shows the

24 hour water demands output signals with respect to time in second. The red line in the figure represents the average water demands.

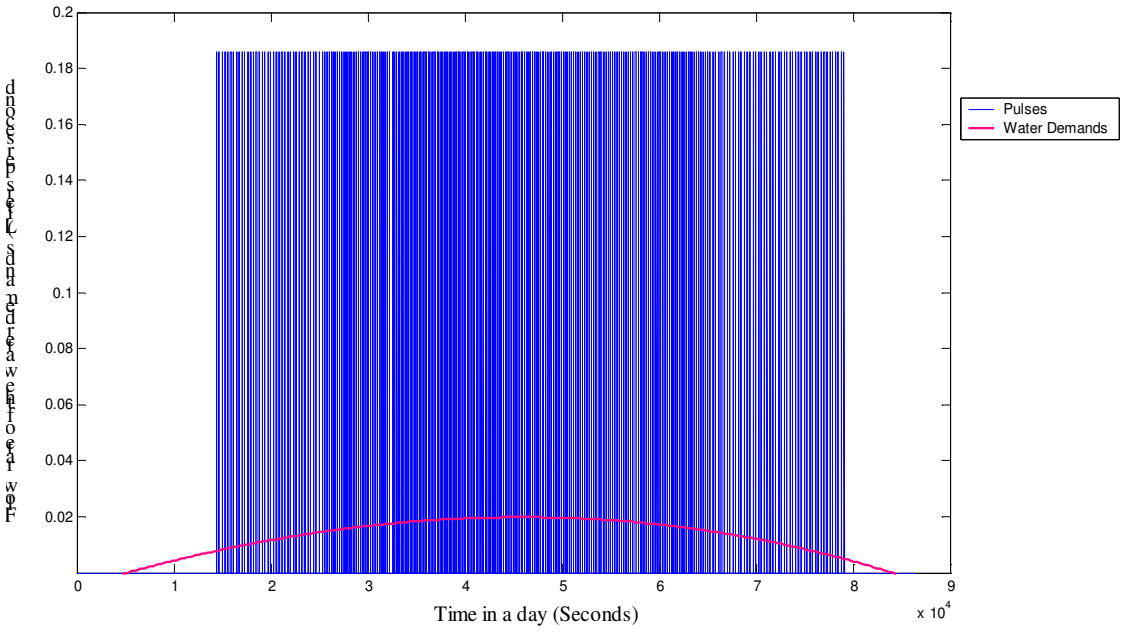

Figure 6.4 - Plot of Water demands in 24 hours

6.1.3 Weekly Water Demand Modelling

The water demand was also modelled for a weekly period (7 days). Due to the fact that the variation of the water usage was unknown, the assumption was made that the water demand of each week day was identical. Using the Matlab model of 24 hour water demands, 7 days' water demands were created and shown in figure 6.6.

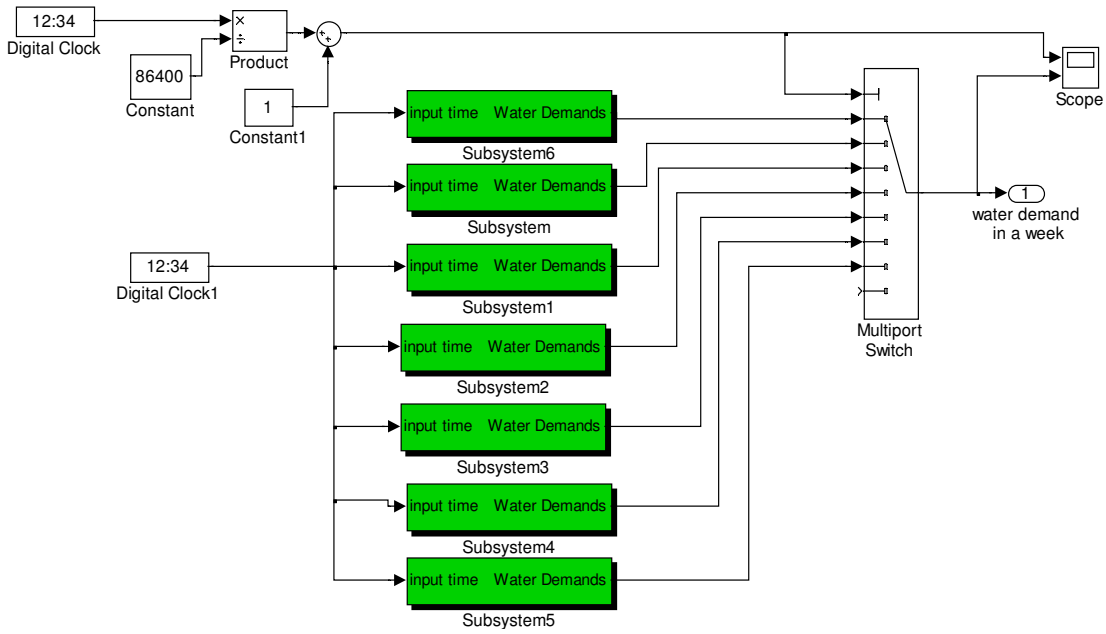

Figure 6.5 – Weekly water demand model

6.2 PID Control Modeling

From the function block provided in Simulink, nonlinear PID control was chosen. However this control block needs to be tuned. Since the PID block was formerly masked, first thing required was to look under the mask in order to understand the mechanism of the block diagram. The loop tuning was carried out later on and depicted in the following sections.

The flow rate is the main variable needs to be regulated. The range between its highest and lowest values was confined. Then the pilot PID controller was connected into the RO system and tested for tuning purposes. The refined PID controller was exhibited in figure 6.8. Special attention was needed to find the appropriate values for the gain of PID loop. It was discovered that the loop output variable (motor frequency) would be unstable when the PID gain was too high. Yet, the loop output variable could not reach its desired value when the PID gain was small. Hence, calibration was done with many different values of gain in different situations where the feed water conductivity changes from 2000 to 10000ppm. The one that produces the best performance was chosen as the value for PID gain. What is more, the system noise and sensor noise was chosen as 20% and 5% respectively.

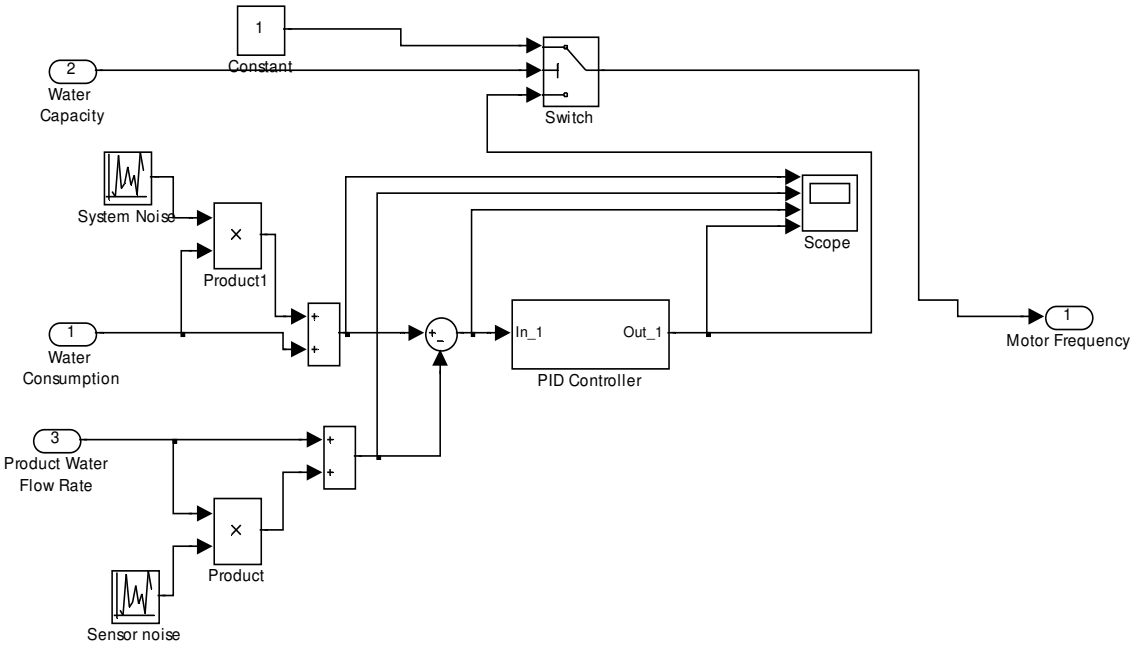

Figure 6.6 - PID controller in automatic mode

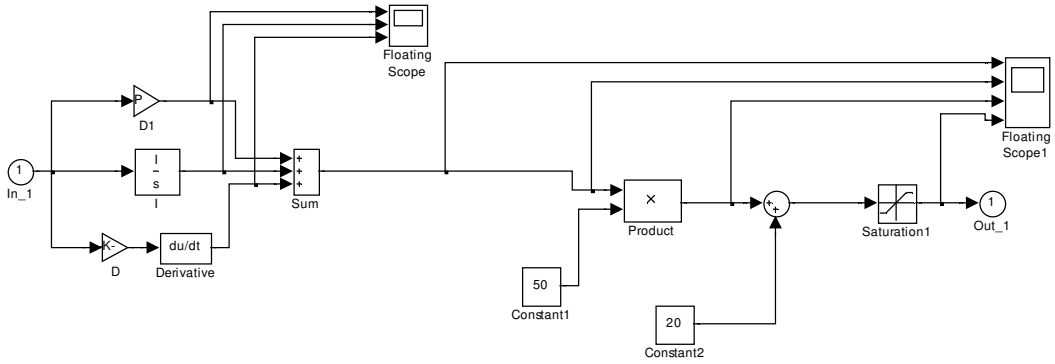

Figure 6.7 – Block diagram of PID controller

6.3 Feed-forward Control Modeling

The mathematical model of feed-forward control is illustrated in chapter 5. Based on that, the feed-forward control system is built in Matlab. As seen in figure 6.8, the feed-forward control loop contains a feed-forward gain and PID controller.

Tuning of the feed-forward control loop was required. The feed-forward gain and the parameters of PID controller are the tunable variables. The output (motor frequency) of the control was measured while maximum membranes permeate

reached its maximum flow rate. This output value was tuned by using *math operator* function blocks. Again, the system noise and sensor noise was set as 20% and 5 % respectively.

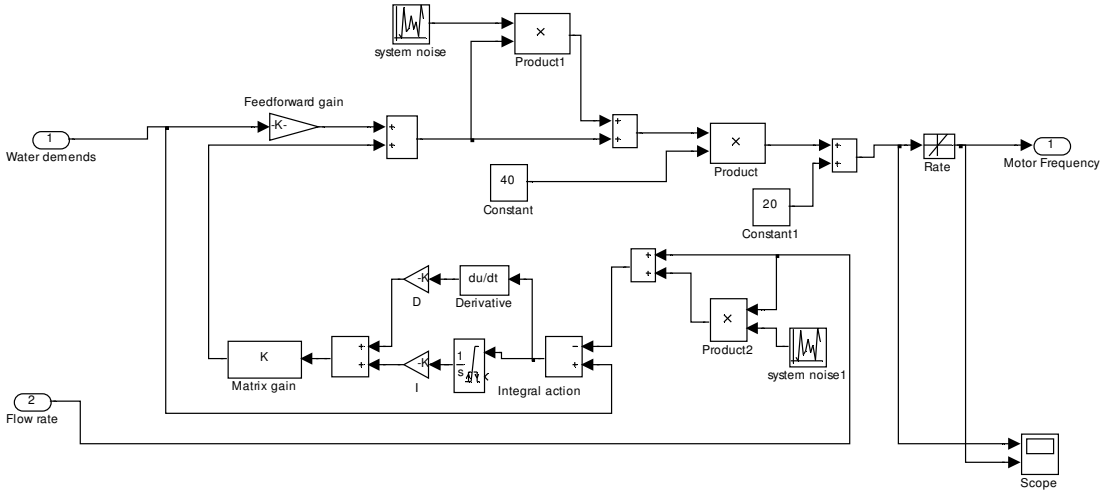

Figure 6.8 – Detailed Matlab model of feed-forward control for the RO system

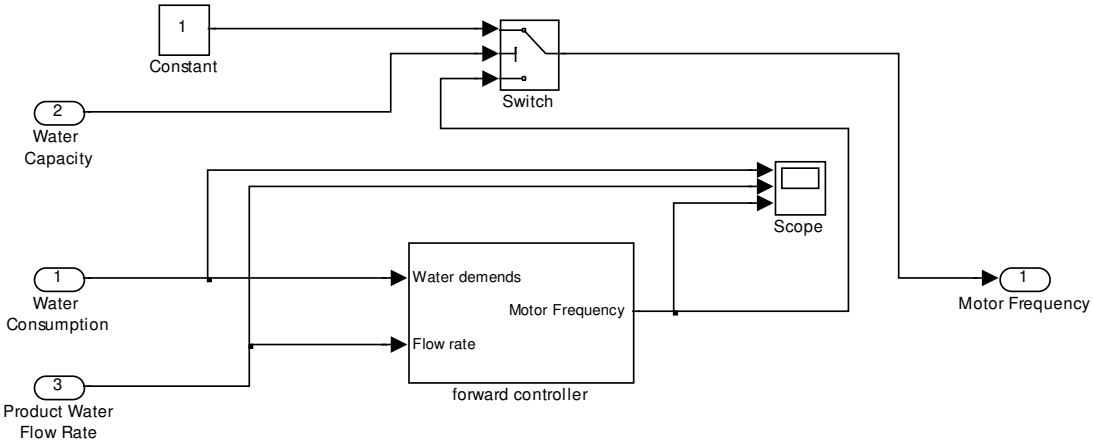

Figure 6.9 – Feed-forward control model in automatic mode

6.4 Toggle Control Modeling

In Chapter 5, the conventional control strategy-toggle control was depicted in terms of its operation principle and control rationale. This control idea was modeled in Matlab shown in figure 6.8.

A flip-flop function is used to translate the idea of toggle control described in chapter 5. The lowest value for the water level in the product tank is 20 percent; the

highest one is 80 percent of the tank capacity. 50 Hertz is set to be the operation frequency of the motor when the low water level sensor is triggered. An auto-switch is used to turn on and off the high pressure pump.

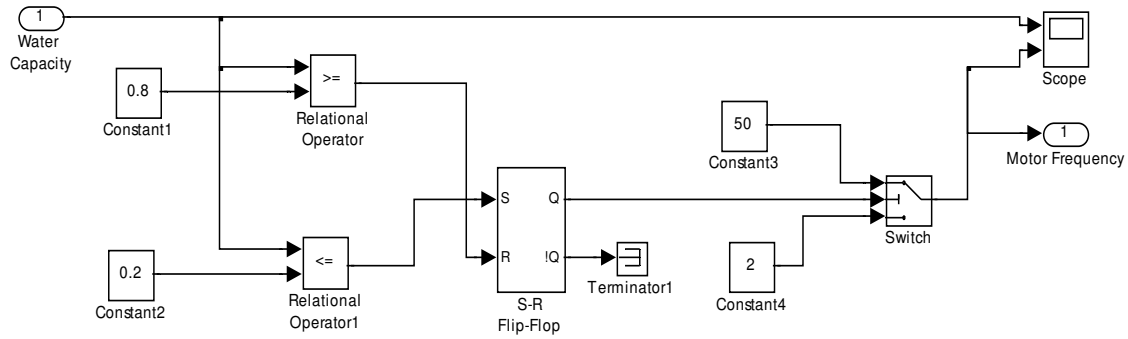

Figure 6.10 – Toggle controller with an auto-switch

6.5 Matlab Model for the RO System

Based on the Mathematic models of the control system done in chapter 5, Matlab models of water demands, energy consumption and RO system controllers were created in Simulink. The transient energy consumption and fresh water productivity were displayed and recorded into workspace of Matlab, so was the total energy consumption and water productivity during the period of simulations.

The control systems of the RO system was assembled together with the system components' models presented in chapter 4. The Matlab model of the whole RO system was established and displayed as below. A switch was used for selecting the control mode.

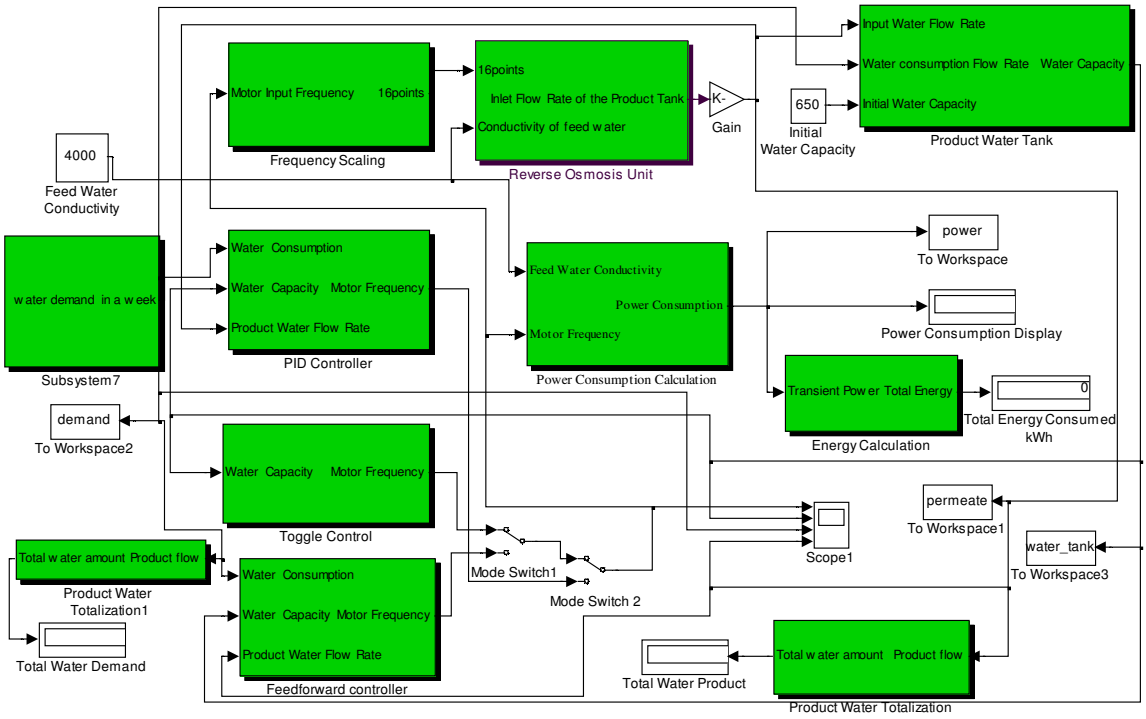

Figure 6.11 - Simulink model of the entire RO system

6.6 System Simulations and Results Analysis

6.6.1 System Simulations

At the first stage of the simulation, the simulations were carried out in toggle control mode, PID control mode, and feed-forward control mode. Simulation time in each control mode was set to be 24 hours which equals to 86400 seconds. The feed water conductivity was chosen to be in a span of 2000 to 10,000 ppm, having 1000 ppm as an interval.

At the second stage of the simulation, the simulations were still run in those three control modes but simulations' time were changed to be 168 hours (7 days).The feed water conductivity was chosen to be 4000ppm.

Assuming that the water storage can sustain at least one day's water usage for 300 people, the water tank capacity is chosen to be 1300 litres and the initial water volume in the tank is set as 650 litres which is half of the total capacity.

6.6.2 Simulation Results

With the water demand of 1003 litres per day, series of the results were produced from simulations. They are displayed as below.

6.6.2.1 System Short Term Performance in Each Control Mode

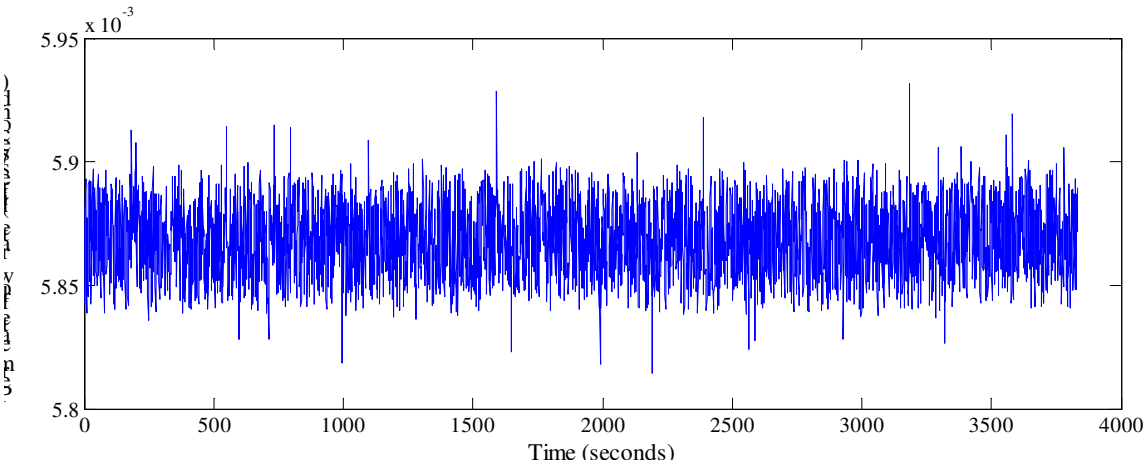

Figure 6.12 – The effect of the system noises on the permeate flow

The importance of the simulation is to be as comprehensive as possible. The operational environment of the RO system needs to be thoroughly envisaged. As mentioned in previous sections, the noise factors are considered in terms of the sensor noise that have intelligible effects on the output of the system. This is visually depicted in figure 6.12.

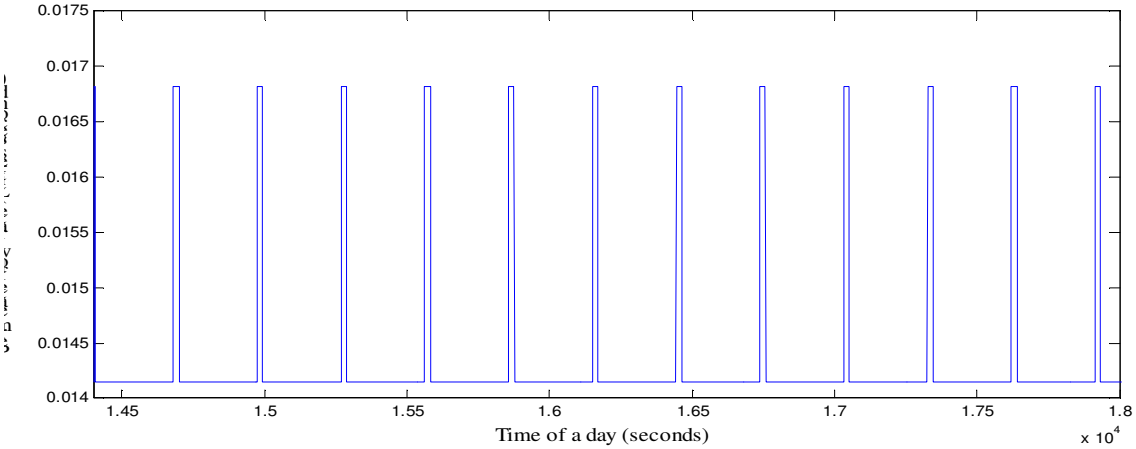

Figure 6.13 – Product water flow rate in PID control mode over an hour

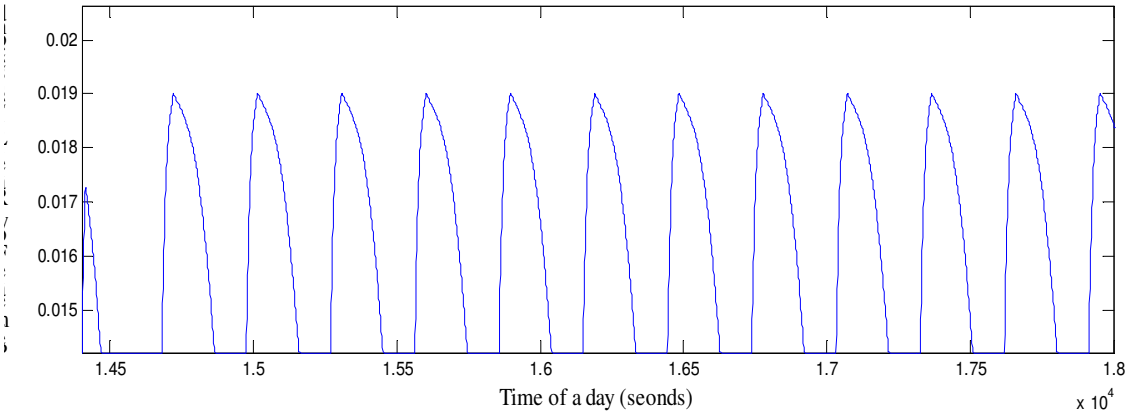

Figure 6.14 - Product water flow rate in feed-forward control mode over an hour

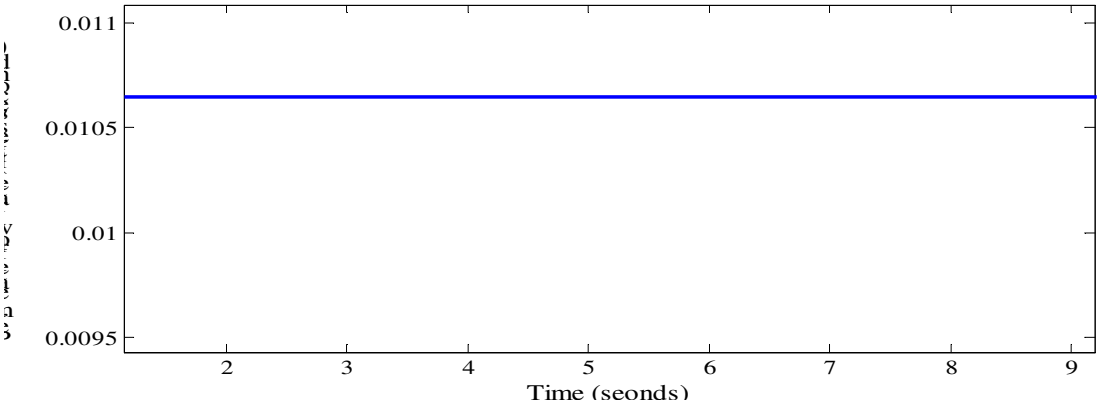

Figure 6.15 - Product water flow rate in toggle control mode over an hour

Figure 6.13, 6.14, 6.15 shows the zoomed-in view of the permeate flow rate over one hour simulation time. It can be noticed that the PID and feed-forward control produced the teeth-saw curves because of their load trailing feature while the permeate flow rate is maintained level for it does not control the motor frequency.

Because the product water flow rates were recorded in unit of liters per second and the system maximum productivity has a maximum size of 1500 liters (refer to chapter 3), the values of the permeate flow in each control mode are small.

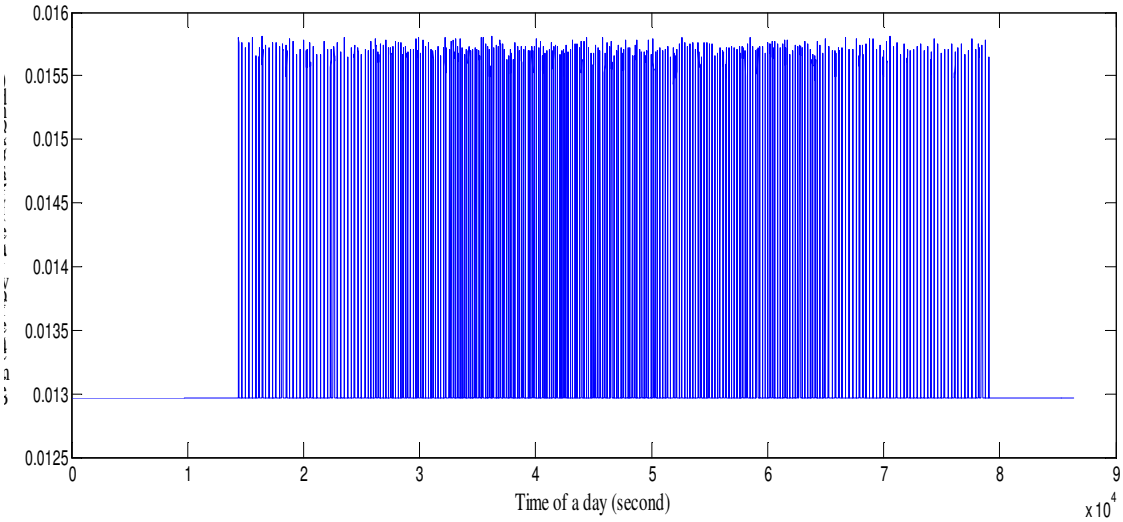

Figure 6.16 – Flow rate of the permeate in PID control mode over 1 day

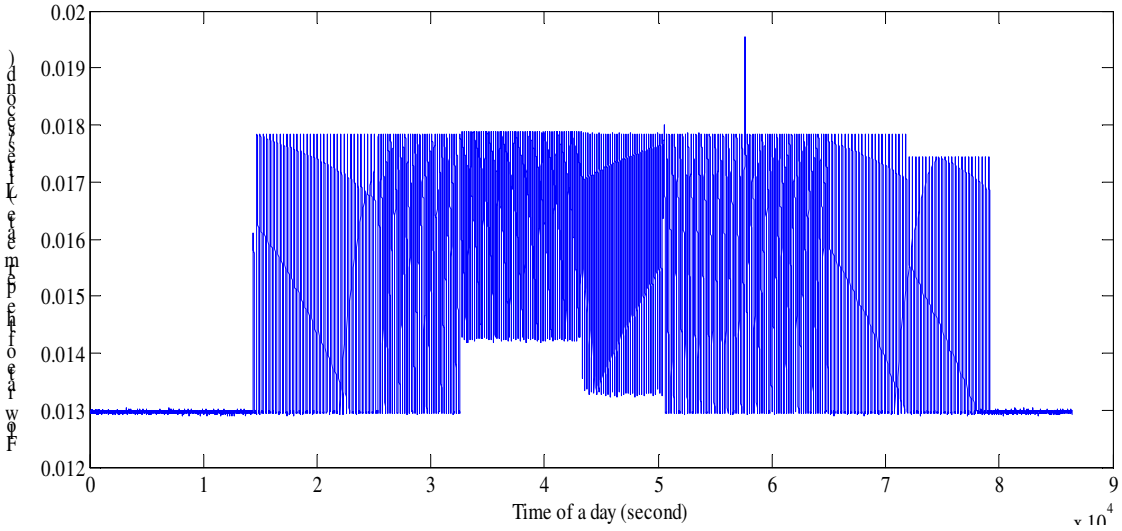

Figure 6.17 Flow rate of the permeate in feed-forward control mode over 1 day

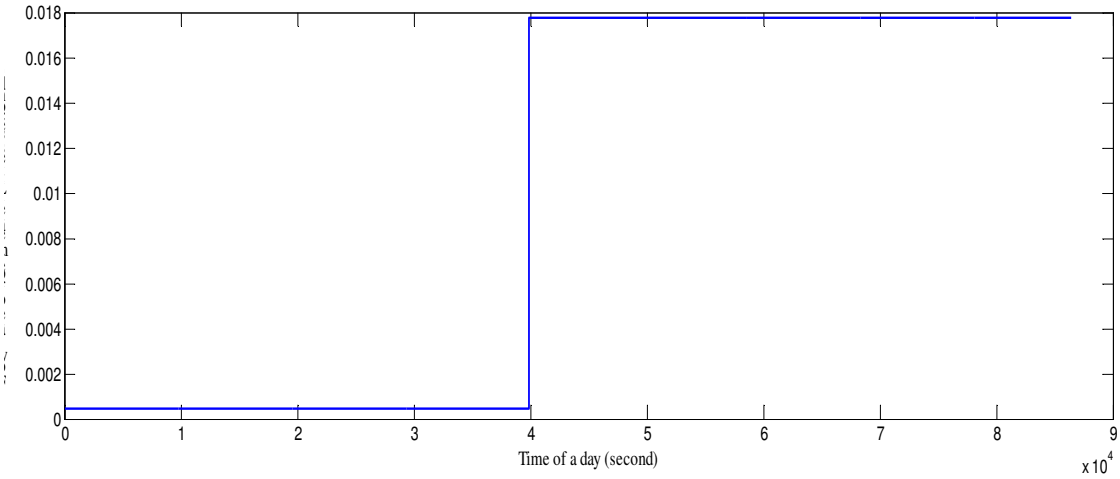

Figure 6.18 – Flow rate of the permeate in toggle control mode over 1 day

Over a 24 hour time period the simulations in each control mode generated useful data that interpreted the performance of the RO system, especially in terms of the permeate flow, power consumption, and water level in the product water tank.

Figures 6.16, 6.17, 6.18 present the trending of the permeate flow rates over 24 hours. The permeate flow is totalized to reveal the entire water volume produced by the RO system. The transient power consumptions of the system in each control mode are recorded in Matlab and plotted as observed in figure 6.19, 6.20, and 6.21.

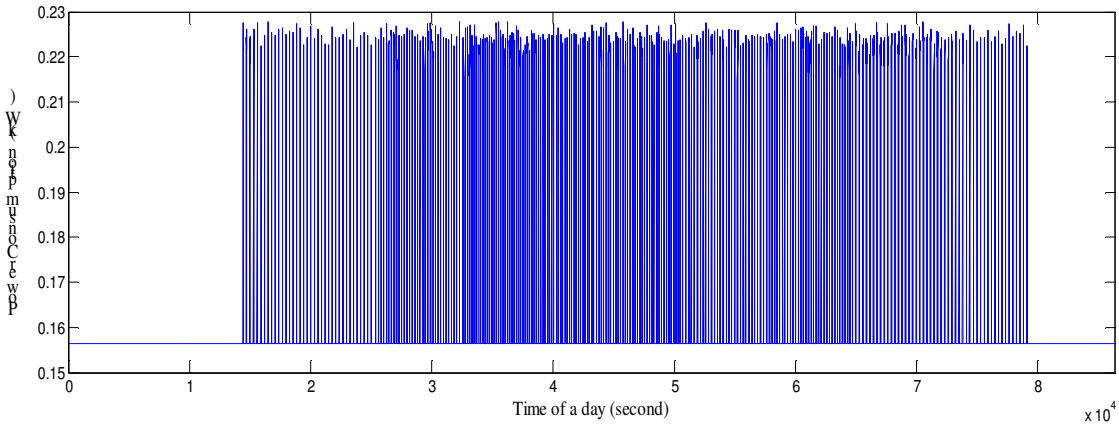

Figure 6.19 – RO System power consumption in PID control mode over 1 day

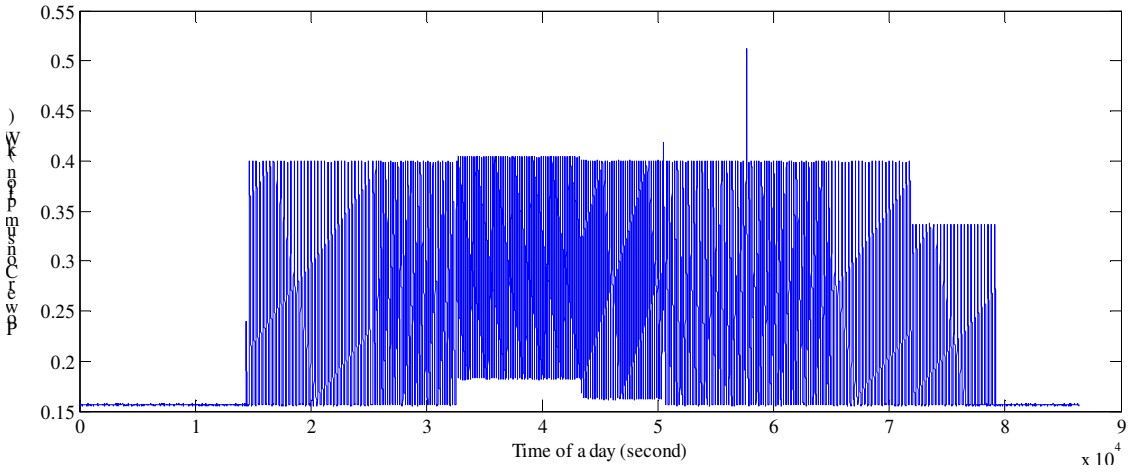

Figure 6.20 – RO System power consumption in feed-forward control mode over 1 day

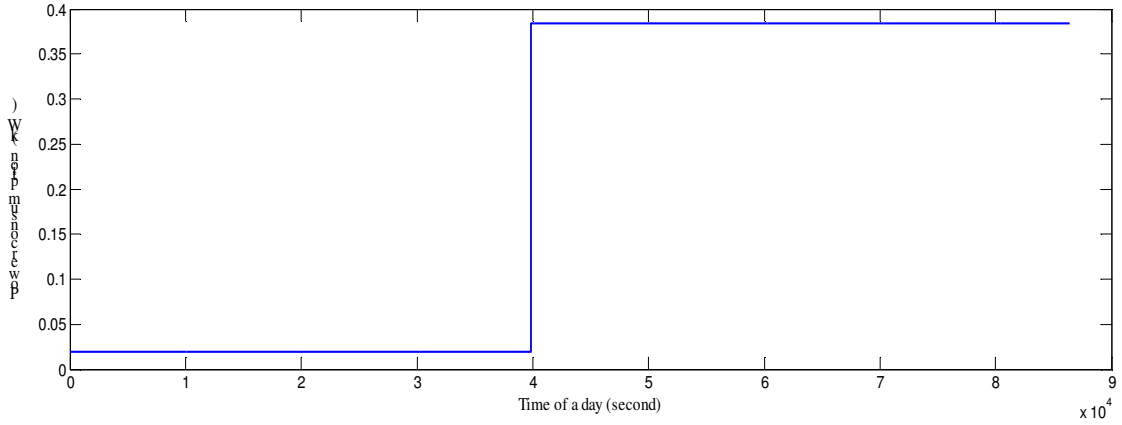

Figure 6.21 – RO system power consumption in toggle control mode over 1 day

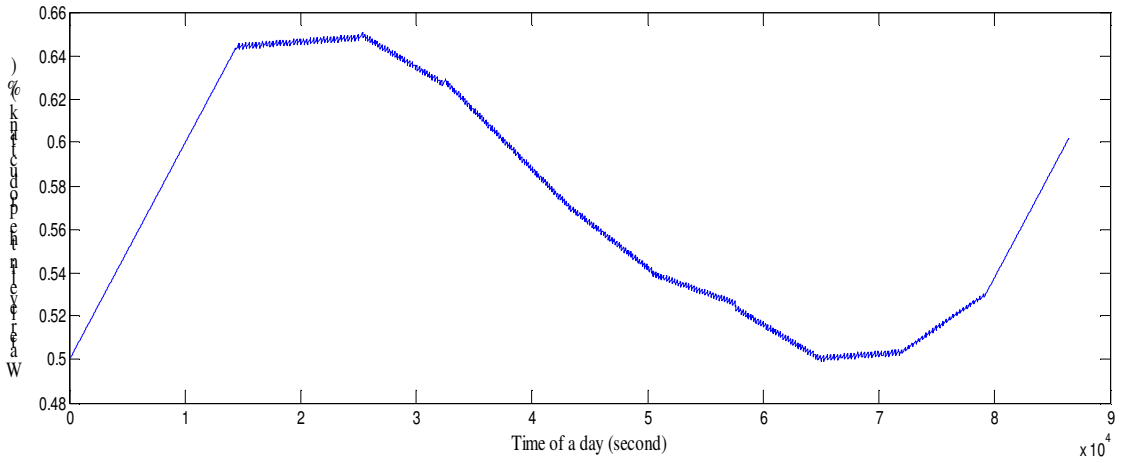

Figure 6.22 – Water level in the product in the PID control mode tank over 1 day

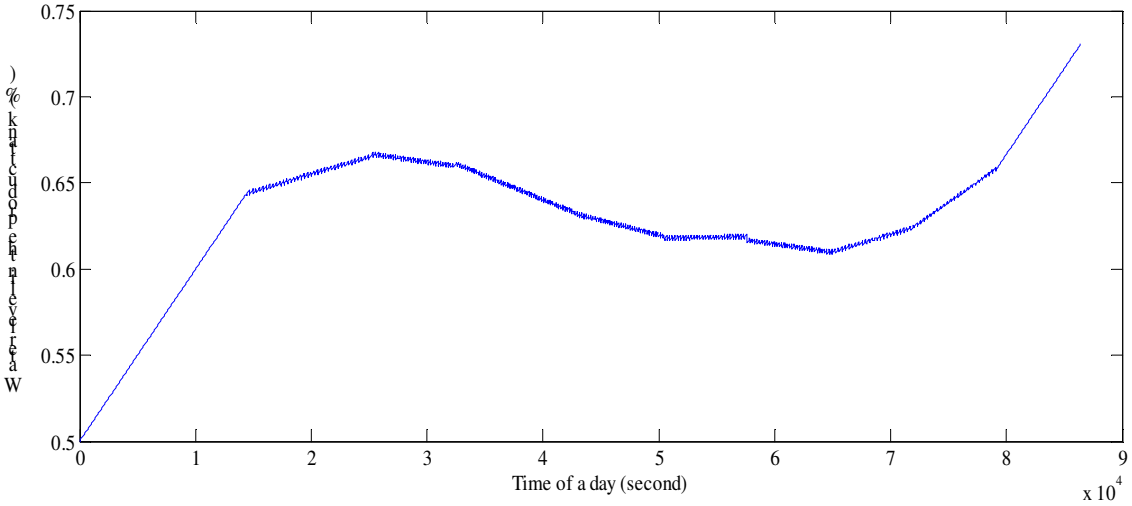

Figure 6.23 – Water level in the product tank in the feed-forward control mode over 1 day

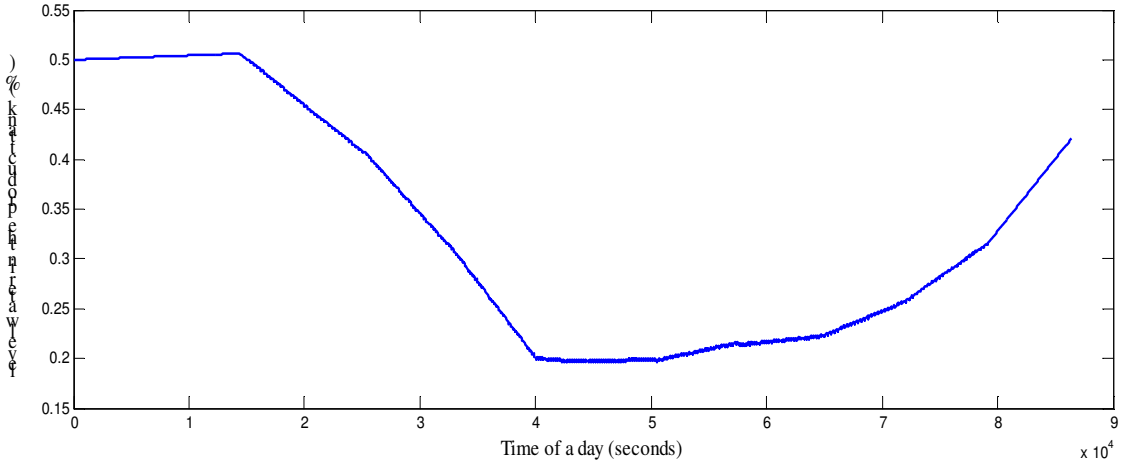

Figure 6.24 – Water level in the product tank in the toggle control mode over 1 day

Water levels in the storage tank are trended and displayed in figure 6.22, 6.23 and 6.24. They are the plots in sequence of PID control, feed-forward control and toggle control. All of the curves start at 50%, as the initial water level is set as half of the capacity of the product tank. It is seen that the water level drops down to 20% at around mid-day when the water consumption is relatively higher than some time around twilight.

6.6.2.2 System Long Term Performance in Each Control Mode

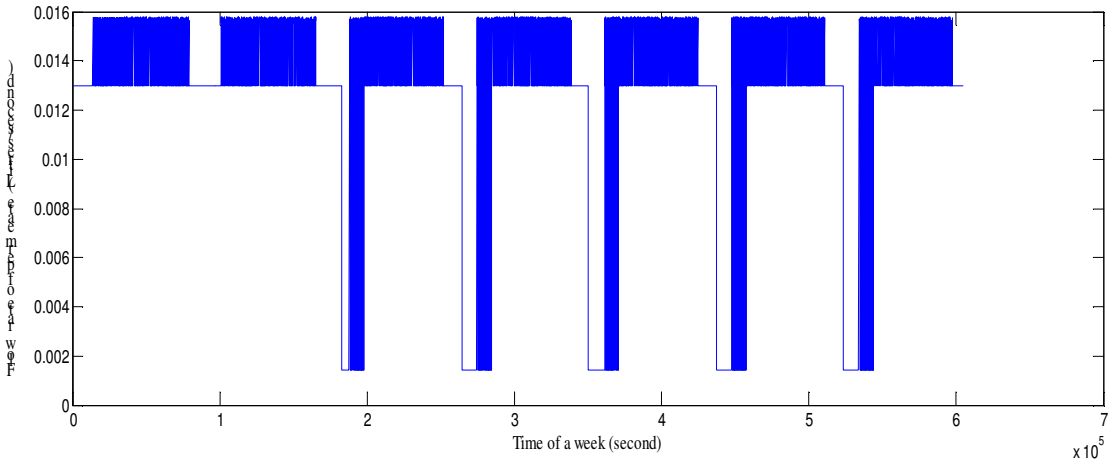

Figure 6.25 – Permeate flow rate of the RO system in PID control mode over 7 days

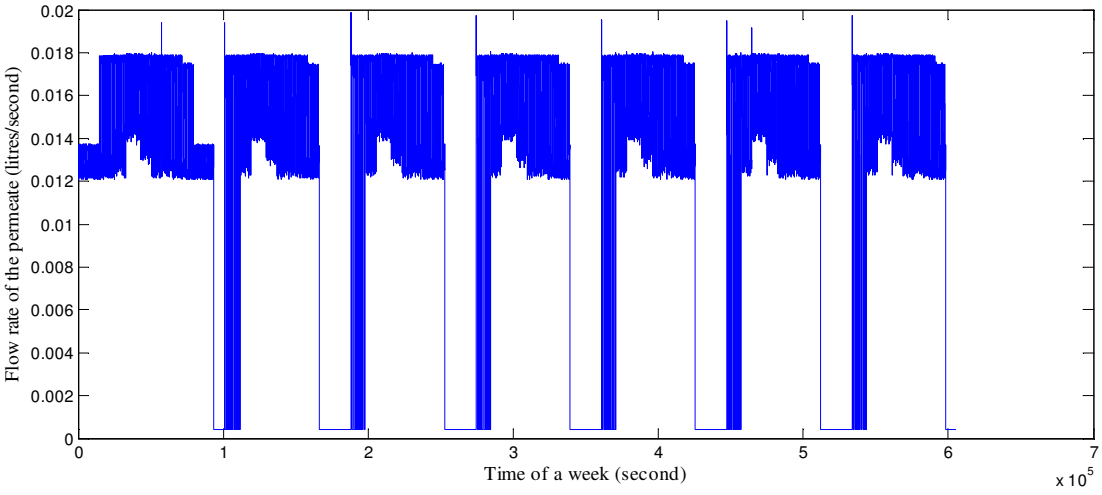

Figure 6.26 - Permeate flow rate of the RO system in feed-forward control mode over 7 days

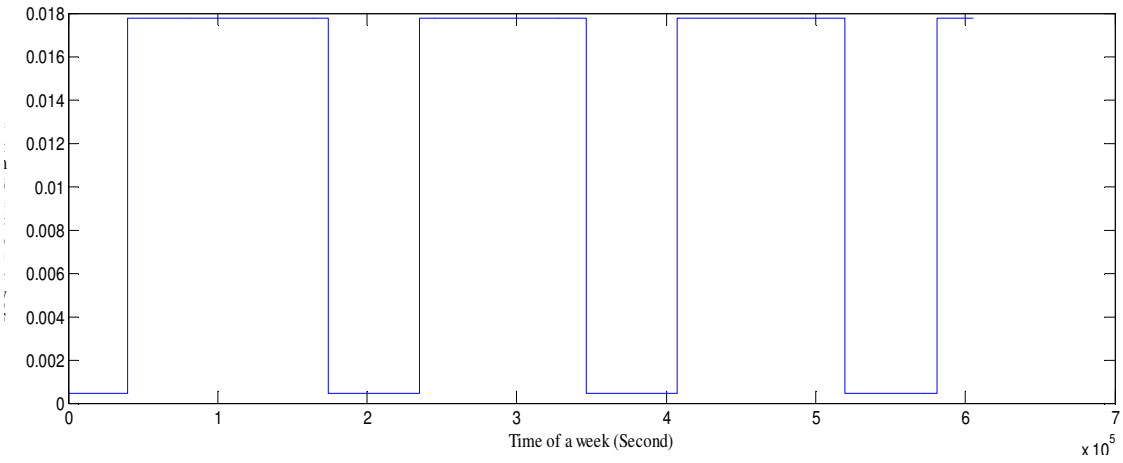

Figure 6.27 – Permeate Flow Rate of the RO system in toggle control mode over 7 days

The System inputs and outputs were monitored and recorded over 7 days in which the simulations were running continually. During those periods, the permeate flows of the RO system are trended and shown in figure 6.25 and 6.26 in the sequence of PID control and toggle control. The water levels in the product tank are exhibited in figure 6.27 and 6.28. In toggle control mode, the tank's water level fluctuates in between 20% and 80% over the week. It is found that the tank's water level stayed at above 60% most of time while the system was in PID control mode (figure 6.27).

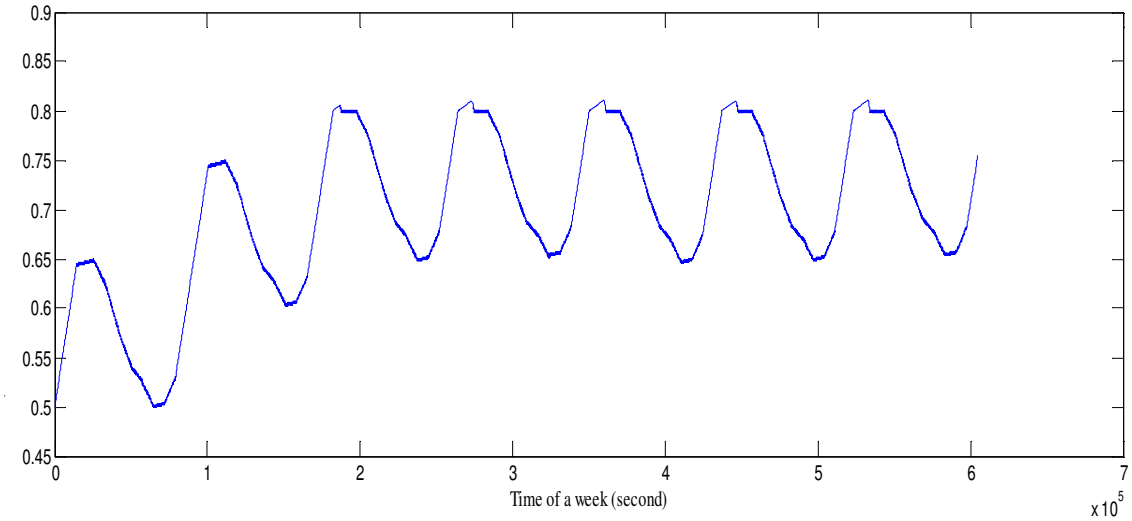

Figure 6.28 - Water level in the product tank in PID control mode over 7 days

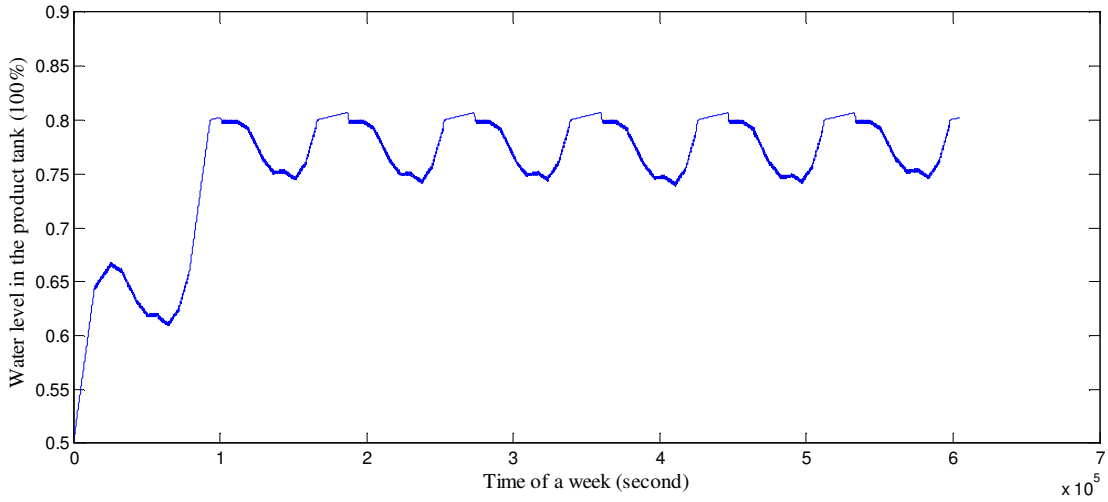

Figure 6.29 – Water level in the product tank in feed-forward control mode over 7 days

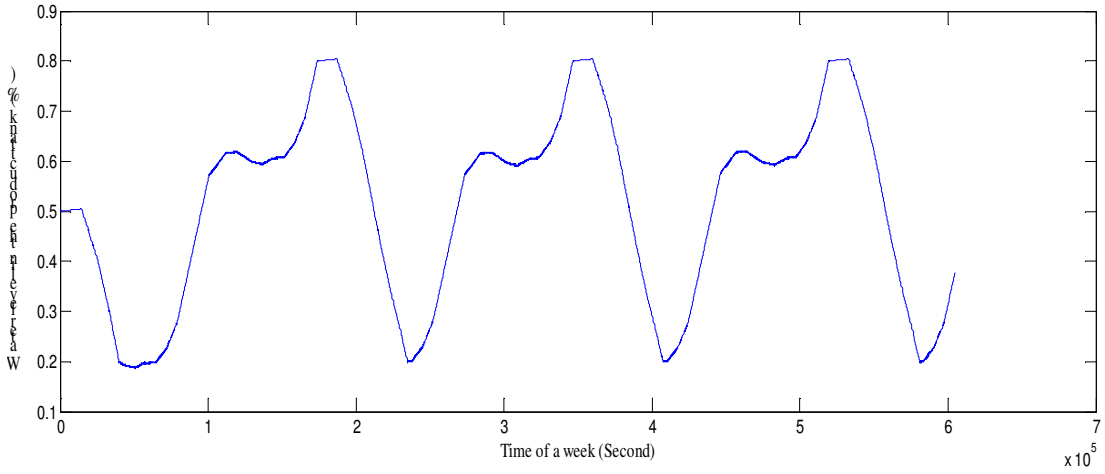

Figure 6.30 – Water level in the product tank in toggle control mode over 7 days

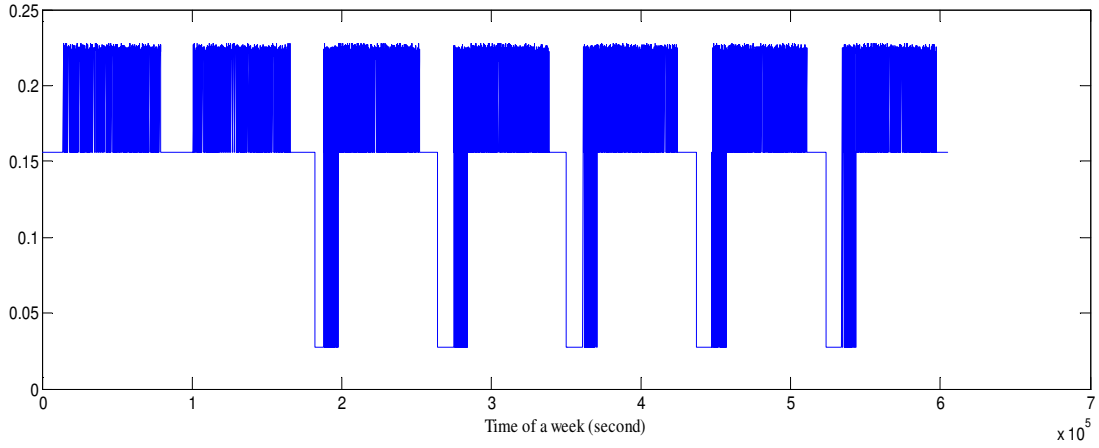

Figure 6.31 – Power consumption of the RO system in PID control mode over 7 days

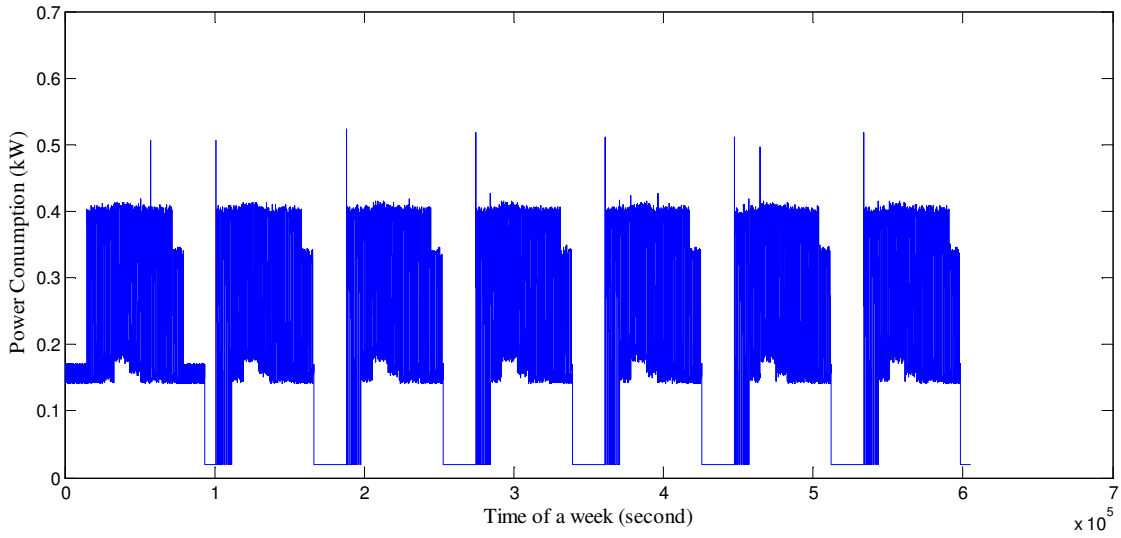

Figure 6.32 – Power consumption of the RO system in feed-forward control mode over 7 days

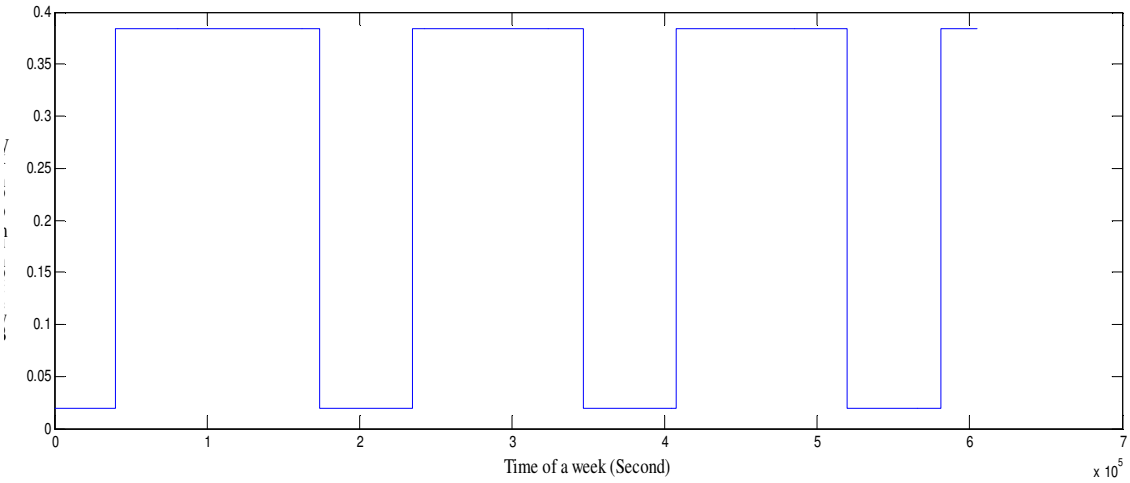

Figure 6.33 – Power consumption of the RO system in toggle control mode over 7 days

6.7 Simulation Results Analysis

6.7.1 Improvement to the Productivity of the System

Productivities of the RO system with those three control strategies were compared and displayed in figure 6.31. Noticeably, the feed-forward control and PID control have better productivities than the toggle control. Particularly, PID control and feed-forward control can produce a greater volume of the fresh water which is up to

392.7 litres and 490.6 litres than the toggle control. Furthermore, the productivities of all those control systems decline as the feed water conductivities increase.

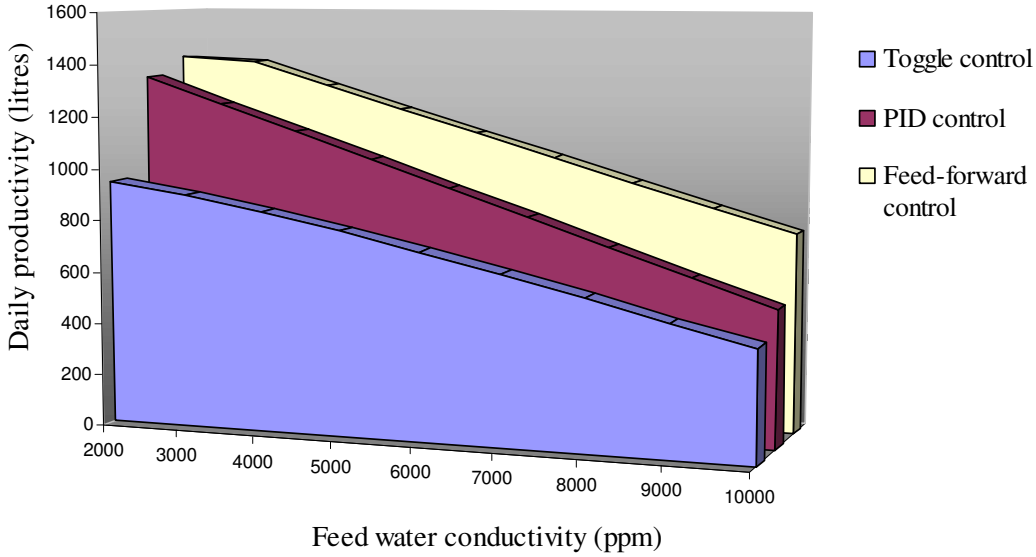

Figure 6.34 – Water productivities of the RO system in different control modes over a series of feed water conductivities

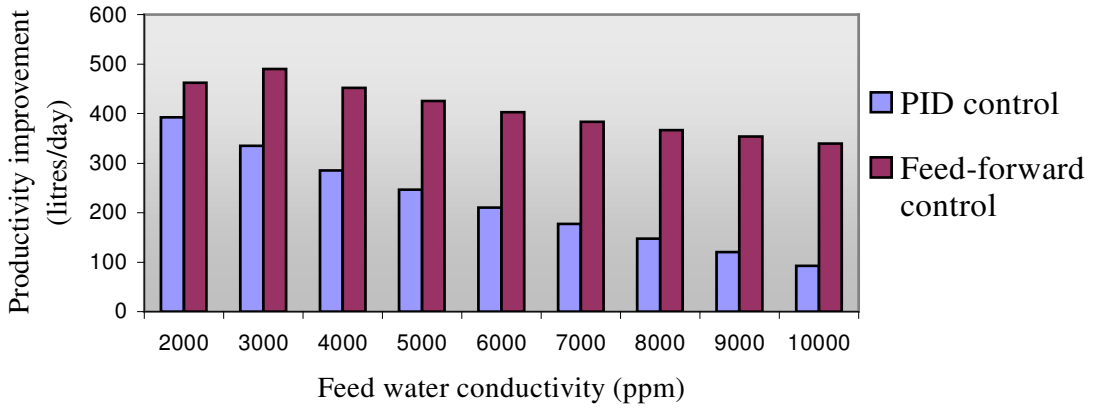

Figure 6.35 – Daily productivity improvement of the RO system with PID and feed-forward control compared to the toggle control

With PID and feed-forward control, the improvements of productivity of the RO system are significant. As shown in figure 6.35, the net increase of the fresh water is at least 100 litres and 360 litres respectively by using PID and feed-forward control. In particular, the improvement of the system productivity from using feed-forward

control is dramatic and static which indicates that the feed-forward control would be capable of providing more fresh water than the PID and toggle control within any feed water salinity condition.

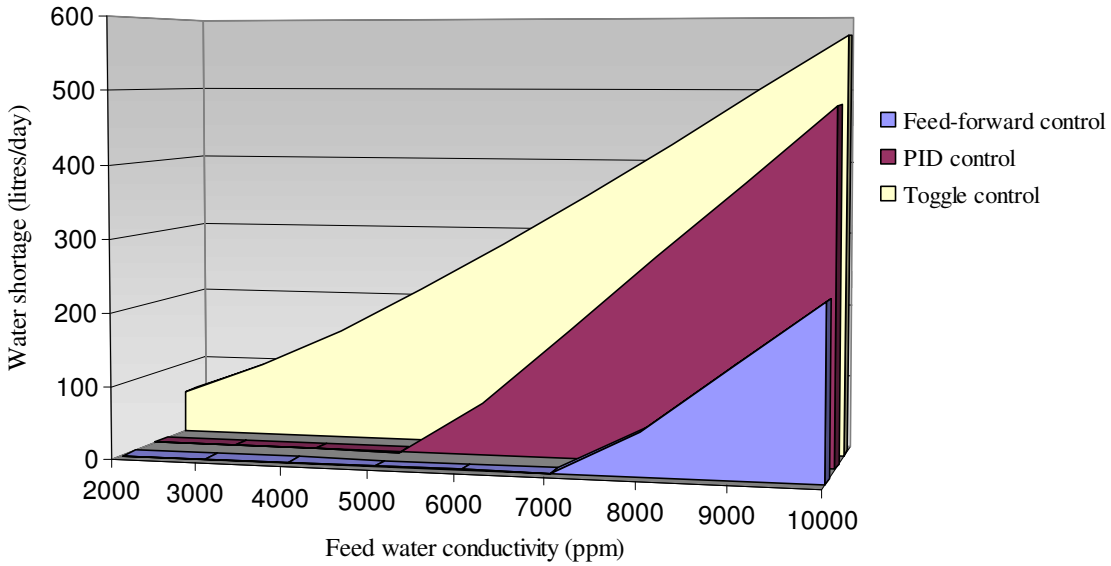

Figure 6.36 – Daily Water supply shortage in different control modes over a series of the feed water conductivities

Observing in figure 6.36, the daily water supply shortage for each control system is charted by comparing the water demands created in section 6.1.1. When the feed water conductivity is at the high levels, a shortage of the water supply occurs. This tends to become significant for the toggle control to which the deficiency of water supply is always problematic.

PID control does have water supply shortage; however that only happens when the feed water conductivity reaches up to 5,000ppm. The shortage turns out to be more serious when the source water conductivity goes higher than 5,000ppm. The biggest deficiency is about 420 litres water as the source water concentration is 10,000ppm.

Feed-forward control does a good job in terms of maintaining the lower rate of water supply deficiency. It only allows 200 litres water shortage when the feed water concentration is 10,000ppm.

6.7.2 Reduction in the Energy Consumption of the System

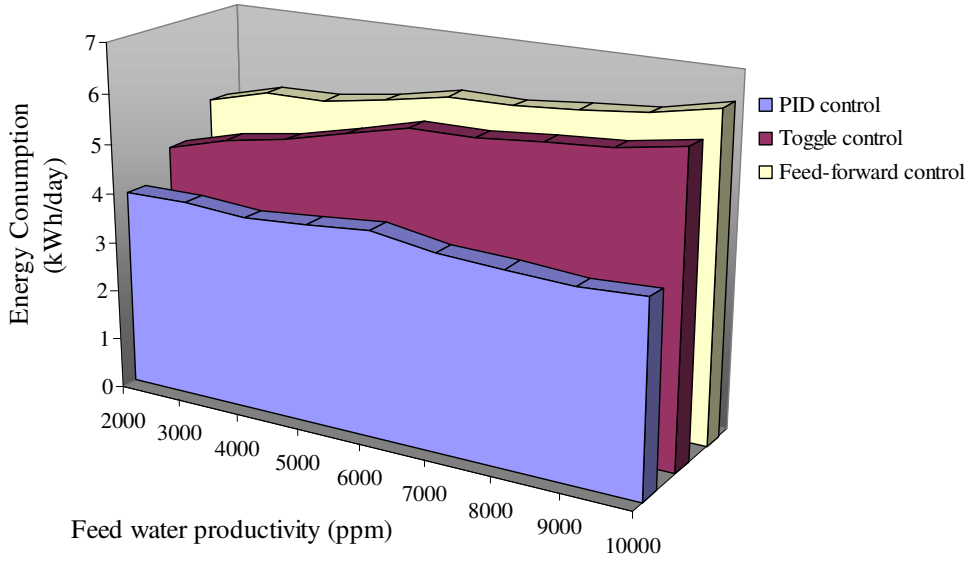

Figure 6.37 - Energy consumptions of the RO system in control modes over a series of feed water conductivities

Although the RO system having the feed-forward control system gives the best performance in productivity, it has the highest daily energy consumption which is presented in figure 6.37. Yet, the PID control system has the profile of the least daily energy consumption. This leads to the envisagement in the energy saving of the RO system using PID control.

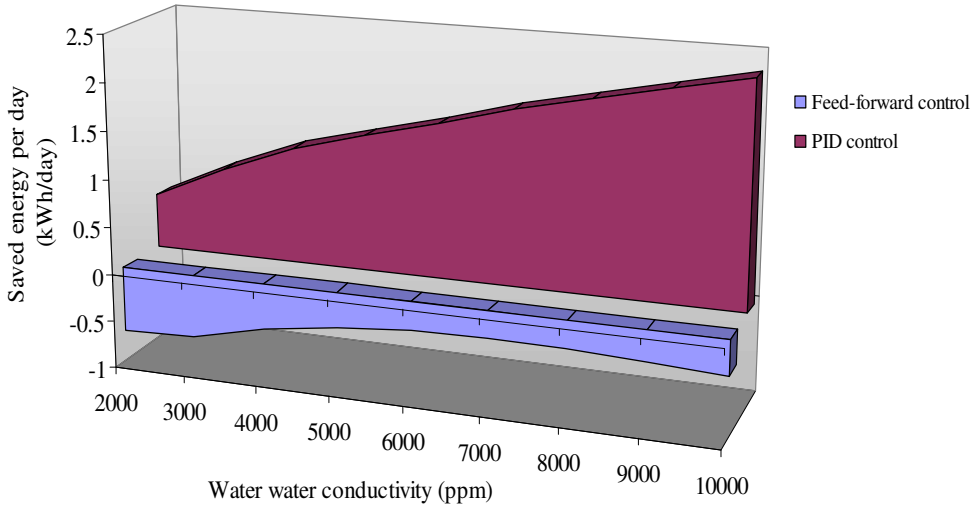

Figure 6.38 – Daily energy saving of the RO system with PID control and feed-forward control compared to the toggle control

6.7.3 Enhancement in the RO System Efficiency

Efficiency study is the main theme throughout the work. It has a formidable role in making a selection from the listed control strategies, because the high efficiency of the RO system will bring up the system productivity with the least amount of energy. In order to find the RO system efficiencies for each control scheme, the equation is used and given as:

$$Efficiency = \frac{productivity}{Consumption} \tag{6.1}$$

Where

Productivity states the volume of the water produced from the RO system in litres.

Consumption means the total energy consumed by the RO system daily, kJ.

Based on this the equation above, the efficiencies of the RO system with different control systems were calculated and articulated in figure 6.39. It shows that the efficiency of the RO system decreases for all control systems when the source water conductivity is lowered. However, the PID control is always at a higher efficiency level than the others. This states that the designed PID loop is capable of efficiently controlling the RO system.

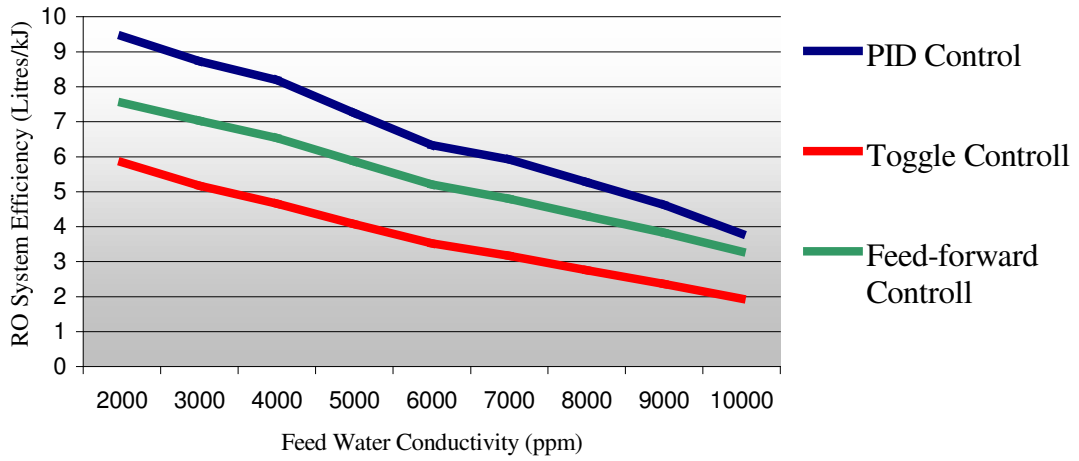

Figure 6.39 – RO System efficiencies in different control modes over a series of feed water conductivities

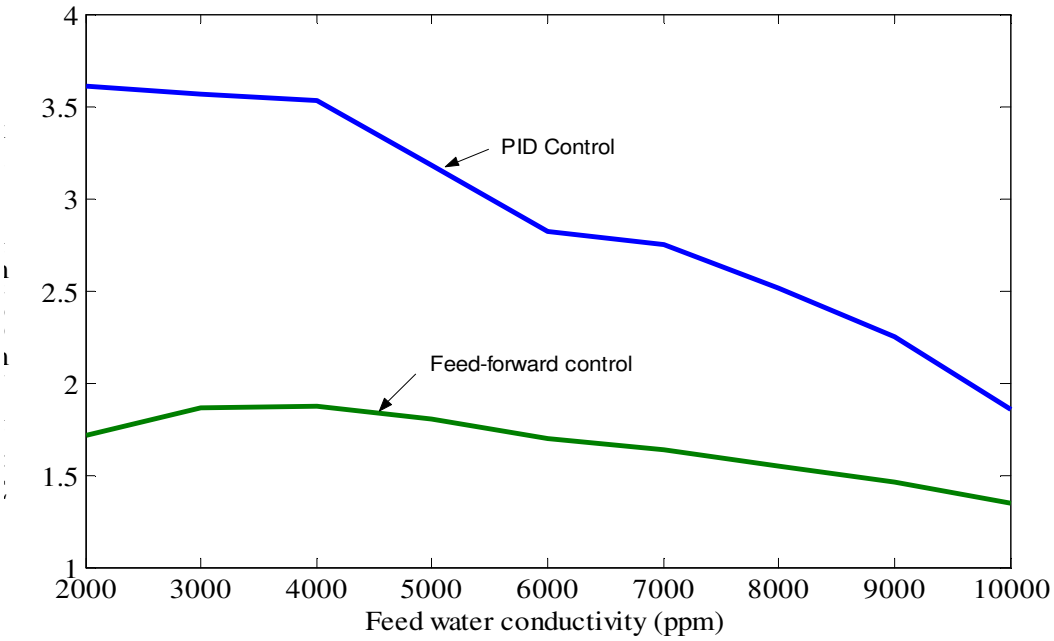

Figure 6.40 – Efficiency improvement of the RO system with PID control and feed-forward control compared to the toggle control

Comparing the efficiencies of the RO system with those three control systems, a more vivid observation can be obtained in terms of the system efficiency improvement. As seen in figure 6.40, PID control overwhelms the feed-forward control and increases the system efficiency up to 3.5 Litres/kJ in contrast to the toggle control. This result from the simulations predicts the functionality of the PID control and its outstanding performance in enhancing the RO system efficiency.

6.8 References

[1] Kaikhurst Eric T., "Village Electrification an Evaluation of Options in remote Area systems," *The World Directory of Renewable Energy Suppliers and Services*, 1998

[2] Marcos S., David I., A wind-powered seawater reverse osmosis system without batteries. *Desalination* (2002), 153, 9-16.

[3] Al-Alawi, A., *An integrated PV-diesel hybrid water and power supply system for remote arid regions*, Curtin University, Perth, 2004.

[4] Slater, CS, Brook, CA, III. *Development of a simulation model predicting performance of reverse osmosis batch system*, Separation Science and Technology, 1992, 27(11), 1361-1388.

[5] The MathWorks Inc., Natick, and MA 01760-1500. *SIMULINK (R), Dynamics System Simulation for MATLAB (R) Version 2.2 edition*, 1998.

[6] The Mathworks. *Matlab Documentation (Using MATLAB Version 6.5)*, 2001.

[7] Http://www.nps.gov/rivers/waterfacts.html [Access in 2006].

CHAPTER 7 EXPERIMENTAL EVALUATION OF A SMALL-SCALE REVERSE OSMOSIS DESALINATION SYSTEM

In order to implement the ideas generated in chapter 5 regarding the new control strategies, a reverse osmosis desalination system was built and series of experiments were conducted. For the time and geophysical limitations, the RO system was not able to be tested in the mini renewable energy power supply system. However, the idea regarding load following control was implemented and proved to be more efficient than the conventional toggle control. Experimental Data was plotted and provided in this chapter.

7.1 Experimental Set-up

With the specification listed in chapter 3, components were assembled according to their functions. The system was divided into three major groups of components: the PLC and SCADA unit; the reverse osmosis desalination unit; the variable speed inverter. Additionally, some other components such as signal conditioners, power supply, sensors and transducers are required to be set up.

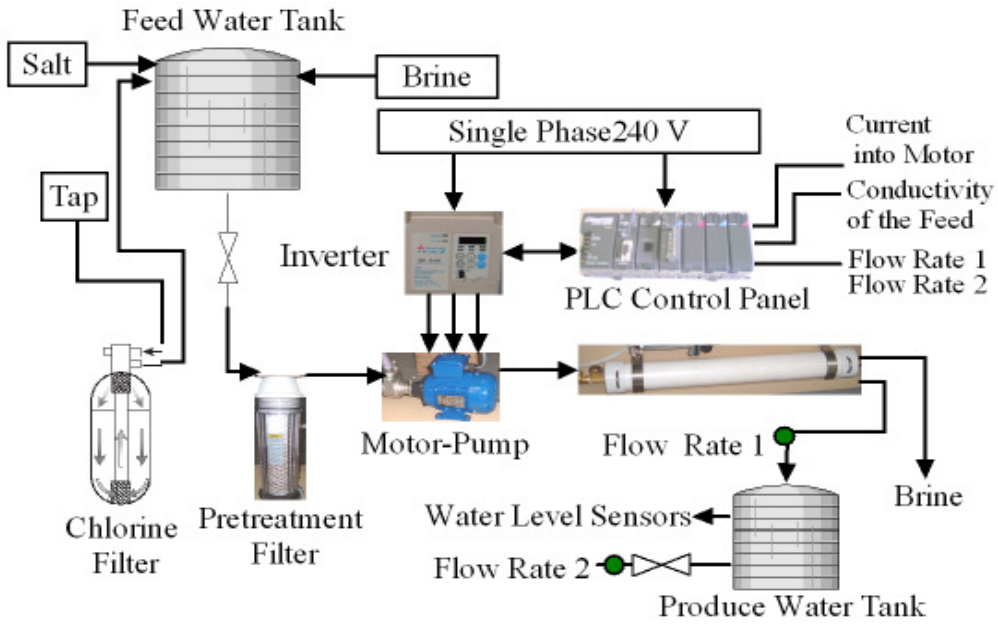

Figure 7.1 -The experimental set-up for RO system

7.1.1 Setup of the PLC and SCADA

The layout of the PLC control panel is displayed in figure 7.2. The PLC requires 230 V AC power source as well as a 24 V DC power supply. As seen in figure 7.2, two 24 V DC power supplies (the one drawn with dotted line is a backup power supply) are mounted beside controller to supply the power for sensors, transducers, and a DC water pump.

There are totally 43 terminals needed for wiring up the instruments with the PLC. Most of the then can share the common lines. 250 ohm resister is required to connect in parallel to the analogue signal input channel of variable speed drive.

Table 7.1
Terminal allocation in PLC

I/O Type	Channels	Terminals per channel	Common	Terminals
Digital Inputs	7	2	1	15
Digital Outputs	5	2	1	11
Analogue Inputs	7	2	1	15
Analogue Outputs	1	2	0	2
			Total	43

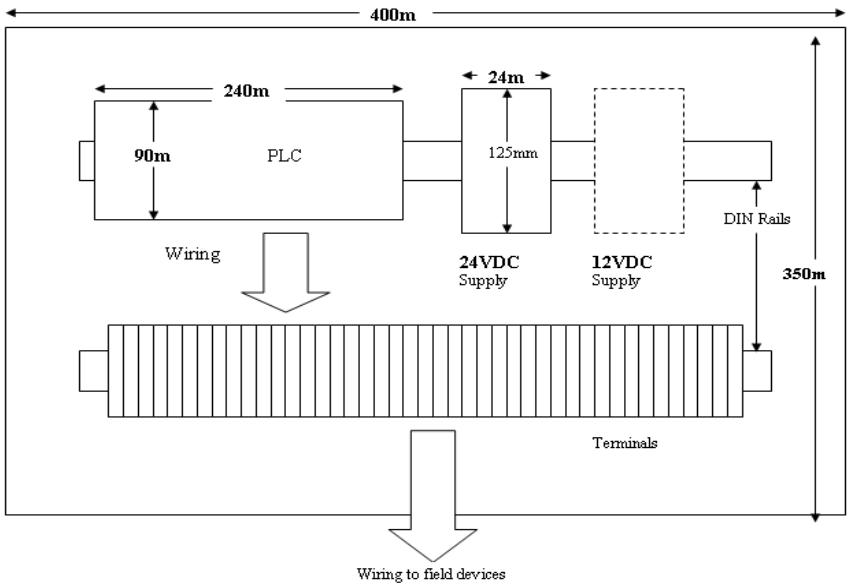

Figure 7.2 -Layout of the PLC panel

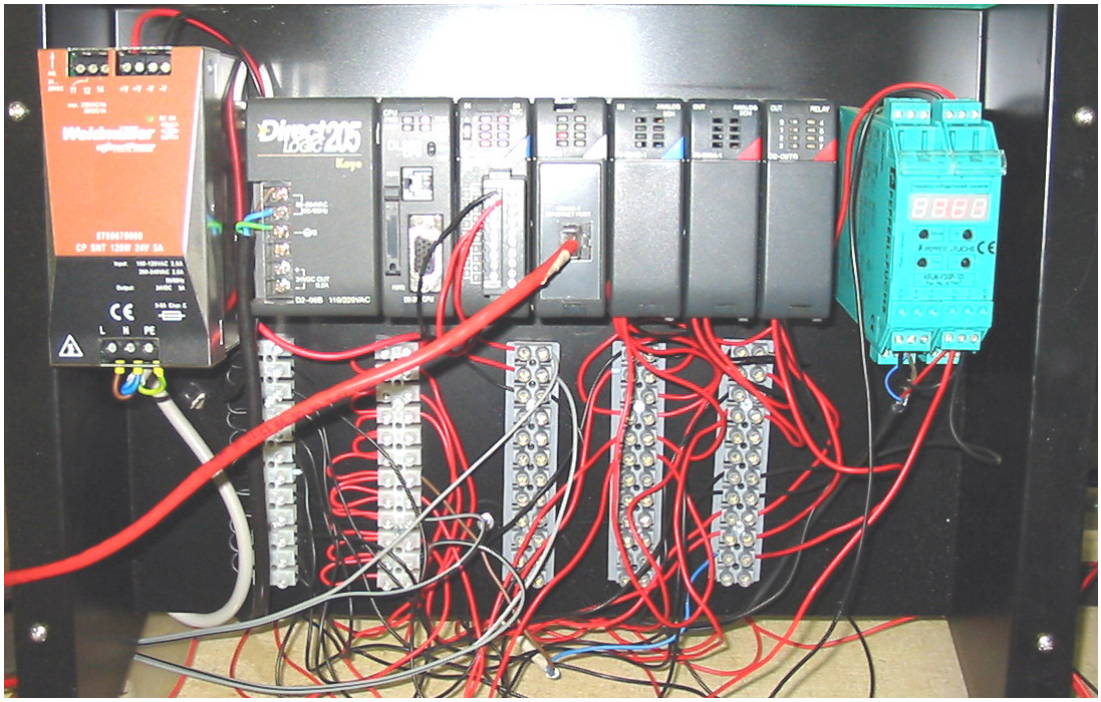

Figure 7.3 – Photo of the PLC with a 24 V DC power supply and terminals

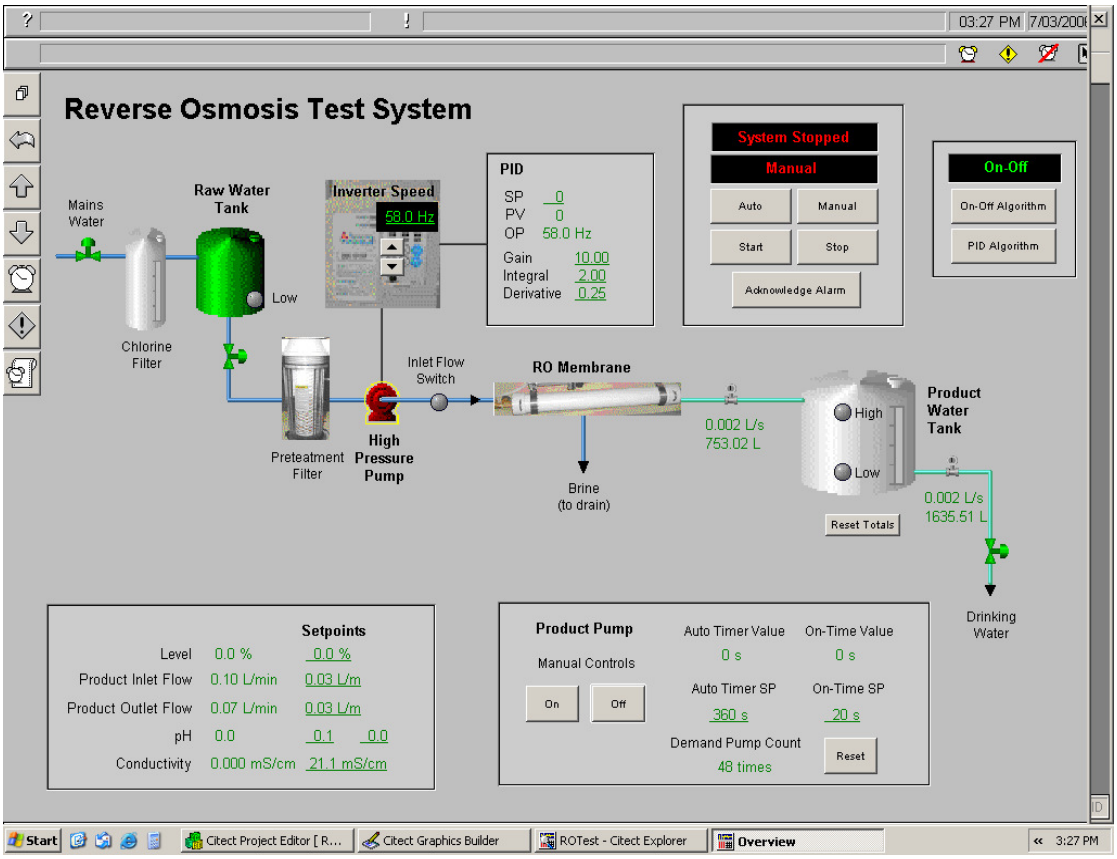

Figure 7.4 - Screen image of the main page of Citect SCADA

7.1.2 Set-up of the Reverse Osmosis Unit

Two flow meters were carefully positioned onto the reverse osmosis unit. One was mounted at the outlet of the membrane cylinder and another one was fixed at the outlet of the product water tank. Signal conditioners (frequency to current converter, frequency to voltage converter, voltage to current converter) were connected between the flow meters PLC. An analogue pressure meter originally mounted together with RO membrane unit supplied pressure reading that can be obtained from manual observations. The motor of the RO unit gains its power from the variable speed drive.

Figure 7.5 - Photo of the motor-pump section of the RO unit

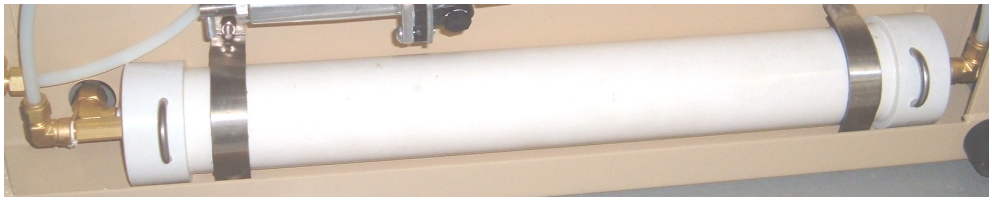

Figure 7.6 - Photo of the membrane cylinder

7.1.3 Set-up of the Water Tanks

A water tank with the capacity of 315 liters is used to store the salt water (feed water). It has an input connected with a water tap. Certain amount of the salt was weighted and dissolved into the water in the tank before every experiment.

Another water tank with the capacity of 20 liters is used to hold permeate (product water) produced by the RO membrane. A DC water pump is placed at the bottom of the tank to draw the water out of the tank. This pump is used in the simulation of the different water demands. It can be controlled automatically and manually.

Figure 7.7 – Photo of the feed water tank

7.1.4 Set-up of Variable Speed Inverter

The single phase to three-phase inverter described in chapter 3 was assembled into the RO system. It takes in the single phase AC power from the local power grid and inverts to be three-phase AC power which then is supplied to the motor drive. It has a digital manual control panel where parameters for different functions can be set up. It also has a RS485 communication terminal that allows another controller to access this inverter via a 3 cords communication cable. Unfortunately, this terminal was tested and proved to be in faulty conditions. However, the inverter has another set of control terminals which were found functioning positively. By connecting to these terminals, the controller is able to switch on and off the inverter's power supply to the motor. Also, the frequency reference of the inverter can be changed by the controller via an analogue output channel of the PLC. This analogue output signal was produced in current format ranges from 4-20mA and needs to be scaled into operation range of the inverter.

Figure 7.8 - Photo of the variable speed inverter

7.1.5 Set-up of signal conditioners

Signal conditioners were wired into the system, particularly the output of the signal conditioners were connected to input module of the PLC. The photos of these signal conditioners are displayed as below (Figure 7.9 – 7.11).

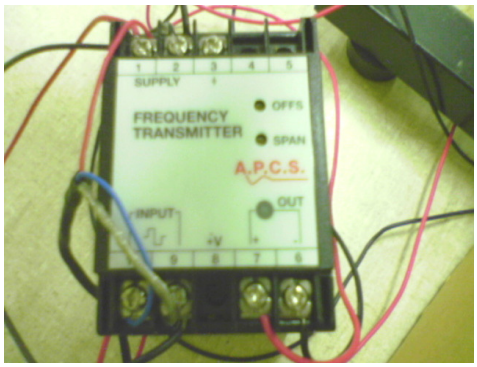

Figure 7.9 – Photo of the frequency to voltage converter

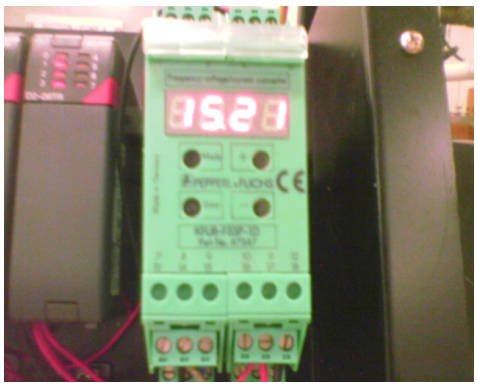

Figure 7.10 – Photo of the frequency to current converter

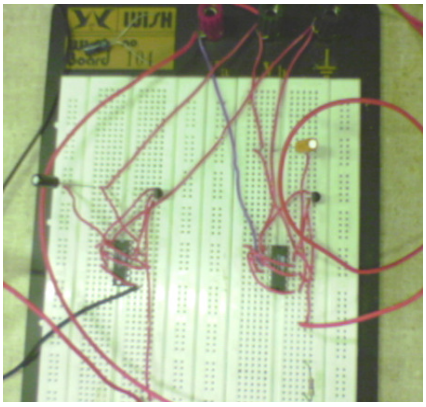

Figure 7.11 – Photo of the circuitry of voltage to current converter

7.1.6 Set-up for sensors and transducers

Two flow meters were fixed at the inlet and outlet of the product tank, respectively. Energy Meter (Fluke) was attached to the variable speed inverter. The photos of these meters were shown as below (Figure 7.12 – 7.14).

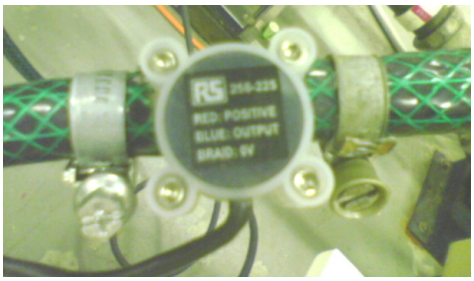

Figure 7.12 – Photo of the flow meter

Figure 7.13 – Photo of the Fluke meter

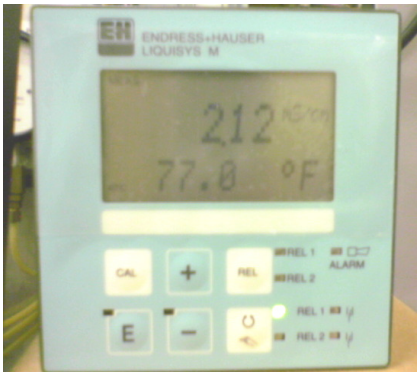

Figure 7.14 – Photo of the conductivity meter

7.1.7 Photo of the Experimental Set-up of the RO system

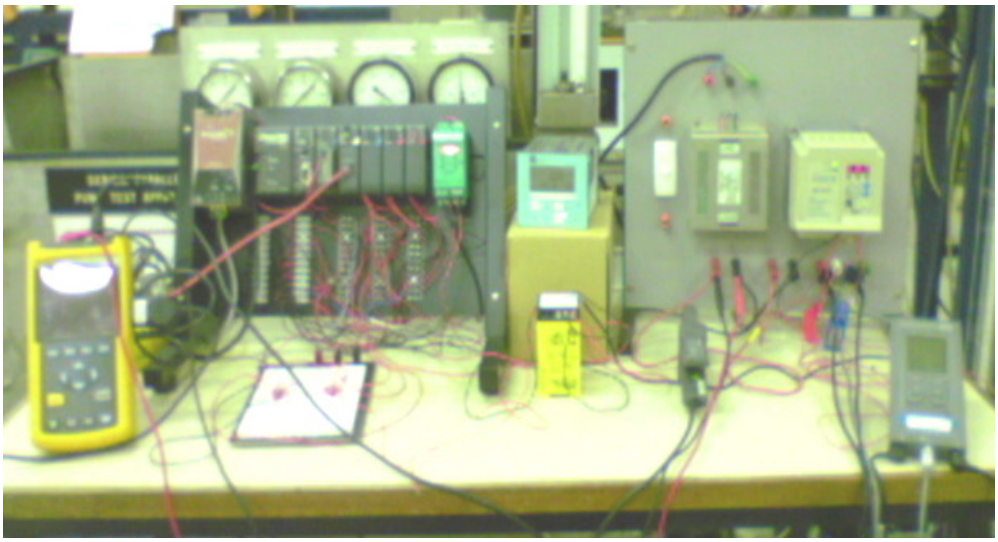

Figure 7.15 – Photo of the RO system experimental set-up

7.2 Experimental Procedure

7.2.1 Programming for Water Demands

7.2.1.1 Functions of the Product Water Pump

The following are the test characteristics of the test RO system:

- Product tank capacity is 20 litres

- 3 litres water can be pumped out of product tank using a DC water pump over 20 seconds
- 1.10 litres water can be produced at 50Hertz power supply frequency per minute when the conductivity of the feed water is 3000ppm

The purpose of the test is to find the efficiency of the novel algorithm compare with the conventional On-Off control. In reality, the water tank is bigger than the 20 litres. And the water in the tank will be completely drawn out relatively slower. Hence, the simulated water demands will be somehow less than the water input. The water level in the tank will be seen rising gradually until it reaches the high level set-point and RO pump stops. Afterwards the water level will drop as the demand continues until it hits the low level switch and RO pumps resumes running.

7.2.1.2 Calculation for the water demand

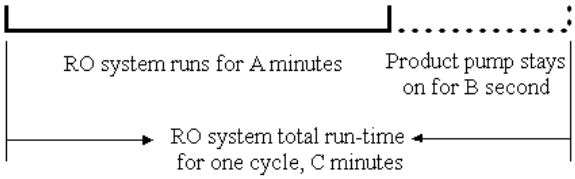

Figure 7.16 Simulation cycle of water demands

Set the length of time as **a** (mins), during this period, product water goes into tank without any consumption. After A mins, the demand is turned on while the RO system still producing water.

For criteria (1):

$$1.08 \times (a + \frac{1}{6}) - 1.4 > 0$$

Hence,

$$a > 2.96 \approx 13 \min s$$

Which means, the demand side pump shall be turned on every 13 mins at 50 Hertz

As it is noticed, product tank will be filled out over the certain length of time. This period is set as parameter B. For the test purpose, B is designed to be closer to reality. Thus, B is chosen to be 1 hour.

For criteria (2):

$$\frac{20}{1.08A - 13.82} \times (a + \frac{1}{6}) = B = 60 \min s$$

Thus,

$$a = 18.58 \approx 19 \min s$$

The criteria 2 tells how long it takes to fill out product tank (20 litres) at the pump rate a.

7.2.1.3 Water Demand Scenarios

The water demands are varying depends on the geography, climates, population density and other specific factors. For the RO system is designed as a generic prototype, in accordance with producing ability (1000 litres/ day) and average water consumption per capita (3 litres/ day), water consumption is scaled into three major scenarios:

High water demand:

$$\frac{1000}{24} \div 1.4 \approx 30 times\,, \frac{1 \times 60}{30 times} = 2 \min s$$

Which means the product pump runs every 2 mins.

Medium water demand:

$$\frac{600}{24} \div 1.4 \approx 18 times\,, \quad \frac{1 \times 60}{18 times} \approx 3 \min s \text{ and 30 seconds.}$$

Which means the product pump runs every 3 mins.

Low water demand:

$$\frac{155}{24} \div 1.4 = 4.6 \approx 4 \text{ and half times. } \frac{1 \times 60}{4.5 times} \approx 13 \min s$$

Which means the product pump runs every 13 mins.

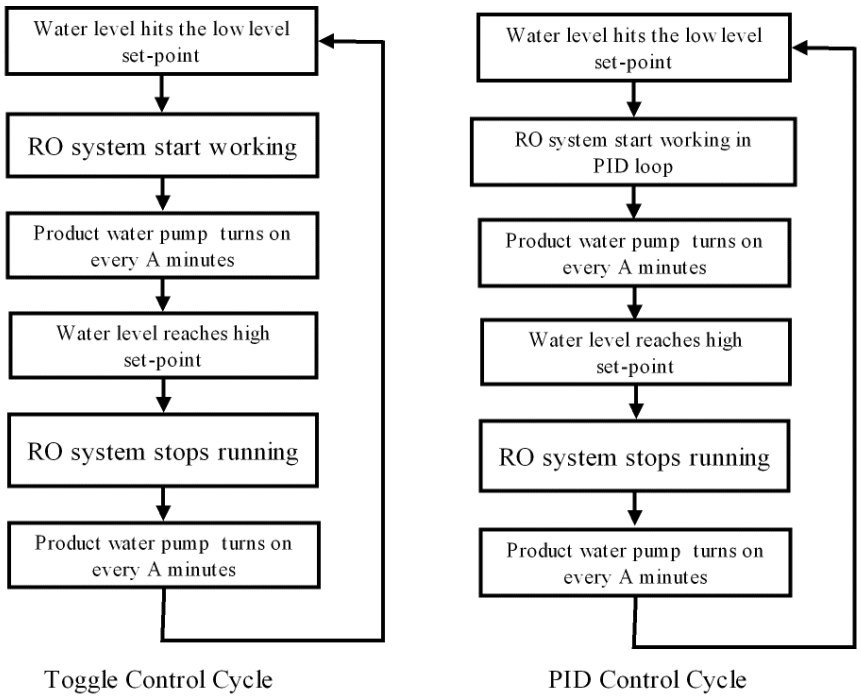

Figure 7.17 Different Control cycles in a certain water demand scenario

7.2.1.4 Product Water Pump Programming

The product pump requires 24 V DC power. This is supplied by the 24 V DC power source on the control penal. Power wire of this pump is connected to one of the relay out put on the PLC in serial. So, the PLC controls the operations of the pump. This makes it feeble to simulate the aforementioned water demand scenarios. By reading and using the time register in PLC, the water demands in larger scale and longer period can be simulated. For example, the PLC has a register-V7770 where the hour of a day is held. A rung of the ladder program shows (Figure 7.18) that if the hour of a day is equal to zero (i.e. midnight), PLC will read the information from register K180 where the certainly type of water load is programmed and stored.

Figure 7.18 - The image of the PLC ladder diagram about using the "hour" register

7.2.2 Experimental Results

7.2.2.1 Short Term Performance

The following experiments were conducted on 15th Feb., 2006. Power consumptions of each test was retrieved from the power meter (Fluke) mentioned in chapter 3. Over the tests' periods, the following values were recorded: operation mode of the controller, temperature and conductivity of the feed water, parameters of PID loop, length of tests, average power consumptions. Inlet and outlet flow rates of the product water tank, transient power consumptions were trended in PLC and Fluke energy meter respectively.

Table 7.2
PID control test in experiment 1

Operation Mode	PID
Water Demands	Medium
Total Length (m)	21
PID Parameters	10,2,0.25
Conductivity (ppm)	2000
Temperature (C^0)	26
Average Power (kW)	0.22
Total Energy Consumption (kJ)	277.2
Start-up Level of Water in the Product Tank (L)	1.5
Number of Switch-on of Product Pump	3
Stop Level of Water in the Product Tank (L)	18

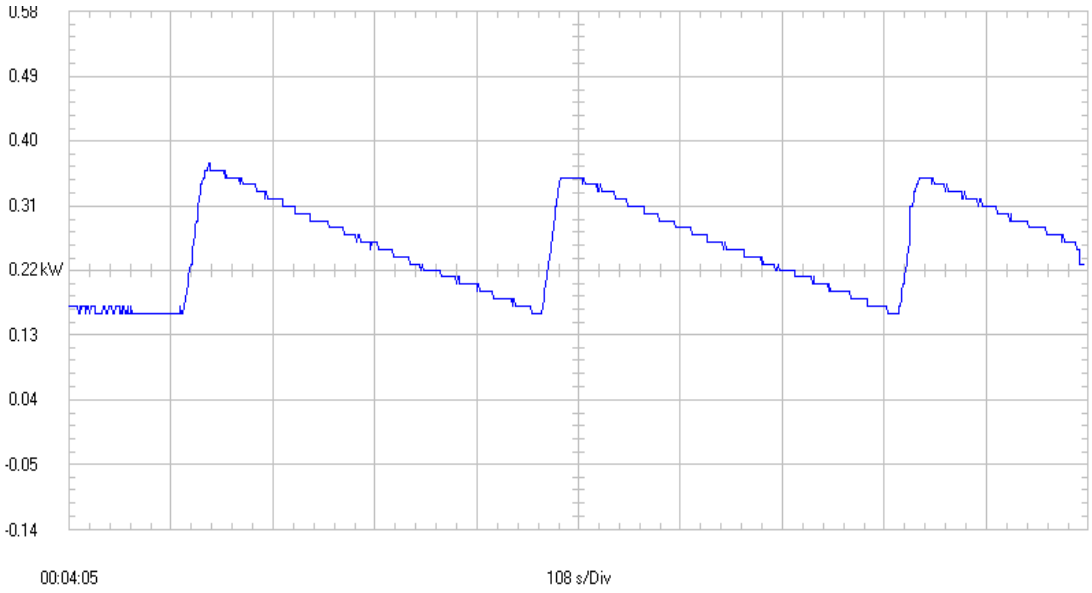

Figure 7.19 - Transient power consumption of the RO system with PID control

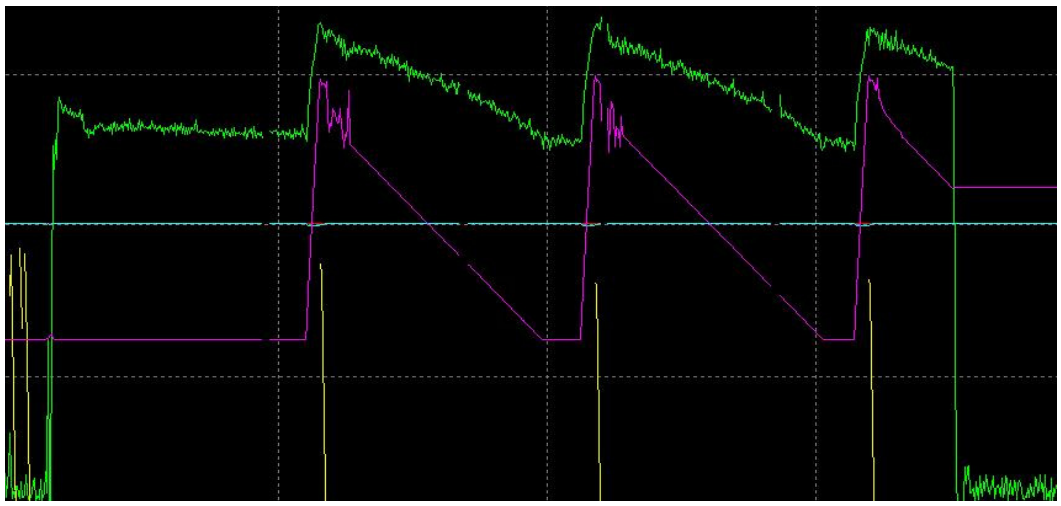

Figure 7.20 – Trends of inlet and outlet flow of the product tank in PID control (Green curve is the inlet flow of the tank, yellow curve is the outlet flow of the tank)

Table 7.3
Toggle control test in experiment 1

Operation Mode	Toggle control
Water Demands	Medium
Total Length (m)	16
Supply motor frequency (Hertz)	50
Conductivity (ppm)	2000
Temperature (C^0)	26
Average Power (kW)	0.37
Total Energy Consumption (kJ)	355.2
Start-up Level of Water in the Product Tank (L)	1.5
Number of Switch-on of Product Pump	2
Stop Level of Water in the Product Tank (L)	18
Membrane Pressure (kPa)	1200

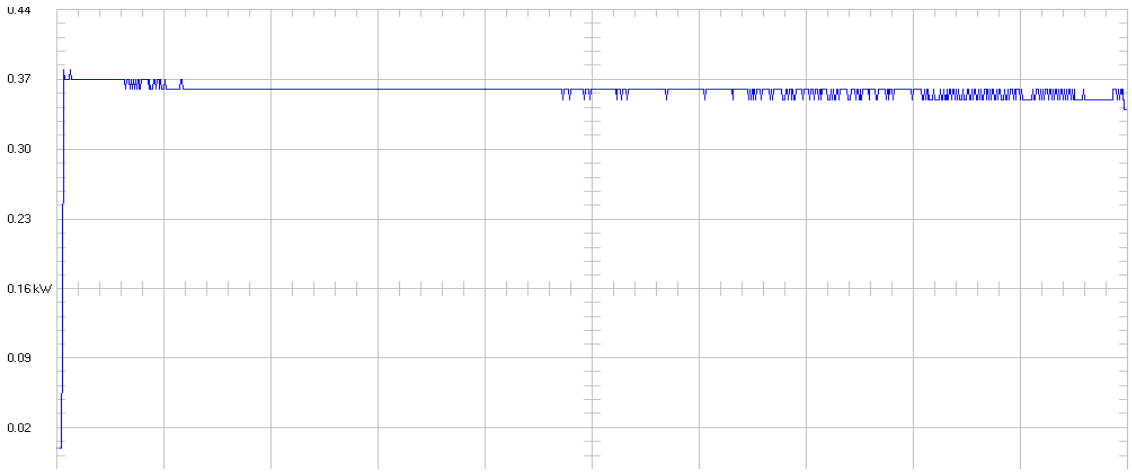

Figure 7.21 – Transient power consumption of the RO system with toggle control

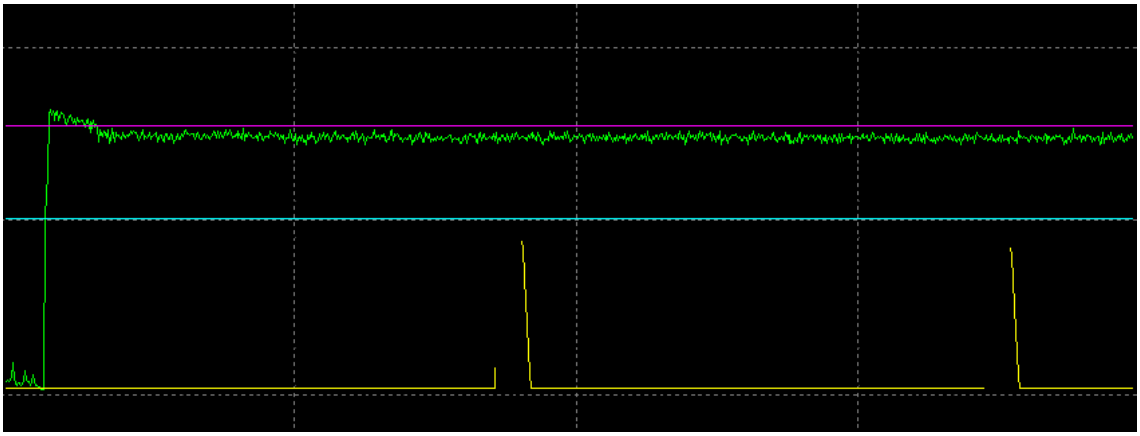

Figure 7.22 - Trend of the inlet and outlet flow rate of the product tank in toggle control (Green curve is the inlet flow of the tank, yellow curve is the outlet flow of the tank)

Table 7.4
PID control test in experiment 2

Operation Mode	PID
Water Demands	Medium
Total Length (m)	23.5
PID Parameters	10,2,0.25
Conductivity (ppm)	3000
Temperature (C^0)	25
Average Power (kW)	0.23
Total Energy Consumption (kJ)	324.3
Start-up Level of Water in the Product Tank (L)	1.5
Number of Switch-on of Product Pump	3
Stop Level of Water in the Product Tank (L)	18

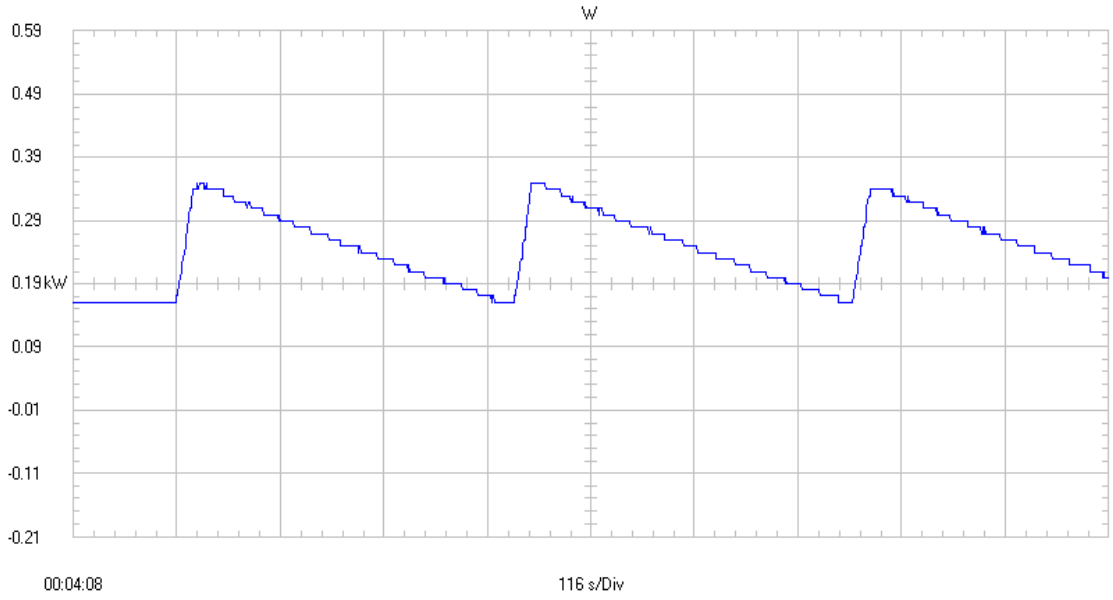

Figure 7.23 – Transient power consumption of the RO system in PID control

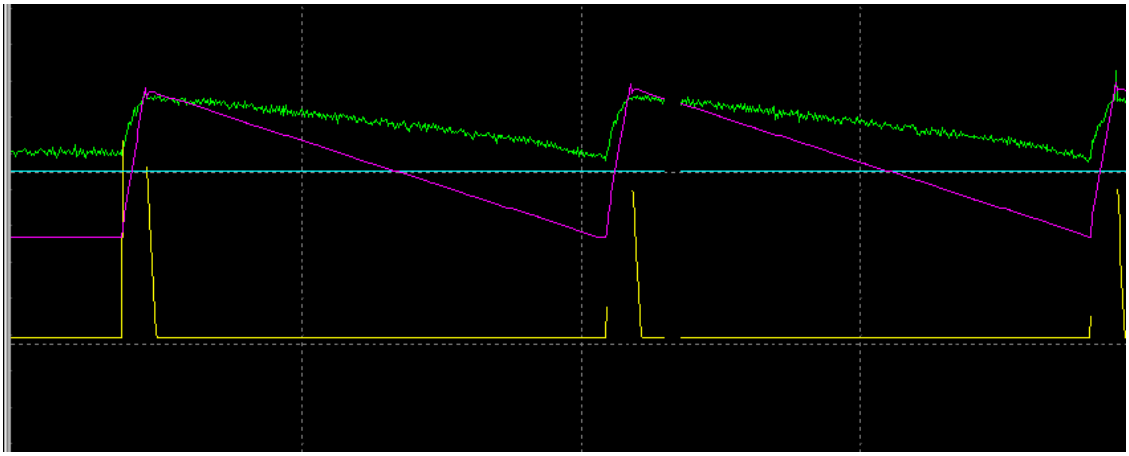

Figure 7.24 – Trend of inlet and outlet flow rate of the product tank in PID control (Green curve is the inlet flow of the tank, yellow curve is the outlet flow of the tank)

In figure 7.20 and 7.22, green curve is the trend for inlet flow of the product water tank. And the yellow line stands for the outlet flow of the product water tank. It can be clearly observed that, in PID control mode, water production of the system follows the pattern of water consumption.

Table 7.5
Toggle control test in experiment 2

Operation Mode	Toggle control
Water Demands	Medium
Total Length (m)	18.67
Supply motor frequency (Hertz)	50
Conductivity (ppm)	3000
Temperature (C^0)	25
Average Power (kW)	0.37
Total Energy Consumption (kJ)	392
Start-up Level of Water in the Product Tank (L)	1.5
Number of Switch-on of Product Pump	2
Stop Level of Water in the Product Tank (L)	18
Membrane Pressure (kPa)	1200

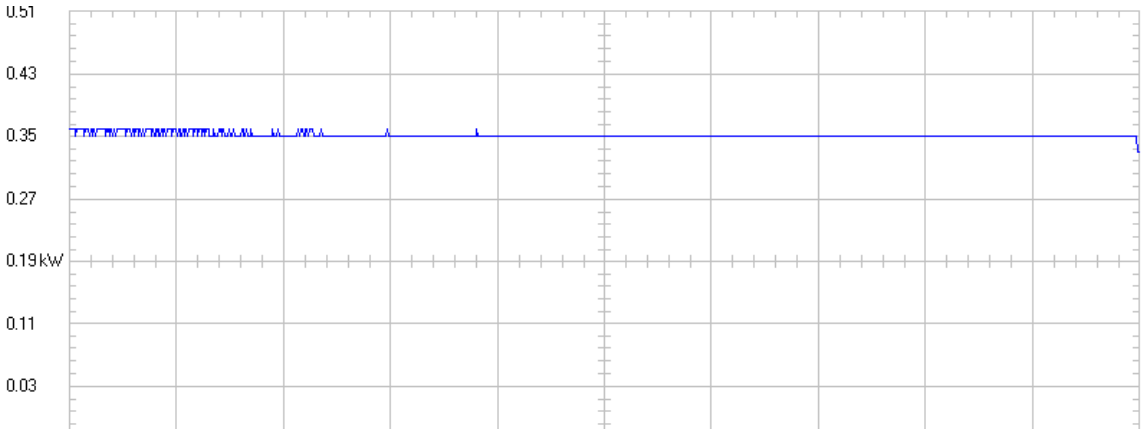

Figure 7.25 – Transient power consumption of the RO system in toggle control

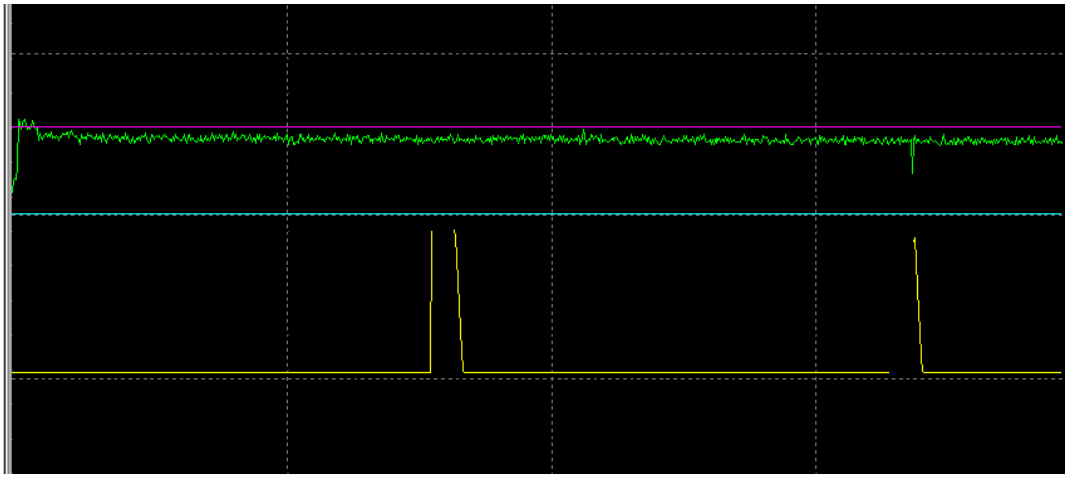

Figure 7.26 – Trend of the inlet and outlet flow rate of the product tank in toggle control (Green curve is the inlet flow of the tank, yellow curve is the outlet flow of the tank)

In figure 7.26, green curve is the trend for inlet flow of the product water tank. And the yellow line stands for the outlet flow of the product water tank. It can be seen that, in toggle control mode, water production of the system remains constant.

7.2.2.2 Long Term Performance

The system was tested in 24 hours in PID control mode and toggle control mode, respectively. The experimental results are revealed as below.

A) System performance in PID control mode

Table 7.6
Experimental condition and results with PID control

Feed Water Conductivity (ppm)	System Operation Time	Average power consumption (KW)	Total Energy Consumption (kJ)	Water consumption (Litres)
4000	25 hrs 17 mins	0.23	20934.6	1058

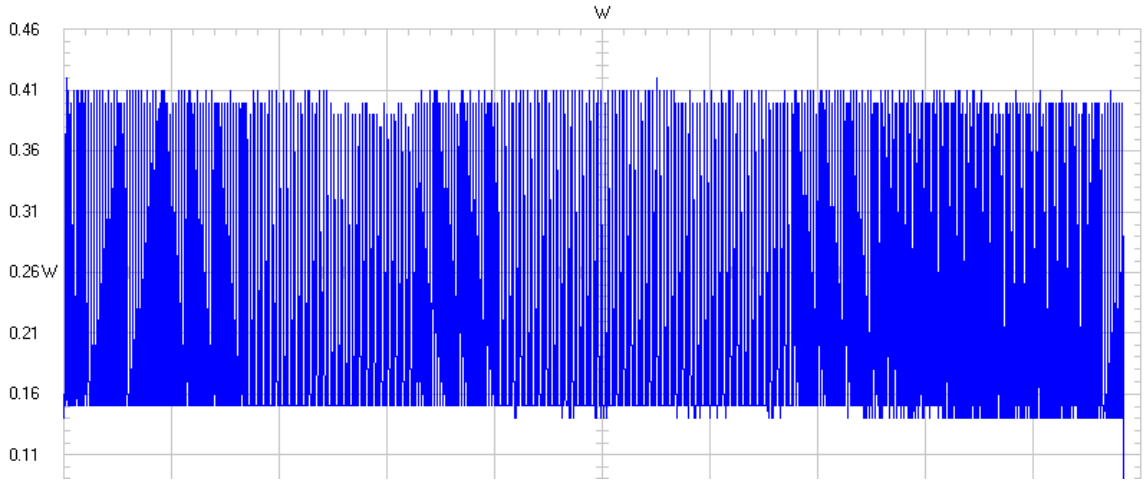

Figure 7.27 – Transient power consumption of the RO system over 24 hours with PID control algorithm

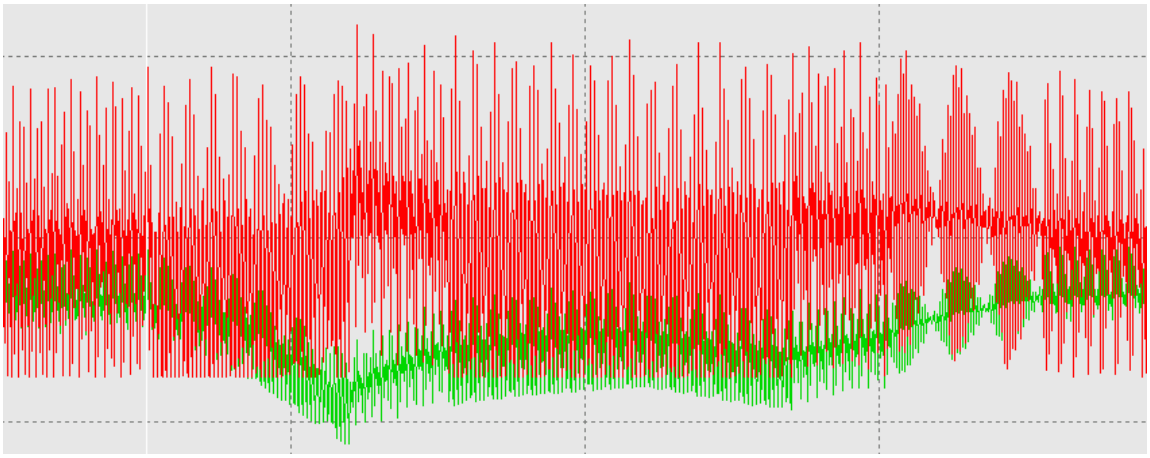

Figure 7.28 – Trend of the inlet flow rate of the product tank and motor frequency over 24 hours with PID control algorithm

Figure 7.28 shows the transient performance of the system in terms of the inlet flow and motor frequency. The red line and green line stands for the motor frequency and inlet flow of the product tank, respectively.

B) System performance in toggle control mode

Table 7.7
Experimental condition and results with toggle control

Feed Water Conductivity (ppm)	System Operation Time	Average power consumption (KW)	Total Energy Consumption (kJ)	Water consumption (Litres)
4000	25 hrs 17 mins	0.33	30036.6	1053

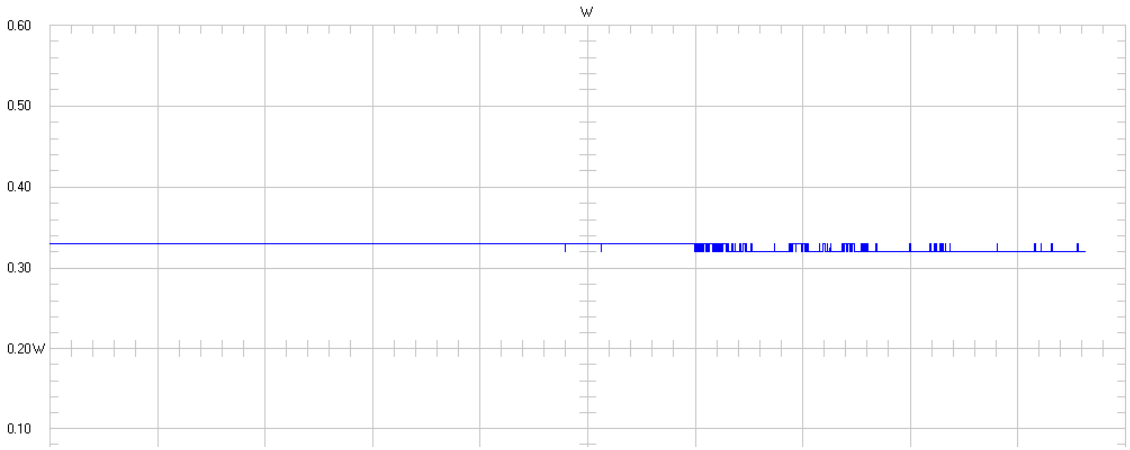

Figure 7.29 – Transient power consumption of the RO system over 24 hours with toggle control algorithm

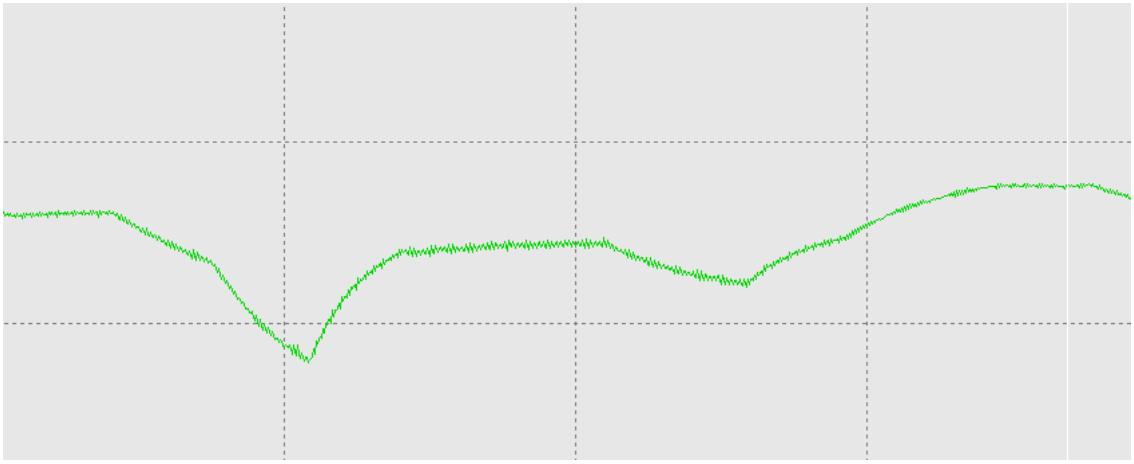

Figure 7.30 – Trend of the inlet flow rate of the product tank over 24 hours with toggle control algorithm

7.2.3 Experiment Results Analysis

7.2.3.1 Short term performance

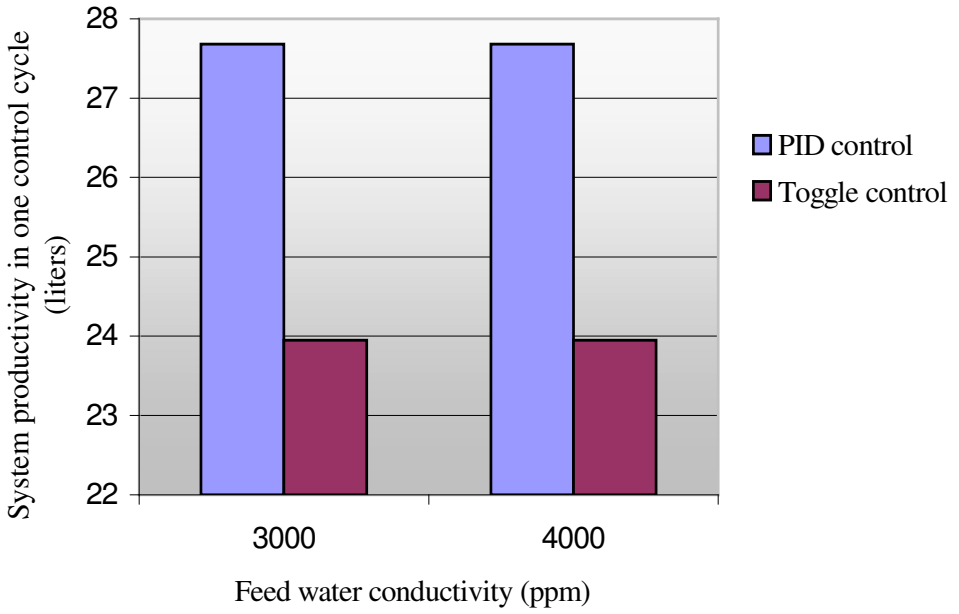

Figure 7.31 - System productivity in one control cycle for PID control and toggle control

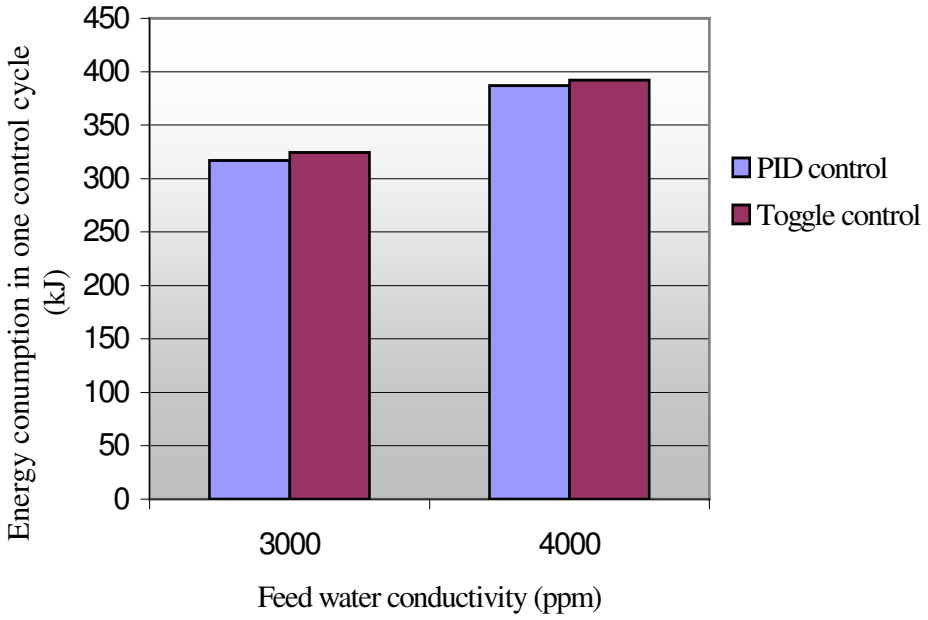

Figure 7.32 – Energy consumption of the system in one control cycle for PID and toggle control

When the feed water conductivity is 4000ppm, in one PID control cycle, 27.68 litres water was produced with 324.3kJ energy consumption in total, whereas, in one On-Off control cycle, 23.95 litres water was produced with 392kJ energy is drawn from the grid (can be seen in figure 7.31, 7.32). This determined that the PID Automatic Control spent less energy than On/Off control. Additionally, the system efficiency is improved (8.54%) with PID control, while the efficiency of the conventional control is 6.11% (seen in figure 7.33).

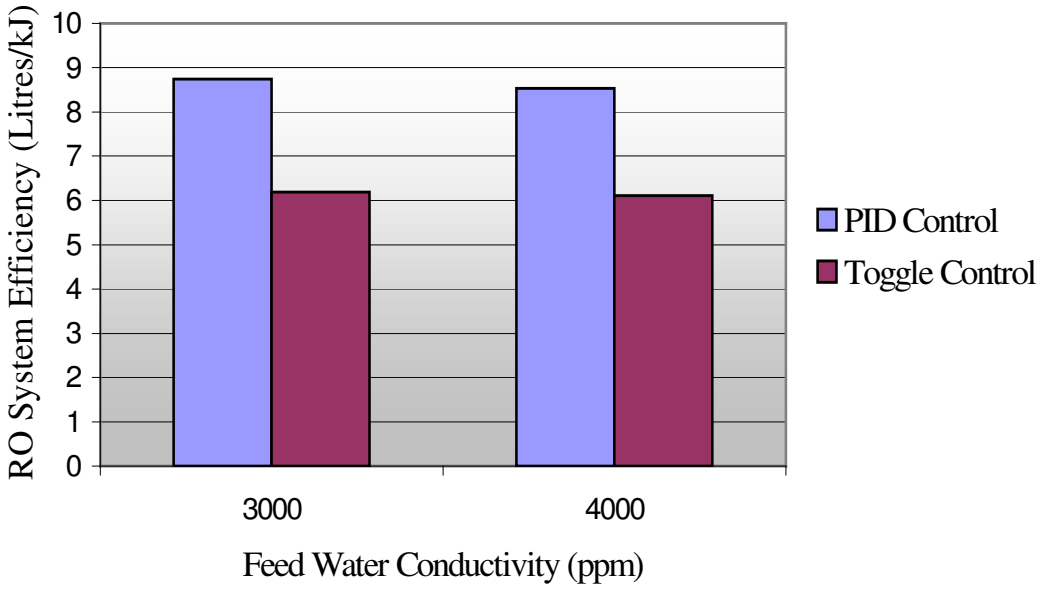

Figure 7.33 – Comparison of the system efficiency between PID control and toggle control

Therefore, from the short term performance of the system with each control strategy, it is shown that the system with PID control can produce greater amount of water, at the same time, consume less energy than the toggle control. This proves that the new control strategy - PID control is a promising and more suitable solution for the RO system in terms of saving energy and improving the system efficiency.

7.2.3.2 Long term performance

Using the similar analytical tactic, results obtained from the long term experiments were compared and analysed as shown in figure

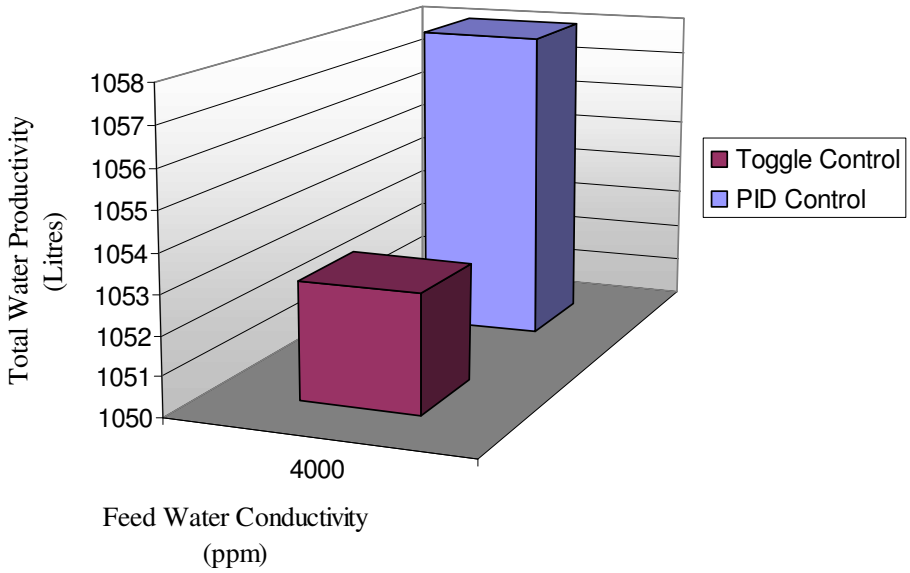

Figure 7.34 - System productivity in PID control mode and toggle control mode over 24 hours

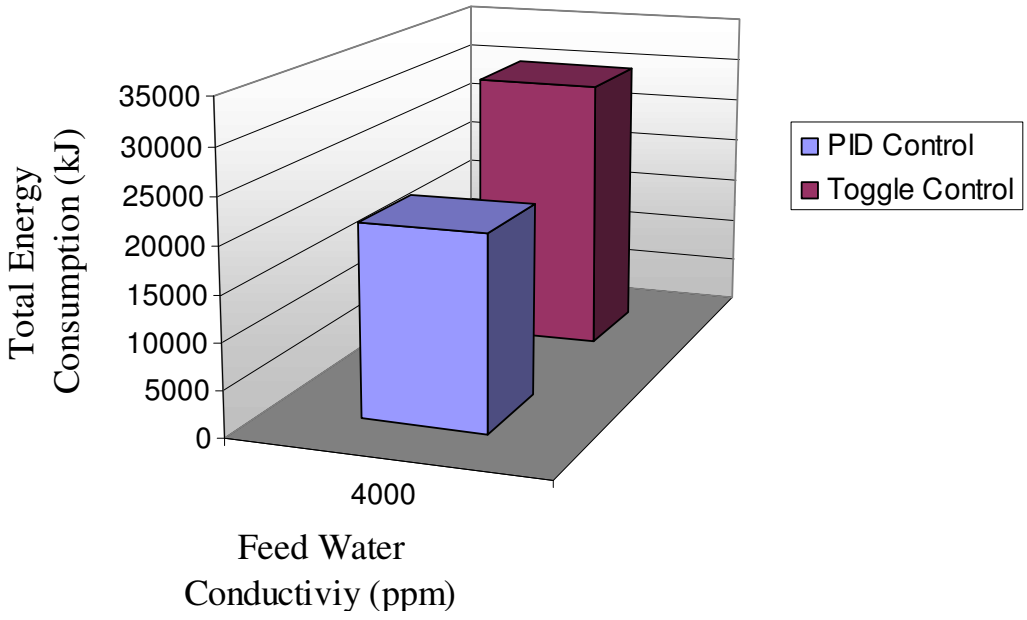

Figure 7.35 – System energy consumption in PID control mode and toggle control mode over 24 hours

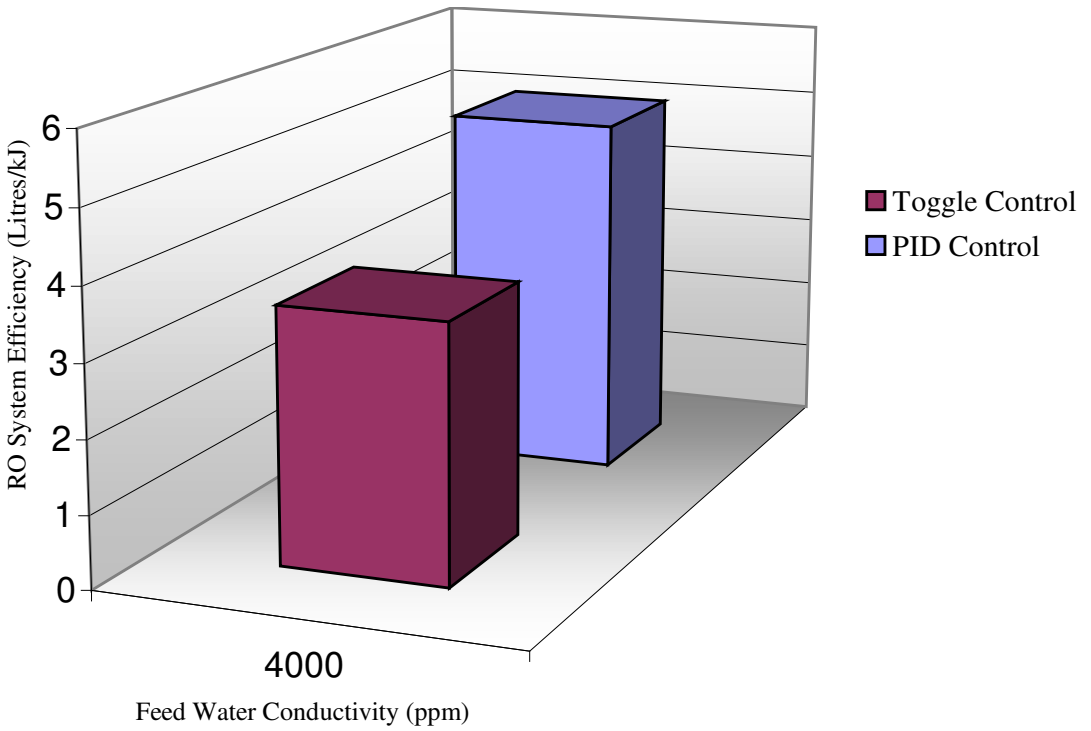

Figure 7.36 – System efficiency in PID control mode and toggle control mode over 24 hours

From figure 7.34, 7.35 and 7.36, it can conclude that the RO system had better performance while it was operating with PID control algorithm over 24 hours period of time. With PID controller, the RO system not only consumed less energy, but also produced more water. Substantially, the efficiency of the RO system was enhanced by implementing the PID controller. The improvement in system efficiency was up to 1.51 percent while the feed water conductivity was 4000 ppm. This proved the correctness of the computer modelling and simulation conducted in chapter 4, 5, 7. At last, the functionality of the PID controller was tested to be outstanding and the objective of efficiency improvement for the RO system was achieved.

7.3 References

[1] CITOR, Instruction Manual-Designator, Perth, 2005.

[2] TECO, 7*200J* Inverter-Instruction Manual, Taiwan, 1987.

[3] DL205 User ManualVolume 2, Automationdirect.com Incorporated, Http:// www.Automationdirect.com [accessed 2005].

[4] Marcos, M., *Small-scale Wind Powered Seawater Desalination without Batteries*, Loughborough: PhD Thesis, Loughborough University, 2003.

[5] Citect HMI, Manual of the SCADA, http://www.citect.com/products-and-services/citect-hmi.html [accessed 2005].

[6] Nayar C. V., Phillips S. J., James W. L., Pryor T. L., and Remmer D., "Novel wind/diesel/batter hybrid energy system." *Solar energy*, vol. 51 pp. 65-78, 1993.

CHAPTER 8 CASE STUDY- APPLICATION OF THE RO DESALINATION IN A MINI RENEWABLE ENERGY POWER SUPPLY SYSTEM

With the empirical results gained in chapter 5, the entire RAPS system includes the RO system needs to be proved applicable. Mundoo island of Maldives was selected to be the place where the proposed RO system can be implemented and evaluated. Infrastructures were devastated on this island after being hit by tsunami in late 2004 and since then the restorations of power supply and fresh water supply facility were being continual issues. With estimated daily load the simulations were undertaken in this chapter. By comparing the results to the expected local price of the electricity, the promising performance of the entire RAPS system was noticed.

8.1 Selection Process for the RO System

8.1.1 Location of Mundoo Island

Selecting an appropriate site for the RO desalination system is unveiled by choosing an appropriate location for RAPS system for it will be the ground where RO system designed to embed. The site selected for this project is Mundoo Island in Hadhdhunmathee Atoll. The exact location of the island is Longitude 73° 32’ 00” E and Latitude 02° 00’ 45” N [6]. The physical dimensions of Mundoo are approximately 1420m long and 220m wide at most. Figure 8.1 show a map of the island whose approximate area is 0.197 km^2.

Figure 8.1 - Map of Hadhdhunmathee (Source: MAD)

8.1.2 Population of Mundoo

By July 2004, Mundoo had a registered population of 760, out of which resident population was about 580 as the rest were living in Male' and elsewhere [7]. However, the resident population further declined after the tsunami as Mundoo was swept with 10 feet high waves. Following the tsunami disaster, 255 people migrated to nearby Gan Island and took temporary accommodations as refugees. Hence current resident population of the island is considered as 325 people comprising of men, women and children.

Before tsunami (December, 2004), the total number of fully built-up houses were 94 and 90 houses out of that were occupied. After the tsunami, number of occupied houses remained as 46 because many buildings were completely destroyed by the disaster [7].

8.1.3 Power Generation

Currently, public electricity supply in Mundoo is in an erratic status as all pre-tsunami generators were damaged by the disaster. For the time being, power supply is managed with the pre-tsunami 60 kVA being partly repaired and operational with some restrictions [11]. Since the central government is providing free diesel fuel for

electricity supply, the present routine is set to 12 hours night time which is expected to continue till the end of June. After June, the Island Development Committee (IDC) does not plan to use the 60 kVA as they feel that the generator is too costly to run with public financing. Therefore the Mundoo community is looking for ways to improve their power supply systems with other alternatives in future [3].

8.1.4 Water Supply Situation

Water supply is a dreadfully agony after the tsunami. All of the original water supply facilities were destroyed. The existing drinking water sources were mostly contaminated. Apart from the problems of water safety, on some island of Maldives, the underground water stays salty (around 4000ppm) due to their geophysical locations. At the moment, the drinking water supplied for the island is largely transported from other places. Meanwhile, three desalination plants are being constructed by Germany. Therefore, local habitants confront a long term shortage of drinking water. Quick and prompt solutions are needed for establishing quality water supply facilities.

8.1.5 Load Devices

Majority of the houses have typical domestic appliances such as TV, radio, oven, refrigerator, ceiling fans and light fixtures. Some houses have deep freezers, small grinders and few other kitchen appliances. No house has an air conditioner or any other high power rated machine [2]. Table 8.1 lists typical load devices used daily in a household earning a high income.

Table 8.1

Typical load devices used in a household earning a medium income

Electrical Device	Description	Rated Power (W)	Qty. (nos.)	Total Hourly Consumption (W)
Radio	A simple radio with tape player	40	01	40
TV	21" Color TV	78	01	78
Refrigerator	4' high refrigerator with freezing compartment	60	01	30
Lights 1	Tungsten filament bulb	5	05	25
Lights 2	Fluorescent tube	10	02	20
Lights 3	Fluorescent tube	20	04	80
C. fan 1	900mm diameter Blades ceiling fans in 3 bedrooms	30	03	90
C. fan 2	1200mm diameter Blades ceiling fan in living room	55	01	55
C. fan 3	900mm diameter Blade ceiling fan in dining room	30	01	30

Apart from the above listed items, almost all household in the medium and high income category have washing machines and irons too [2]. However, before tsunami, using washing machines was restricted in a certain time period of a day to ensure that there is enough reactive power in the supply grid to keep the generators operating properly.

8.1.6 Metering, Billing and Unit Cost

All connected houses, two mosques, school and office have mechanical electrical meters with necessary safety devices. IDC takes readings on monthly basis

and issue bills to all customers but power consumed by two telephone booths owned by the country's telecommunication company.

Before tsunami, in Mundoo, the charge of the unit rate was of AU$ 0.50 per kWh, which was subject to change with diesel price variations. According IDC, the residents feel that pre-tsunami rate is too high and practically unaffordable [3]. Hence, IDC plans to lower rate to at least AU$ 0.25 per kWh at maximum or set a rate structure similar to the rates which is shown in Table 7.2.

Table 8.2
Electricity unit rates in Mundoo

Customer groups	Unit rate (AU$ / kWh)	
	Below 200 kWh	Above 200 kWh
Residential	0.175	0.225
Government	0.225	0.275
Commercial	0.325	0.375

8.2 Evaluation of the RO System for Mundoo

8.2.1 Methodology

It was decided to use a simulation-software, to evaluate all the possible scenarios for the proposed RO desalination system implement in Mundoo. Homer was chosen because it is a useful simulation tool to evaluate the performances of RAPS systems in almost any load conditions. It also provides economical results in terms of the initial investment units' rates, etc, which can give more realistic ideas in the over all scales. The basic rationale is to simulate the entire renewable energy power supply system (described in chapter 3) of which the RO system is one of the primary loads. The simulations will save a lot of time as well as expenses by avoiding real implementation of projects with trial and error constructions.

8.2.2 System Architecture

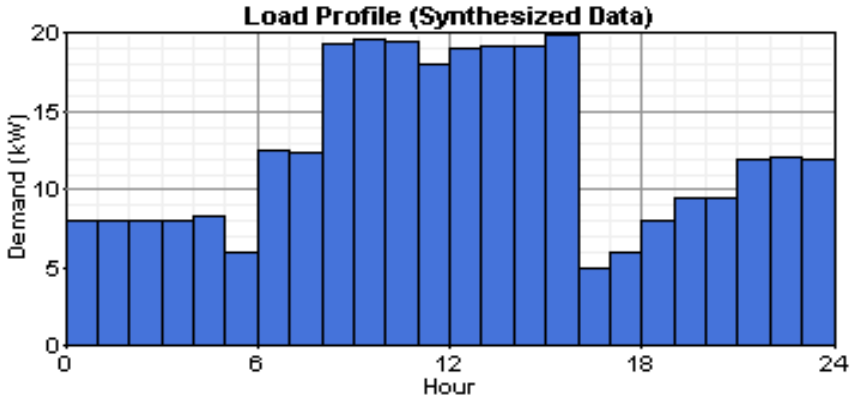

Figure 8.2 - An existing daily load profile in Mundoo

To begin with simulations, a load profile was input into the HOMER as shown in figure 8.2. And a 3kW wind generator, a 5kW photovoltaic generator, two diesel generators, a 40.5kWh battery bank and a 15kW bi-directional inverter were modeled in HOMER in according with the configuration of a mini renewable energy power supply grid previously developed at Curtin University of Technology. Another primary load (shown in figure 8.3) was fed into the simulation as the estimated power consumption for the RO system.

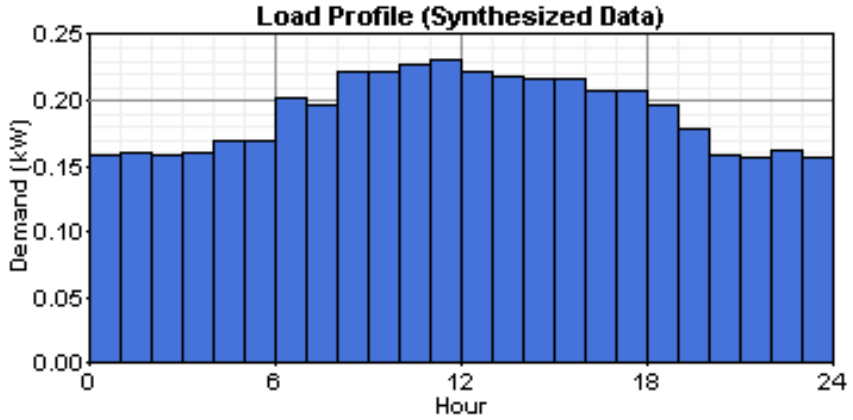

Figure 8.3 - An estimated daily load profile for the RO system in Mundoo

For the existing daily load, daily and hourly noises were added at 2 and 7 percent respectively. The annual average consumption was 299.0 kWh / day while

annual peak reached 25.0 kW. Instead, for the RO system load file, daily and hourly noises were keyed in 15 and 20 percent respectively. The annual average power consumption was 6.3 kWh per day and its peak power is 0.899kW.

Solar resource inputs were downloaded for Mundoo from NASA (National Aeronautics and Space Administration) as shown in Table 8.3 and Figure 8.4.

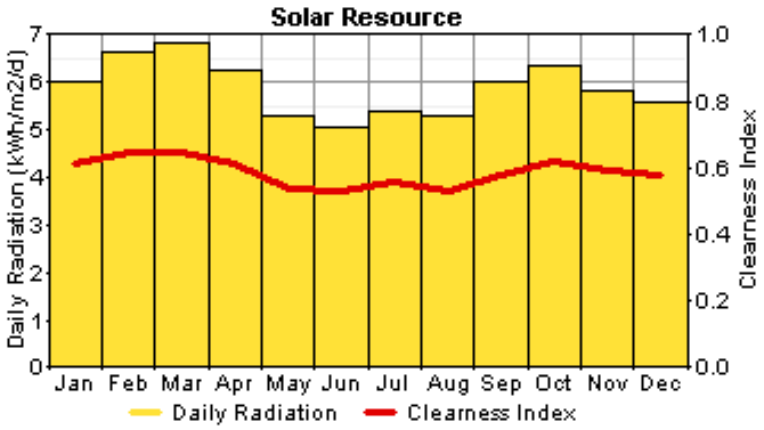

Figure 8.4 – Solar resource chart

Table 8.3

Solar resource in Mundoo (Source: NASA, 2006)

Month	Clearness Index	Average Radiation (kWh/m^2/day)
January	0.610	6.005
February	0.650	6.658
March	0.650	6.810
April	0.610	6.278
May	0.540	5.309
June	0.530	5.046
July	0.560	5.392
August	0.530	5.321
September	0.580	5.999
October	0.620	6.357
November	0.590	5.838
December	0.580	5.609

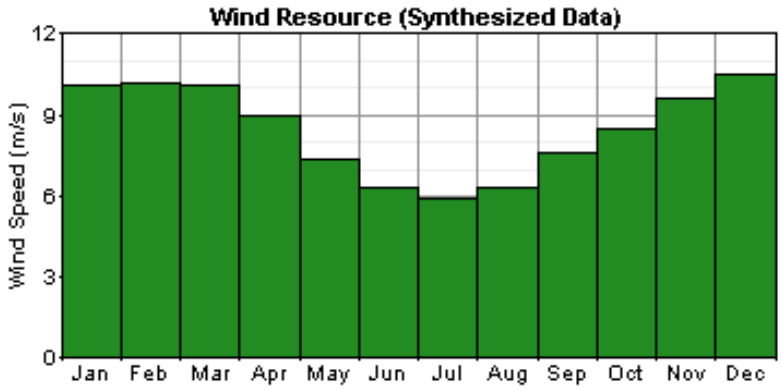

Figure 8.5 - Wind resource chart

Table 8.4 Wind resource in Mundoo, (source NASA, 2006)

Month	Jan	Feb	Mar	Apr	May	Jun	Jul	Aug	Sept	Oct	Nov	Dec
Wind Speed (m/s)	10.1	10.2	10.1	8.9	7.4	6.3	5.9	6.3	7.6	8.5	9.6	10.5

Table 8.5 Cost inputs and specification for PV component

Photovoltaic information						
Size (kW)	Capital cost ($)	Replacement cost ($)	Operation & Maintenance ($/yr)	Quantity	Life time	Derating factor
1.0	7600.00	6900.00	20.00	5	20	90%

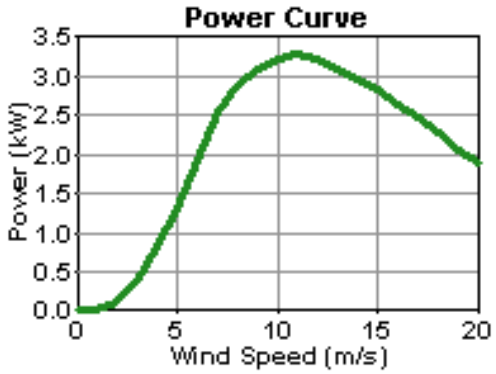

Figure 8.6 Characteristic of the wind turbine

Table 8.6 Cost inputs and specification for wind generator

Wind generator information						
Size (kW)	Capital cost ($)	Replacement cost ($)	Operation & Maintenance ($/yr)	Quantity	Life time (yr)	Hub height (m)
3.0	8200	22500	150.00	1	20	25

Table 8.7 Cost inputs and specification for converter

Bi-directional inverter information							
Size (kW)	Capital cost ($)	Replacement cost ($)	Operation & Maintenance ($/yr)	Quantity	Life time	Inverter Efficiency (%)	Rectifier Efficiency (%)
15.0	19275	19275	240	1	20	90	85%

Table 8.8 Cost inputs battery

Battery information						
Voltage (V)	Nominal capacity (Ah)	Capital cost ($)	Replacement cost ($)	Life time Through out (kWh)	Quantity	Operation & Maintenance ($/yr)
6	225 Ah	180.00	155.00	845 kWh	30	90

Table 8.9 Information of the 15kW generator

Size (kW)	Capital ($)	Replacement ($)	O&M ($/hr)	Life Time (hrs)	Fuel used	Min. load ratio (%)
15	2,535	2,475	0.410	15,000	Diesel	30%

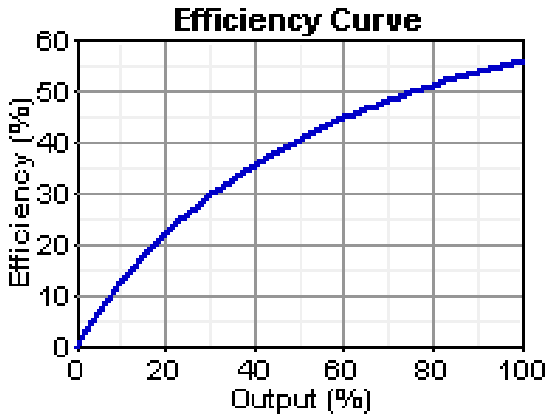

Figure 8.7 Efficiency curve of the 15kW generator

Table 8.10 Information of the 11kW generator

Size (kW)	Capital ($)	Replacement ($)	O&M ($/hr)	Life Time (hrs)	Fuel used	Min. load ratio (%)
11	1,859	1,815	0.40	15,000	Diesel	30%

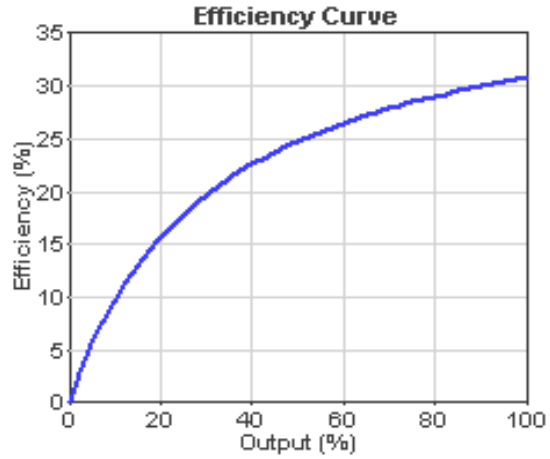

Figure 8.8 Efficiency curve of the 11kW generator

Next stage was to input costs for PV, converter and battery. PV costs include PV modules, mounting hardware, wiring, installation and transport costs.

An initial cost estimation for all three components prices were made with the aid of available prices from various internet sites. The prices were checked against PV

module prices, converter prices and battery prices [1], [4], [5]. However, in case of battery, HOMER required to select a specific battery for any simulation with battery component. Therefore Trojan T-105 battery was selected.

Transportation cost was calculated for shipping from Singapore to Male', and then transporting from Male' to Mundoo by inter-atoll transport boats. Import duty was considered as nil as government always rebates duty for components specifically imported for such projects. Local expertise fees were assumed to be minimal due the nature of the project.

All operational costs for PV, converter and batteries were assumed to be included in the operational costs for diesel generators as shown in Table 8.9 and 8.10 because one technician will be responsible for all components.

The price of diesel is set to be the recently local price: AUS 0.64 per litre. The density and carbon content of the diesel are 820 kg per m^3 and 88% respectively.

Real interest rate was calculated based on 5% borrowing interest and 1% inflation rate. The borrowing rate is based on the interest rates of loans from central government to rural island communities.

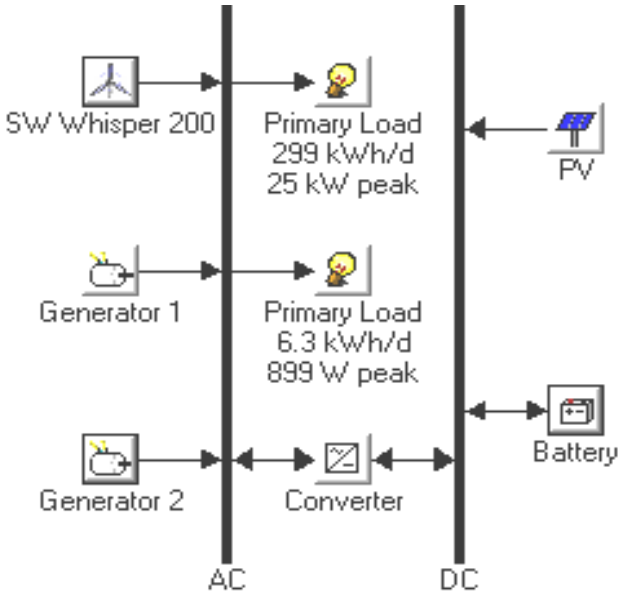

Figure 8.9 Layout of the configured RAPS system with the RO system embedded

Table 8.11
System architecture

Item	Power capacity	Quantity
PV Array:	5kW	1
Wind turbine:	3kW SW Whisper 200	1
Generator 1:	15kW	1
Generator 2:	11kW	1
Battery:	1.35kWh Trojan T-105	30
Inverter:	15kW	1

8.2.3 System Simulation Results and Analysis

Simulations were carried out after the system parameters were confirmed and put into Homer. The power produced by PV, wind and diesel generators was charted. The cost of the power unit was generated. The renewable energy fraction of the whole system is 25%.

Table 8.12
Annual electric energy production

Production(kWh/yr)	Component	Fraction (%)
8,686	PV array	8
20,135	Wind turbine	18
36,279	Generator 1	32
48,614	Generator 2	43
113,714	Total	100

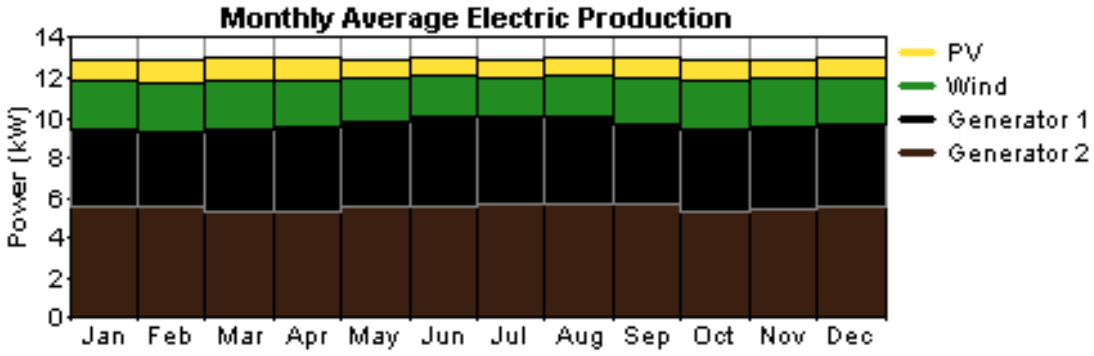

Figure 8.10 - Monthly average electric production

Table 8.13

Annual electric energy consumption

Load	Consumption (kWh/yr)	Fraction (%)
AC primary load	110,803	100
Total	110,803	100

Table 8.14

Cost Summary

Total net present cost:	315,926$
Cost of energy:	0.174$/kWh

The simulation provides positive results that the cost of the unit is AUS$ 0.174 per kWh, which is less than the budget (AUS$ 0.25 per kWh) schemed by Mundoo local government. With the renewable energy fraction settles at 25%, the RAPS system performs more environmentally friendly.

Assume the conductivity of underground water drew in Mundoo is 4000ppm. With the load profile of the RO system introduced in figure 7.3, by looking up the

simulation results in appendix (produced in chapter 6), the volume of the water produced is 1033 Litres per day which matches with the estimated water demands in mundoo. Meanwhile, the energy consumed by the RO system is 4.57 kWh. Hence, the total cost of the water is AUS$0.795. And the water unit cost is AUS$0.77 per m^3. This result reveals that the designed RO system has less power consumption rate than other conventional desalination system (solar still, multi-stage flash, Vapour compression, etc., as mentioned in chapter 2).

8.3 References

[1] Leonics & Regen, *M-400 Series Diesel/Battery/Inverter/ Mini Grid System*, http://www.regenpower.com/hybrid-systems-home.htm, [accessed in 2005].

[2] Julie, C., *Modelling of Renewable Energy Systems in Maldives*, Utrecht: Internship Report, Utrecht University, 2004

[3] Ahmed, N., *Application of a RAPS for the Maldives*, Perth: Master Thesis, Curtin University of Technology, 2005

[4] Information of Whisper 175 (3.2 kW), http://www.solutionmatrix.com/return-on-investment.html [accessed in 2006].

[5] Information of SunWize SW100, 100 Watt Solar Panel, http://www.affordable-solar.com/1138.html, [accessed in 2006].

[6] NASA, *Surface Meteorology and Solar Energy*, National Aeronautics and Space Administration, Washington. Retrieved: May 03, 2005, http://eosweb.larc.nasa.gov/sse/, [Accessed in December 2005].

[7] MHAHE, *First National Communication of the Republic of Maldives to the United Nations Framework Convention on Climate Change*, Ministry of Home Affairs, Housing and Environment, Male'. http://www.mv.undp.org/projects/environment/fnc/index.htm, [Accessed in December 2005].

[8] Camerlynck, J., *Modelling of Renewable Energy Systems in the Maldives*, Utrecht University., http://www.chem.uu.nl/nws/www/publica/I2004-21.pdf. [Accessed in December 2005].

[9] Gilman, P., *Homer Getting Started Guide*, National Renewable Energy Laboratory, Colorado,

http://www.nrel.gov/homer/downloads/HOMERGettingStarted.pdf. [Accessed in December 2005].

[10] HOMER, National Renewable Energy Laboratory (NREL), Colorado, www.nrel.gov/homer/default.asp. [Access in November 2005].

[11] MCST, *Strengthening Maldivian Initiatives for a Long-term Energy Strategy*, Ministry of Communication, Science and Technology, Male', http://www.mcst.gov.mv/projects/smiles. [Accessed in November 2005].

CHAPTER 9 CONCLUSION

The most significant steps of the research work are highlighted. In light of the procedures adopted and the results obtained, the contributions of research are discussed and recommendations for future development are outlined. Finally, the main conclusions of the work are drawn.

The lack of a reliable source of drinking water poses an evident obstacle for human development. Meanwhile, the energy inefficiencies of existing desalination systems raise the issue of saving the energy, especially the energy generated from renewable energy resources for they are relatively scarce and expensive. Reverse Osmosis was chosen to be the desalination technique on which the design was based. The reference to, and even the effective use of, renewable energy sources have been a constant in proposed solutions targeting isolated areas with unreliable power supplies. However, the main focus of the research is laid on the regulation of water demands, i.e. load following control; the designed desalination system can be applied in any place, which experiences problems of water salinity. Therefore, the renewable energy power supply system remains an option for the specific applications of the desalination system.

Considering this background, this research concentrates on the study of the efficiency of small-scale reverse osmosis desalination. The conventional control strategy which is toggle control on the water demands could not satisfy the objective of energy saving. A new control idea was created by using the concept of PID control. A variable speed drive was selected to provide a driving force for the high pressure pump for the purpose of implementing the variable speed controlling.

A review of the work is presented from the perspective of the main achievements and contributions. The recommendations for future research are presented.

9.1 Review of the Work

The review of the optimization of the system based on the characteristic of the reverse osmosis membrane was focused on the analysis of water demand scenarios. Hence, PID control is used as a tool to fulfill the purpose of load following and reduce the energy consumption over the system operational periods.

Empirical results were collected from the past experiments conducted on the membrane, motor-pump, and inverter. The experimental data were plotted and analyzed. The curve fitting technique (non-linear data regression) was used to equate the characteristic of the membrane and power consumptions of the system, especially for the discovery of the relationship between the motor input frequency and membrane output water. This was one of the contributions of this work, although it is believed further improvement could be achieved, particularly with regard to the variation of the membrane performance with different temperatures.

With the discovered relationships amongst each system component, the transfer functions were generated and used in the computer modeling carried out using MATLAB software. The entire RO unit was modeled by using MATLAB/Simulink function tools. This model will benefit further research in terms of the membrane efficiency study and rotary vain high pressure pump study.

A profile was created to represent a typical daily water load with a 1000 liters water demanded per day. Simulations of the RO system were carried out in a span of 24 hours with different feed water conductivities. The efficiencies of the RO system with different control strategies were plotted and analyzed as a chart. The results prove that the proposed design achieved the goal of energy saving with greater water productivity. Most importantly, the total efficiency of the system was improved noticeably in operation of PID control. The figures of improvements are shown in Table 9.1.

Table 9.1
System improvement compared PID control with toggle control

Feed Water Conductivity	2000	3000	4000	5000	6000	7000	8000	9000	10000
Efficiency Improvement (Litres/kJ/day)	0.0361	0.0356	0.0353	0.0318	0.0282	0.0275	0.0251	0.0225	0.0185
Productivity Improvement (litres/day)	392.7	334.6	285	246.2	210.1	177.5	147.8	120.4	92.6
Saved Energy (kWh/day)	0.567	0.915	1.217	1.415	1.605	1.8	1.996	2.158	2.323

The efficacy of the new control strategy proposed has been shown to be very promising from the simulation results obtained. To allow similar implementation in practice, Koyo PLC was used as the controller of the system. A reverse osmosis unit which included a membrane cylinder, AC motor drive, high pressure pump, chlorine filter, and pretreatment filter was purchased and assembled. The proposed control strategy as well as the conventional control technique (toggle control) was programmed into PLC in format of ladder diagram. Flow sensors, water level indicators, conductivity meter, and variable speed inverter were calibrated and installed in the system to extract the real-time readings of water flow rates, water levels, water conductivities, and frequency of the motor. It has to be noted that the signal conditioners were built in order to meet the requirement of analogue input of the PLC. The conditioner contains a frequency to current converter, a frequency to voltage converter, and a voltage to current converter.

On tuning the controller, it is acknowledged that the gain was set empirically, through observation of simulation results. Experiments on the RO system were conducted in short term as well long term. The performances of the system produced satisfactory results that revealed an energy saving feature of the new control scheme.

A case study was done by selecting Mundoo Island to be the location for the applications. Simulation of the RAPS system with which the RO system embedded was carried out in HOMER. The assumed daily water demand was used as the estimated drinking water demand for the local residents (around 300) on the island. Power consumption of the RO system was gained from previous simulation results in MATLAB, and it was integrated as part of the loads of the RAPS system. The final simulations, generating positive results, showed the energy cost (A$0.174) is under

the local government's budget (A$0.48). And volume of fresh water produced out of the designed RO system is 1033 litres per day that stays above water demand (1000 litres per day).

9.2 Future Study Recommendation

9.2.1 Load Leveling Control

Load regulation, also known as demand side management, stands in a formidable role in the RAPS systems. It can reduce the system total cost in terms of maintenance and fuel consumption. A typical electric load (Figure 9.1) has noticeable differences between its peak and lowest values. And the load may vary significantly in the smaller scale (For example, from 9:00 to 16:00 hours, a load sag happens around 13:00). This phenomenon can lead the system into an unstable condition. Diesel generators may have to be forced to work to compensate for the power deficits. Hence, the annual running time of the diesel generator could remain high, which consequently introduces extra expenses in operation and maintenance.

Load regulations can be done by using variable speed drives which have great flexibilities. In the RO system, the AC variable speed drive can also be used as a load regulator regardless of the variation in water demands if the product water tank has a large dimension. In figure 9.2, it is can be observed that the leveled load has a smoother profile. However, with larger size of RO desalination system, the load leveling control can be performed more effectively. Therefore, the future research may focus on the greater scale of RO unit (above 5000 Liters per day).

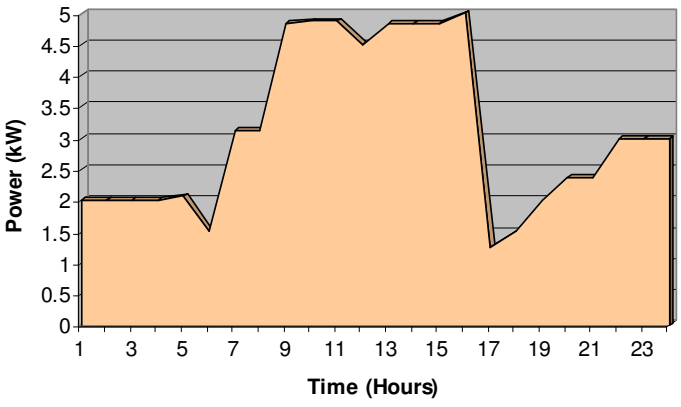

Figure 9.1 - A typical electric load profile

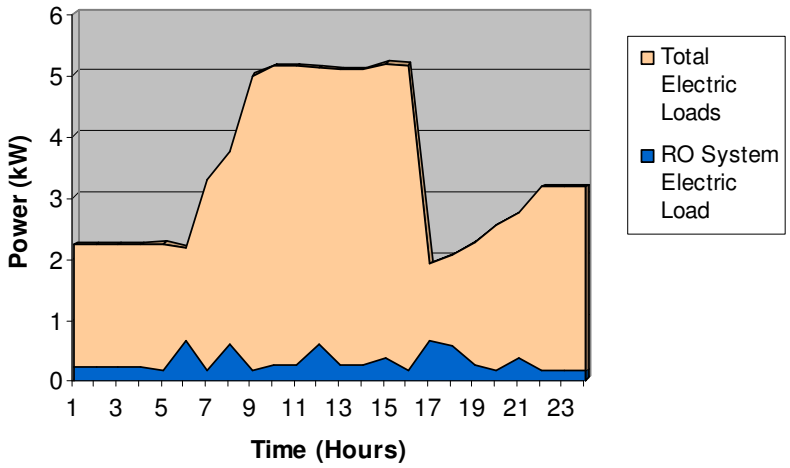

Figure 9.2 - Electric load levelled by the RO System load

9.2.2 Impact from Temperature Variations

Temperature is another parameter that affects the productivity of the RO system. However, the design does not refer to the variation of temperature due to the limited research funding and duration. From the literature review, it is known that higher feed water temperature brings greater water productivity. This point has to be proved from both simulations and experiments.

9.3 Final Comments

The aim of this work was to propose and assess an alternative system configuration which would enable the small-scale desalination of salt water (2000-10,000ppm) using Revers Osmosis technology and performs more energy efficiently than the existing RO systems that mostly use the toggle control technique.

The performance predictions from computer simulations (MATLAB) and experiments acquired from a prototype test rig are encouraging and corroborate its technical viability. An economic analysis done in another computer simulator (HOMER) also indicates that, having this RO unit as one of the electric loads, the mini renewable energy power supply grid is economically viable.

It is believed that the proposed RO system would be useful to reliably supply portable water in a sustainable and environmental friendly way.

APPENDIX A

LOOK-UP TABLES

Table A.1
Flow rate of the Product water vs. motor frequency and feed water conductivity

ppm / Hertz	2000	3000	4000	5000	6000	7000	8000	9000	10000
20	0.95	0.84	0.76	0.67	0.59	0.51	0.48	0.4	0.37
25	1.03	0.93	0.85	0.75	0.65	0.56	0.55	0.47	0.45
30	1.1	1.01	0.93	0.83	0.7	0.61	0.6	0.5	0.51
35	1.13	1.05	0.95	0.86	0.75	0.67	0.62	0.56	0.53
40	1.16	1.07	1.01	0.91	0.8	0.7	0.67	0.59	0.56
42	1.18	1.08	1.02	0.91	0.82	0.72	0.68	0.62	0.59
44	1.19	1.11	1.02	0.93	0.82	0.72	0.7	0.63	0.6
46	1.2	1.12	1.04	0.95	0.86	0.75	0.71	0.64	0.61
48	1.21	1.13	1.04	0.96	0.89	0.76	0.72	0.67	0.62
50	1.23	1.13	1.05	0.98	0.89	0.77	0.73	0.67	0.63
52	1.23	1.15	1.07	0.98	0.92	0.77	0.74	0.68	0.64
54	1.24	1.15	1.08	1	0.92	0.81	0.76	0.7	0.65
56	1.25	1.17	1.08	1.01	0.92	0.83	0.76	0.7	0.66
58	1.25	1.17	1.1	1.01	0.94	0.83	0.78	0.73	0.67
60	1.26	1.18	1.12	1.02	0.94	0.85	0.78	0.73	0.68
62	1.27	1.19	1.12	1.03	0.95	0.85	0.78	0.74	0.69

Table A.2
Power consumption vs. motor frequency and feed water conductivity

	2000	3000	4000	5000	6000	7000	8000	9000	10000
20	0.16	0.16	0.16	0.17	0.17	0.16	0.16	0.16	0.16
25	0.20	0.20	0.19	0.19	0.20	0.19	0.19	0.19	0.19
30	0.23	0.23	0.23	0.23	0.24	0.23	0.23	0.22	0.23
35	0.27	0.27	0.28	0.27	0.27	0.27	0.26	0.26	0.26
40	0.32	0.31	0.31	0.31	0.31	0.30	0.30	0.30	0.30
42	0.33	0.33	0.32	0.33	0.33	0.33	0.32	0.32	0.32
44	0.34	0.34	0.34	0.34	0.34	0.34	0.33	0.33	0.33
46	0.36	0.36	0.35	0.36	0.36	0.35	0.35	0.35	0.35
48	0.38	0.37	0.37	0.37	0.37	0.37	0.36	0.36	0.36
50	0.39	0.38	0.38	0.38	0.38	0.38	0.37	0.37	0.37
52	0.40	0.40	0.40	0.39	0.40	0.39	0.38	0.38	0.39
54	0.42	0.41	0.41	0.41	0.41	0.41	0.40	0.40	0.40
56	0.43	0.43	0.43	0.42	0.43	0.42	0.42	0.42	0.42
58	0.45	0.45	0.45	0.44	0.45	0.43	0.43	0.44	0.44
60	0.47	0.46	0.46	0.46	0.46	0.46	0.46	0.45	0.45
62	0.48	0.48	0.48	0.48	0.47	0.47	0.47	0.47	0.47

APPENDIX B

EXPLICIT RAPS SIMULATION REPORTS

Table B.1

Cost breakdown

Component	Initial Capital ($)	Annualised Capital ($/yr)	Annualised Replacement ($/yr)	Annual O&M ($/yr)	Annual Fuel ($/yr)	Total Annualised ($/yr)
PV Array	38,000	2,324	0	50	0	2,374
SW Whisper 200	8,200	501	0	10	0	511
Generator 1	2,535	155	300	1,044	4,324	5,823
Generator 2	1,859	114	575	2,183	5,350	8,221
Battery	5,640	345	784	450	0	1,579
Converter	15,000	917	0	15	0	932
Totals	71,234	4,356	1,659	3,752	9,675	19,442

Table B.2

Annual electric energy consumption

Load	Consumption (kWh/yr)	Fraction (%)
AC primary load	111,402	100
Total	111,402	100

Table B.3

Performance of PV generator

Variable	Value	Units
Average output:	23.8	kWh/d
Minimum output:	0.000102	kW
Maximum output:	4.87	kW
Solar penetration:	7.80	%
Capacity factor:	19.8	%
Hours of operation:	4,719	hr/yr

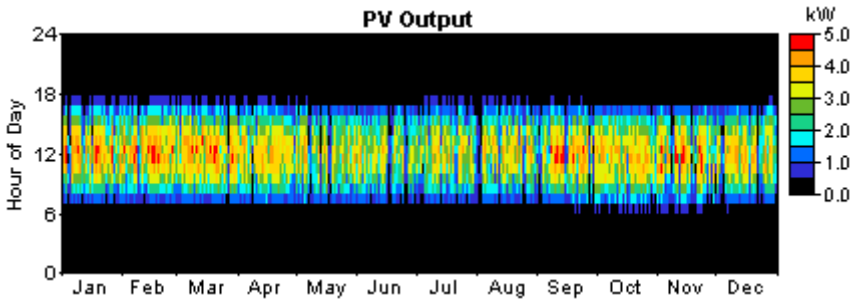

Figure B.1 Electricity product by PV generator

Table B.4

AC Wind Turbine: SW Whisper 200

Variable	Value	Units
Total capacity:	3.28	kW
Average output:	2.30	kW
Minimum output:	0.000	kW
Maximum output:	3.28	kW
Wind penetration:	18.1	%
Capacity factor:	70.1	%
Hours of operation:	8,729	hr/yr

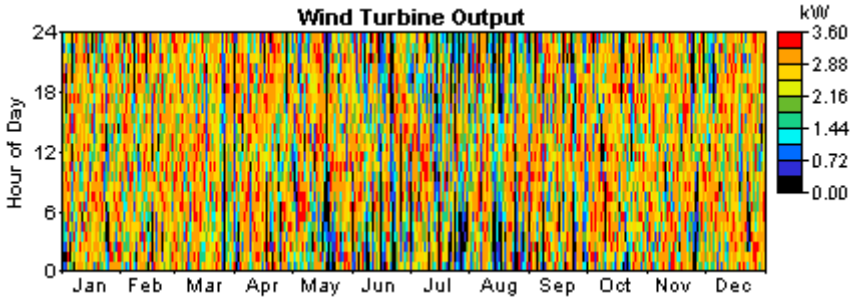

Figure B.2 Electricity produced by wind generator

Table B.5

Cost summary of the generator 1

Variable	Value	Units
Hours of operation:	2,547	hr/yr
Number of starts:	699	starts/yr
Operational life:	5.89	yr
Average electrical output:	14.6	kW
Minimum electrical output:	7.72	kW
Maximum electrical output:	15.0	kW
Annual fuel usage:	6,757	L/yr
Average electrical efficiency:	55.8	%

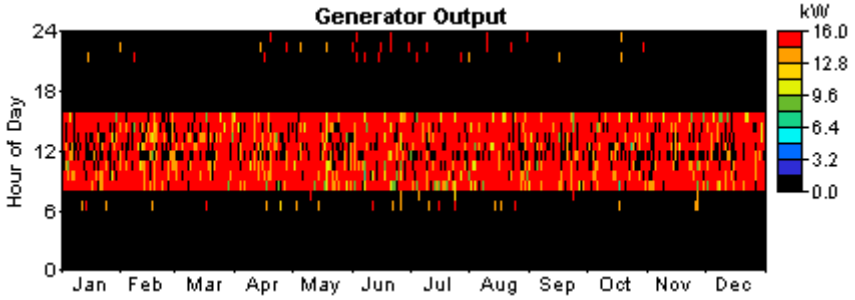

Figure B.3 - Spectrum of the output of generator 1

Table B.6

Cost summary of generator 2

Variable	Value	Units
Hours of operation:	5,457	hr/yr
Number of starts:	1,043	starts/yr
Operational life:	2.75	yr
Average electrical output:	8.87	kW
Minimum electrical output:	4.05	kW
Maximum electrical output:	11.0	kW
Annual fuel usage:	8,360	L/yr
Specific fuel usage:	0.173	L/kWh
Average electrical efficiency:	58.8	%

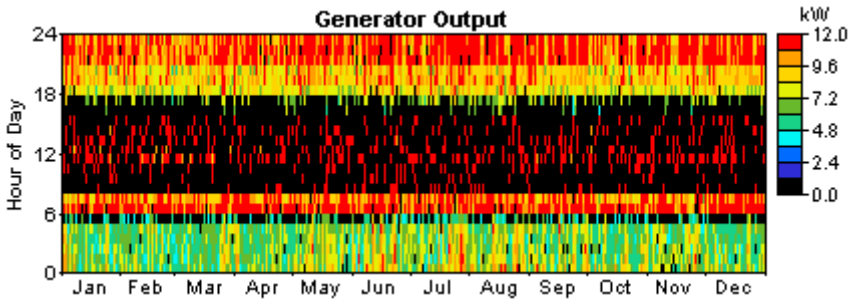

Figure B.4 - Spectrum of the output of generator 2

Table B. 7

Summary of the Battery

Variable	Value	Units
Battery throughput	5,504	kWh/yr
Battery life	4.61	yr
Battery autonomy	2.21	hours

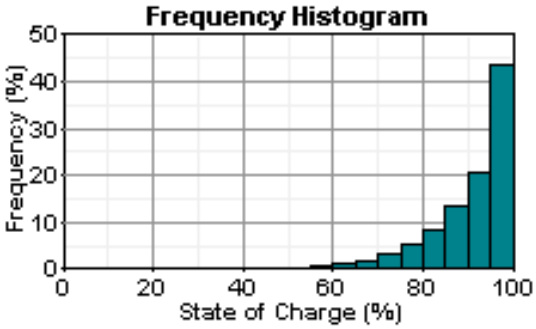

Figure B.5 – State of the charge of the battery

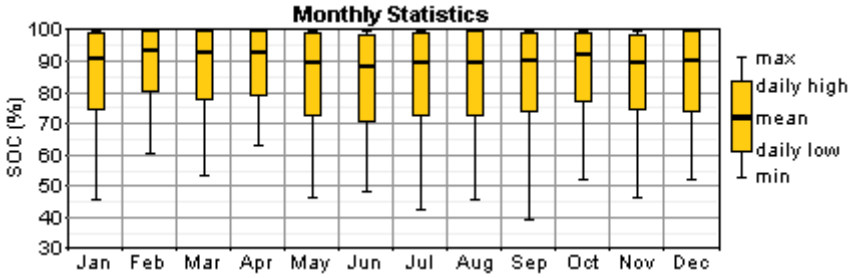

Figure B.6 – Monthly chart of the state of charge of battery bank

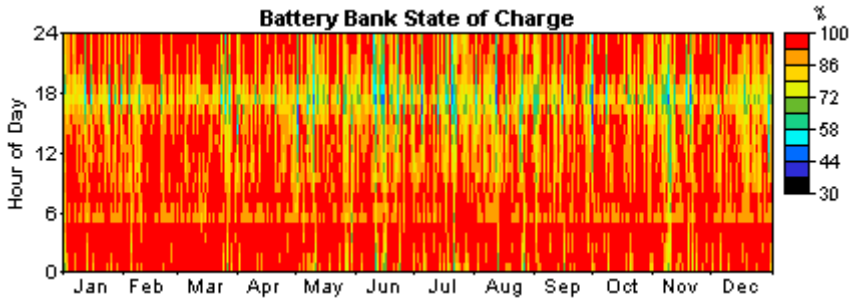

Figure B.7 – Spectrum of the battery bank state of charge

Table B.9

Summary of the Emissions

Pollutant	Emissions (kg/yr)
Carbon dioxide	39,807
Carbon monoxide	98.3
Unburned hydrocarbons	10.9
Particulate matter	7.41
Sulphur dioxide	79.9
Nitrogen oxides	877

APPENDIX C

PLC CODES FOR THE RO SYSTEM

These PLC codes, namely ROtest1, were designed and written in Koyo PLC. During the period from May, 2005 to March, 2006, the program was developed and entered progressively.

APPENDIX D

Sarian MR 2110 Configuration Files for the Establishment of the VPN through the Telstra GPRS Mobile Network

Note: All the codes below were entered in Microsoft notepad and transferred to the routers by using FTP in Linux environment.

```
eth 0 IPaddr "207.33.133.23"
eth 0 mask "255.255.255.240"
eth 0 gateway "207.33.133.29"
eth 0 do_nat 2
eth 0 ipsec 1
eth 0 ipanon ON
eth 1 IPaddr "10.2.0.1"
eth 1 mask "255.255.0.0"
l2tp 0 listen ON
l2tp 0 swap_io ON
l2tp 1 listen ON
l2tp 1 swap_io ON
l2tp 2 listen ON
l2tp 2 swap_io ON
l2tp 3 listen ON
l2tp 3 swap_io ON
l2tp 4 listen ON
l2tp 4 swap_io ON
l2tp 5 listen ON
l2tp 5 swap_io ON
l2tp 6 listen ON
l2tp 6 swap_io ON
l2tp 7 listen ON
l2tp 7 swap_io ON
l2tp 8 listen ON
l2tp 8 swap_io ON
l2tp 9 listen ON
l2tp 9 swap_io ON
def_route 0 ll_ent "ETH"
eroute 0 peerid "*"
eroute 0 locip "217.34.133.23"
eroute 0 locmsk "255.255.255.255"
eroute 0 remnetid "*"
eroute 0 mode "Transport"
eroute 0 ESPauth "MD5"
eroute 0 ESPenc "3DES"
eroute 0 proto "UDP"
```

```
        eroute 0 remport 1701
        eroute 0 ltime 3600
        eroute 0 lkbytes 250000
        eroute 0 authmeth "PRESHARED"
        def_eroute 0 nosain "PASS"
        def_eroute 0 nosaout "PASS"
        ppp 3 defpak 16
        ppp 4 defpak 16
        ppp 5 defpak 16
        ppp 6 defpak 16
        ppp 7 defpak 16
        ppp 8 defpak 16
        ppp 9 defpak 16

ppp 10 l_mru 1500
ppp 10 l_acfc ON
ppp 10 l_pfc ON
ppp 10 l_pap ON
ppp 10 l_chap ON
ppp 10 l_accm "0x00000000"
ppp 10 l_comp ON
ppp 10 r_mru 1500
ppp 10 r_accm "0xffffffff"
ppp 10 r_addr ON
ppp 10 r_callb ON
ppp 10 IPaddr "10.2.0.1"
ppp 10 IPmin "10.2.0.10"
ppp 10 IPrange 1
ppp 10 DNSport 53
ppp 10 ans 1
ppp 10 restdel 2000
ppp 10 lcn 1027
ppp 10 defpak 128
ppp 10 baklcn 1027
ppp 10 mask "255.255.255.255"
ppp 10 netip "0.0.0.0"
ppp 10 l1iface "L2TP"
ppp 10 ipanon ON
ppp 10 l_md5 1
ppp 10 r_md5 1
ppp 10 r_ms1 1
ppp 10 r_ms2 1
ppp 11 l_mru 1500
ppp 11 l_acfc ON
ppp 11 l_pfc ON
ppp 11 l_pap ON
ppp 11 l_chap ON
```

ppp 11 l_accm "0x00000000"
ppp 11 l_comp ON
ppp 11 r_mru 1500
ppp 11 r_accm "0xffffffff"
ppp 11 r_addr ON
ppp 11 r_callb ON
ppp 11 IPaddr "10.2.0.1"
ppp 11 IPmin "10.2.0.11"
ppp 11 IPrange 1
ppp 11 DNSport 53
ppp 11 ans 1
ppp 11 restdel 2000
ppp 11 lcn 1027
ppp 11 defpak 128
ppp 11 baklcn 1027
ppp 11 mask "255.255.255.255"
ppp 11 netip "0.0.0.0"
ppp 11 l1iface "L2TP"
ppp 11 l1nb 1
ppp 11 ipanon ON
ppp 11 l_md5 1
ppp 11 r_md5 1
ppp 11 r_ms1 1
ppp 11 r_ms2 1
ppp 12 l_mru 1500
ppp 12 l_acfc ON
ppp 12 l_pfc ON
ppp 12 l_pap ON
ppp 12 l_chap ON
ppp 12 l_accm "0x00000000"
ppp 12 l_comp ON
28
ppp 12 r_mru 1500
ppp 12 r_accm "0xffffffff"
ppp 12 r_addr ON
ppp 12 r_callb ON
ppp 12 IPaddr "10.2.0.1"
ppp 12 IPmin "10.2.0.12"
ppp 12 IPrange 1
ppp 12 DNSport 53
ppp 12 ans 1
ppp 12 restdel 2000
ppp 12 lcn 1027
ppp 12 defpak 128
ppp 12 baklcn 1027
ppp 12 mask "255.255.255.255"

ppp 12 netip "0.0.0.0"
ppp 12 l1iface "L2TP"
ppp 12 l1nb 2
ppp 12 ipanon ON
ppp 12 l_md5 1
ppp 12 r_md5 1
ppp 12 r_ms1 1
ppp 12 r_ms2 1
ppp 13 l_mru 1500
ppp 13 l_acfc ON
ppp 13 l_pfc ON
ppp 13 l_pap ON
ppp 13 l_chap ON
ppp 13 l_accm "0x00000000"
ppp 13 l_comp ON
ppp 13 r_mru 1500
ppp 13 r_accm "0xffffffff"
ppp 13 r_addr ON
ppp 13 r_callb ON
ppp 13 IPaddr "10.2.0.1"
ppp 13 IPmin "10.2.0.13"
ppp 13 IPrange 1
ppp 13 DNSport 53
ppp 13 ans 1
ppp 13 restdel 2000
ppp 13 lcn 1027
ppp 13 defpak 128
ppp 13 baklcn 1027
ppp 13 mask "255.255.255.255"
ppp 13 netip "0.0.0.0"
ppp 13 l1iface "L2TP"
ppp 13 l1nb 3
ppp 13 ipanon ON
ppp 13 l_md5 1
ppp 13 r_md5 1
ppp 13 r_ms1 1
ppp 13 r_ms2 1
ppp 14 l_mru 1500
ppp 14 l_acfc ON
ppp 14 l_pfc ON
ppp 14 l_pap ON
ppp 14 l_chap ON
ppp 14 l_accm "0x00000000"
ppp 14 l_comp ON
ppp 14 r_mru 1500
ppp 14 r_accm "0xffffffff"

ppp 14 r_addr ON
ppp 14 r_callb ON
ppp 14 IPaddr "10.2.0.1"
ppp 14 IPmin "10.2.0.14"
29
ppp 14 IPrange 1
ppp 14 DNSport 53
ppp 14 ans 1
ppp 14 restdel 2000
ppp 14 lcn 1027
ppp 14 defpak 128
ppp 14 baklcn 1027
ppp 14 mask "255.255.255.255"
ppp 14 netip "0.0.0.0"
ppp 14 l1iface "L2TP"
ppp 14 l1nb 4
ppp 14 ipanon ON
ppp 14 l_md5 1
ppp 14 r_md5 1
ppp 14 r_ms1 1
ppp 14 r_ms2 1
ppp 15 l_mru 1500
ppp 15 l_acfc ON
ppp 15 l_pfc ON
ppp 15 l_pap ON
ppp 15 l_chap ON
ppp 15 l_accm "0x00000000"
ppp 15 l_comp ON
ppp 15 r_mru 1500
ppp 15 r_accm "0xffffffff"
ppp 15 r_addr ON
ppp 15 r_callb ON
ppp 15 IPaddr "10.2.0.1"
ppp 15 IPmin "10.2.0.15"
ppp 15 IPrange 1
ppp 15 DNSport 53
ppp 15 ans 1
ppp 15 restdel 2000
ppp 15 lcn 1027
ppp 15 defpak 128
ppp 15 baklcn 1027
ppp 15 mask "255.255.255.255"
ppp 15 netip "0.0.0.0"
ppp 15 l1iface "L2TP"
ppp 15 l1nb 5
ppp 15 ipanon ON

ppp 15 l_md5 1
ppp 15 r_md5 1
ppp 15 r_ms1 1
ppp 15 r_ms2 1
ppp 16 l_mru 1500
ppp 16 l_acfc ON
ppp 16 l_pfc ON
ppp 16 l_pap ON
ppp 16 l_chap ON
ppp 16 l_accm "0x00000000"
ppp 16 l_comp ON
ppp 16 r_mru 1500
ppp 16 r_accm "0xffffffff"
ppp 16 r_addr ON
ppp 16 r_callb ON
ppp 16 IPaddr "10.2.0.1"
ppp 16 IPmin "10.2.0.16"
ppp 16 IPrange 1
ppp 16 DNSport 53
ppp 16 ans 1
ppp 16 restdel 2000
ppp 16 lcn 1027
ppp 16 defpak 128
30
ppp 16 baklcn 1027
ppp 16 mask "255.255.255.255"
ppp 16 netip "0.0.0.0"
ppp 16 l1iface "L2TP"
ppp 16 l1nb 6
ppp 16 ipanon ON
ppp 16 l_md5 1
ppp 16 r_md5 1
ppp 16 r_ms1 1
ppp 16 r_ms2 1
ppp 17 l_mru 1500
ppp 17 l_acfc ON
ppp 17 l_pfc ON
ppp 17 l_pap ON
ppp 17 l_chap ON
ppp 17 l_accm "0x00000000"
ppp 17 l_comp ON
ppp 17 r_mru 1500
ppp 17 r_accm "0xffffffff"
ppp 17 r_addr ON
ppp 17 r_callb ON
ppp 17 IPaddr "10.2.0.1"

ppp 17 IPmin "10.2.0.17"
ppp 17 IPrange 1
ppp 17 DNSport 53
ppp 17 ans 1
ppp 17 restdel 2000
ppp 17 lcn 1027
ppp 17 defpak 128
ppp 17 baklcn 1027
ppp 17 mask "255.255.255.255"
ppp 17 netip "0.0.0.0"
ppp 17 l1iface "L2TP"
ppp 17 l1nb 7
ppp 17 ipanon ON
ppp 17 l_md5 1
ppp 17 r_md5 1
ppp 17 r_ms1 1
ppp 17 r_ms2 1
ppp 18 l_mru 1500
ppp 18 l_acfc ON
ppp 18 l_pfc ON
ppp 18 l_pap ON
ppp 18 l_chap ON
ppp 18 l_accm "0x00000000"
ppp 18 l_comp ON
ppp 18 r_mru 1500
ppp 18 r_accm "0xffffffff"
ppp 18 r_addr ON
ppp 18 r_callb ON
ppp 18 IPaddr "10.2.0.1"
ppp 18 IPmin "10.2.0.18"
ppp 18 IPrange 1
ppp 18 DNSport 53
ppp 18 ans 1
ppp 18 restdel 2000
ppp 18 lcn 1027
ppp 18 defpak 128
ppp 18 baklcn 1027
ppp 18 mask "255.255.255.255"
ppp 18 netip "0.0.0.0"
ppp 18 do_nat 8
ppp 18 l1iface "L2TP"
ppp 18 l1nb 1
31
ppp 18 ipanon ON
ppp 18 l_md5 1
ppp 18 r_md5 1

```
ppp 18 r_ms1 1
ppp 18 r_ms2 1
ppp 19 l_mru 1500
ppp 19 l_acfc ON
ppp 19 l_pfc ON
ppp 19 l_pap ON
ppp 19 l_chap ON
ppp 19 l_accm "0x00000000"
ppp 19 l_comp ON
ppp 19 r_mru 1500
ppp 19 r_accm "0xffffffff"
ppp 19 r_addr ON
ppp 19 r_callb ON
ppp 19 IPaddr "10.2.0.1"
ppp 19 IPmin "10.2.0.19"
ppp 19 IPrange 1
ppp 19 DNSport 53
ppp 19 ans 1
ppp 19 restdel 2000
ppp 19 lcn 1027
ppp 19 defpak 128
ppp 19 baklcn 1027
ppp 19 mask "255.255.255.255"
ppp 19 netip "0.0.0.0"
ppp 19 l1iface "L2TP"
ppp 19 l1nb 9
ppp 19 ipanon ON
ppp 19 l_md5 1
ppp 19 r_md5 1
ppp 19 r_ms1 1
ppp 19 r_ms2 1
ike 0 ltime 28800
ike 0 deblevel 3
ike 0 debug ON
user 0 name "Sarian"
user 0 epassword "EQ0kDhcc"
user 0 access 0
user 1 name "username"
user 1 epassword "KD5lSVJDVVg="
user 1 access 0
user 2 access 0
user 3 access 0
user 4 access 0
user 5 access 0
user 6 access 0
user 7 access 0
```

```
user 8 access 0
user 9 access 0
user 14 name "*"
user 14 epassword "Gmt4DksY"
32
```